

Magneto-Impedance effect for magnetic sensors: challenges, advances and perspectives

A. Zhukov^{1,2,3,4}, P. Corte-Leon^{1,2}, M. Ipatov^{1,2}, J.M. Blanco² A. Gonzalez^{1,2} and V. Zhukova^{1,3}

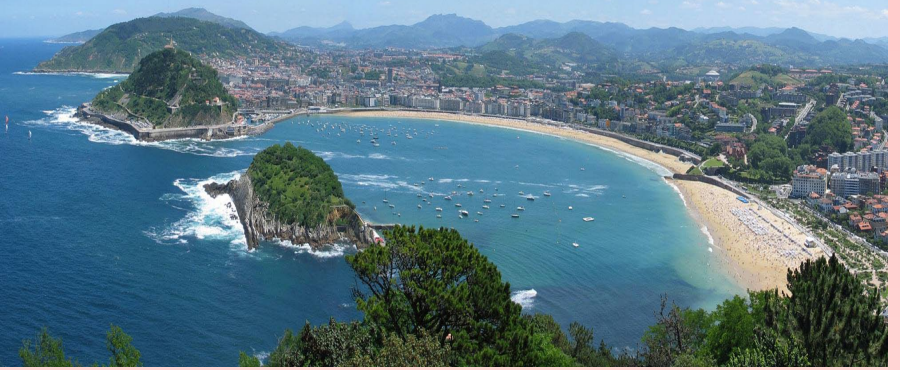
¹Dpto. Polímeros y Materiales Avanzados, UPV/EHU San Sebastián 20009, Spain

²Dpto. de Fís. Aplicada., UPV/EHU San Sebastián 20009, Spain

³Ikerbasque, Basque Foundation for Science , Bilbao, Spain.

⁴ EHU Quantum center





Outline

1. INTRODUCTION

1.1. STATE OF THE ART ON GMI

1. 2. MOTIVATION :

2. MEASUREMENTS METHODS

3. FACTORS AFFECTING GMI

3.1. MAGNETOELASTIC ANISOTROPY

4. LINEARITY OF GMI

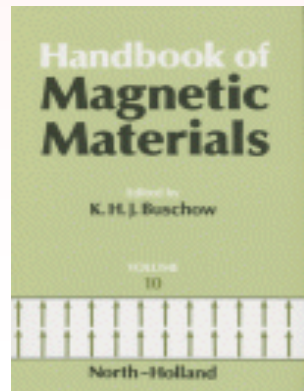
5. GMI HYSTERESIS

6. INTERFACE LAYER

7. CONCLUSIONS

Advances in Giant
Magnetoimpedance of
Materials

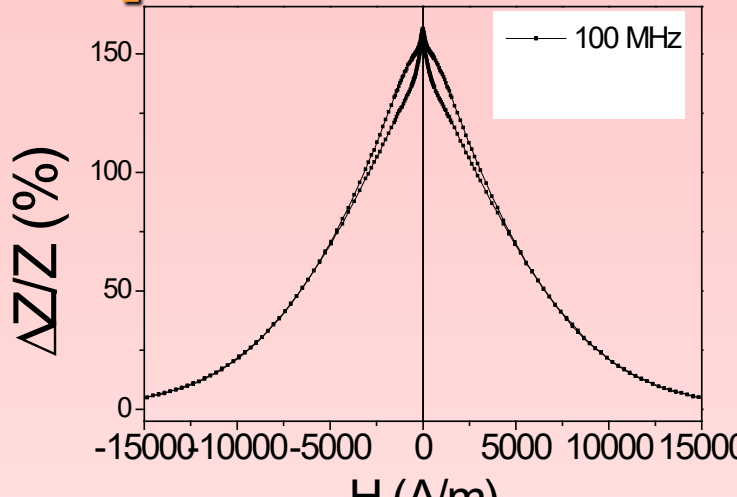
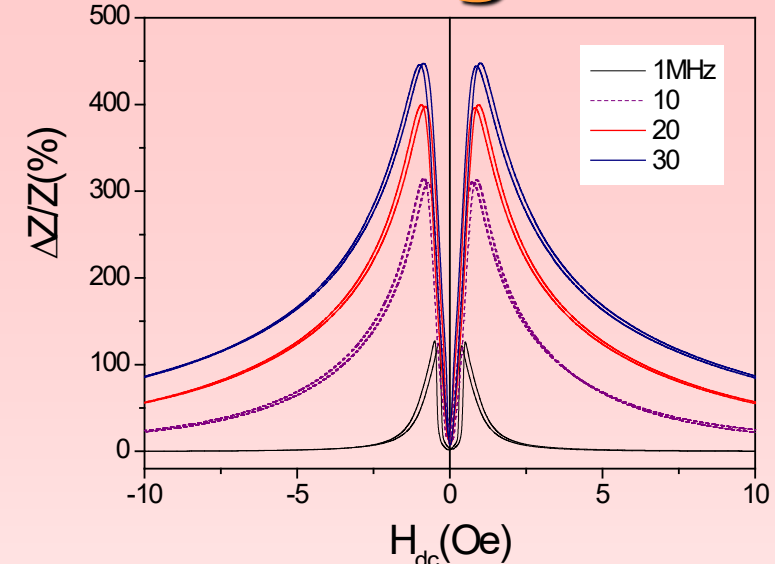
A. Zhukov,^{1,2,3,*} M. Ipatov^{1,2} and V. Zhukova^{1,2}



November 2015

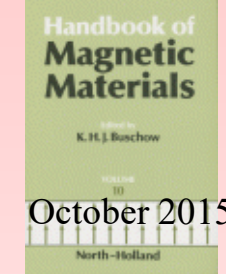


Giant Magneto-impedance effect



Advances in Giant
Magnetoimpedance of
Materials

A. Zhukov,^{1,2,3,*} M. Ipatov^{1,2} and V. Zhukova^{1,2}



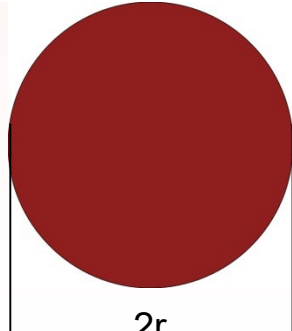
$$\Delta Z / Z = \{ |Z(H_{ex})| - |Z(H_{max})| \} / |Z(H_{max})|$$

Magnetic filed dependence and value are affected by magnetic anisotropy

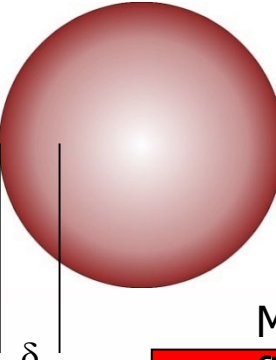
Skin Effect of the Magnetic Conductor

AC current frequency

$f \approx \text{kHz}$



$f \approx \text{MHz}$



$$\mu_\phi \downarrow \rightarrow \delta \uparrow$$

Magnetic
field

Magnetically soft low dimensional magnetic materials

$$\delta = \sqrt{\frac{\rho}{\pi \mu_\phi f}}$$
$$\mu_\phi(H, f)$$
$$\delta < r$$

(at high enough f)

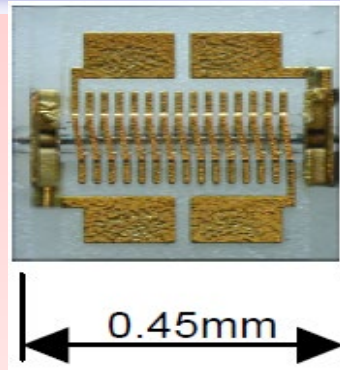
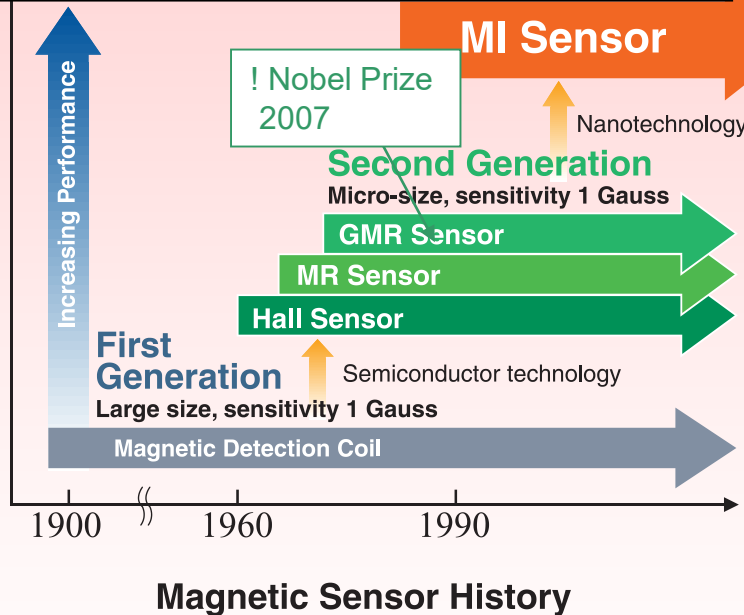
$Z(H)$

Promising GMI applications: 1. Magnetic sensors and smart composites

Third Generation of Magnetic Sensors

Smart composites

MI Sensors with excellent performance!



Based on Amorphous Wwire since 2010



Amorphous wire: (glass-coated wire)
Metal dia. : 11.3 μ m
Total wire : 14.5 μ m
Wire length: 520 μ m
Amorphous Wire 3-axis Electronic Compass chip: A MI 306
Resolution : 0.16 μ T (160 nT) \pm 1.2 mT (\pm 12 Oe)
Dynamic range : 1.7 V
Power voltage Vdd : 150 μ A
Power current Idd : 255 μ W
Power consumption : -45 ~ 80 $^{\circ}$ C
Operating temperature : 2.04 \times 2.04 \times 1.0 mm
Reversibility for big disturbance magnetic field shock ∞



- 1) Micro size and small power consumption (sub-mW)
- 2) High sensitivity with resolution of 0.01 % for dynamic range (Pico-Tesla resolution)
- 3) Quick response with GHz
- 4) High reversibility for big magnetic field disturbance shock ∞
- 5) High temperature stability

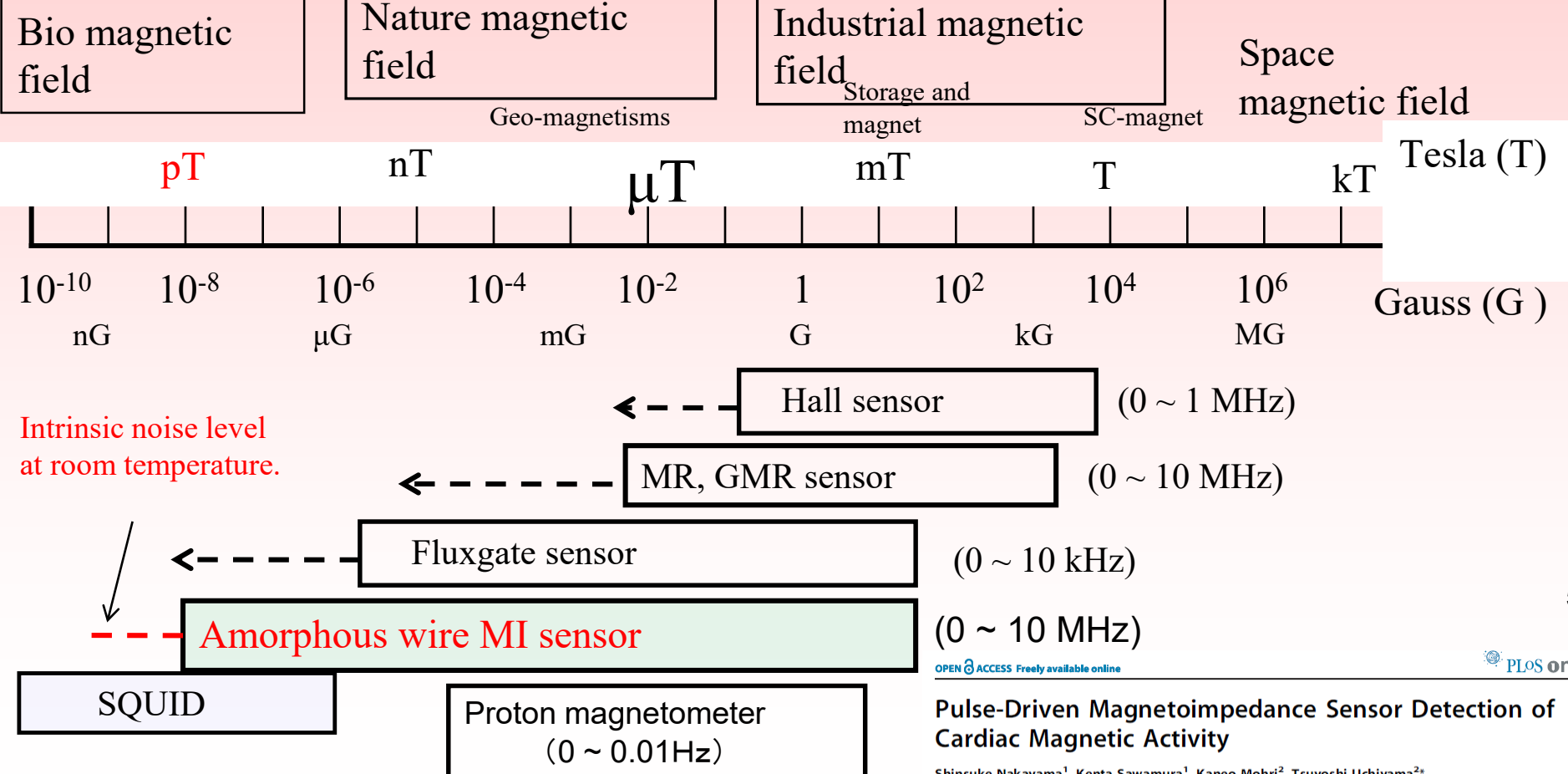
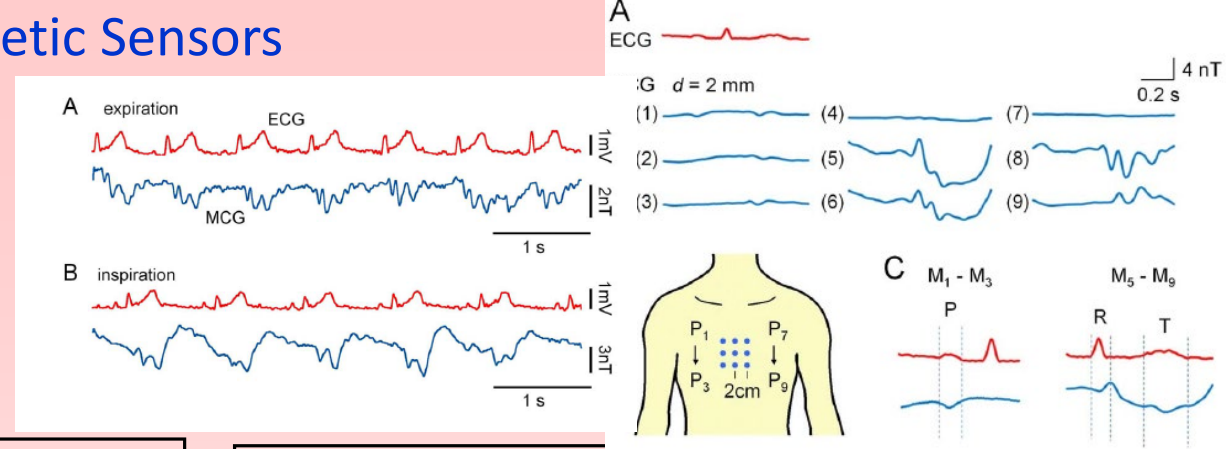
Industrial application in Smart phone using MI sensor

Advanced 3-axis MI sensor chip installed in watch

Last tendencies: Size reduction, frequency increasing Soft magnets are needed

Magnetic Field and Magnetic Sensors

Magnetic wires
(up to 730%),
up to 10%/A/m
pico-Tesla sensitivity !

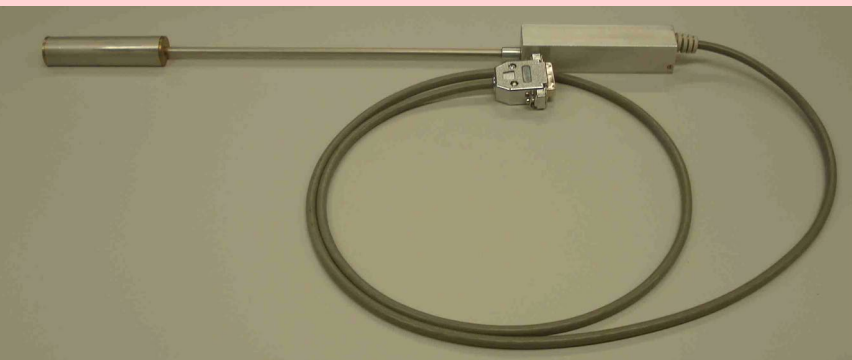


GMI magnetometer versus SQUID and fluxgate

Advantages:

Lower cost

Smaller size



SQUID (superconducting quantum interference device)

All the GMI magnetometer prototypes are made with magnetic wires where the highest GMI ratio is achieved!

Main features and definitions of the GMI effect

The widely used GMI ratio definition [1,2]:

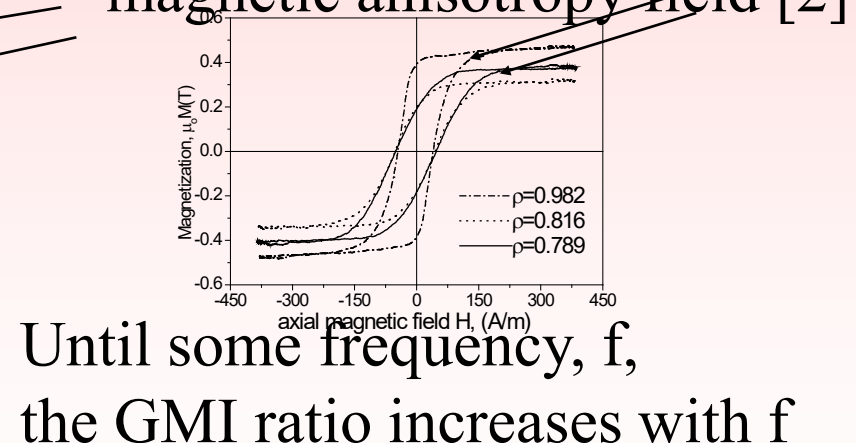
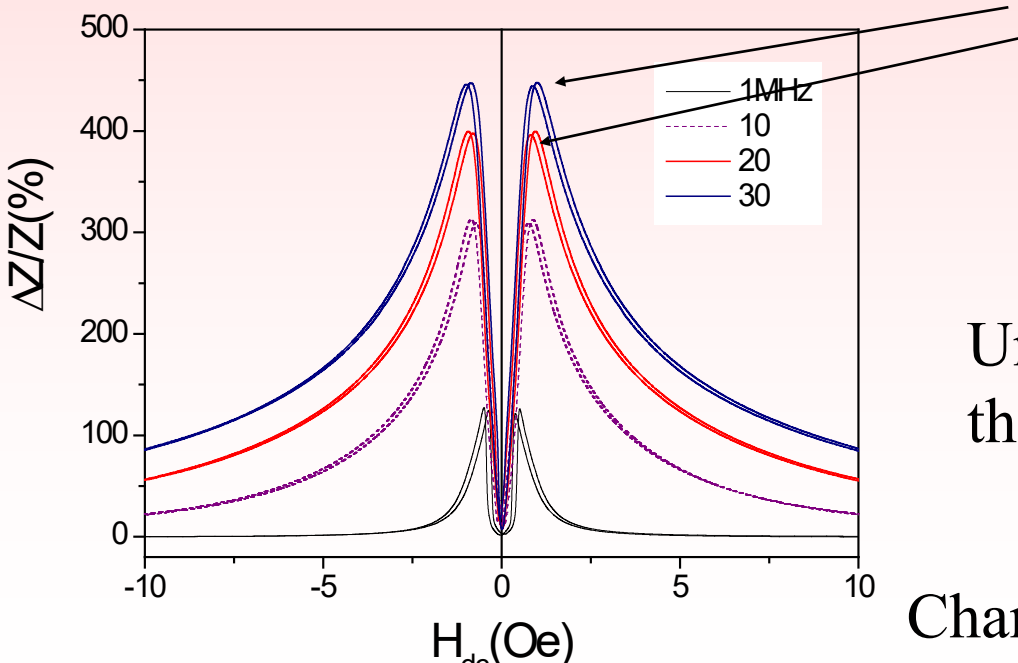
$$\Delta Z / Z = \{ |Z(H_{ex})| - |Z(H_{max})| \} / |Z(H_{max})| \quad (1)$$

where Z is the impedance modulus and H_{max} is the maximum measured field

[1] R. S. Beach, A. E. Berkowitz, *Appl.Phys.Lett.*, **64**, 3652 (1994).

[2] L. V. Panina, K. Mohri, *Appl.Phys. Lett.*, **65**, 1185 (1994). The maximum (if there is) corresponds to the transverse magnetic anisotropy field [2]

Typical GMI ratio curve

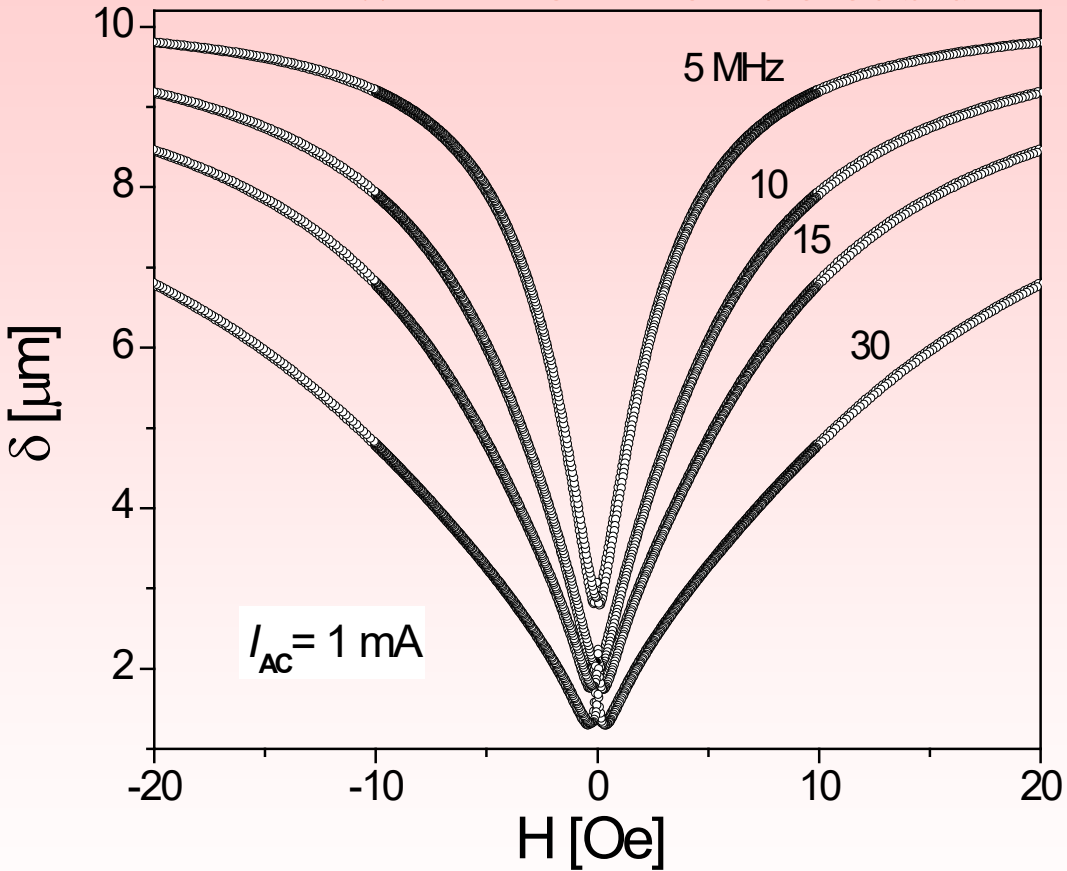


Until some frequency, f ,
the GMI ratio increases with f

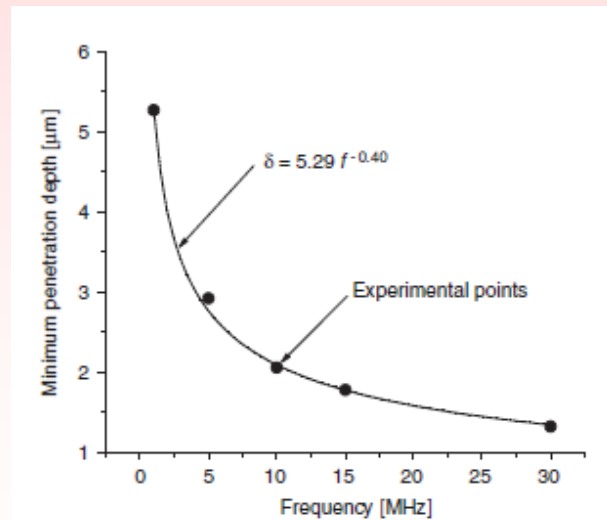
Changing the hysteretic properties
we can modify the GMI effect

GMI effect

Calculated penetration depth vs. axial dc-field at various frequencies of ac-current in $\text{Co}_{67}\text{Fe}_{3.85}\text{Ni}_{1.45}\text{Mo}_{1.7}\text{Si}_{14.5}\text{B}_{11.5}$ microwire with metallic nucleus diameter $22.4 \mu\text{m}$



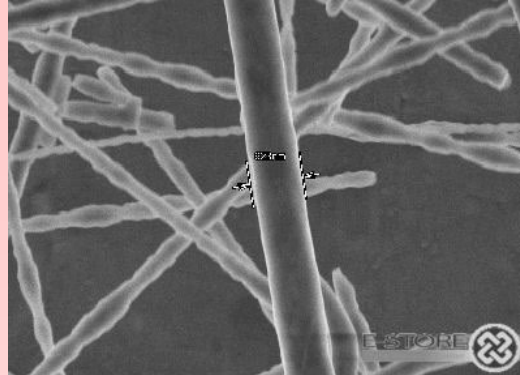
Essentially surface effect. Thin surface layers are involved in the GMI process



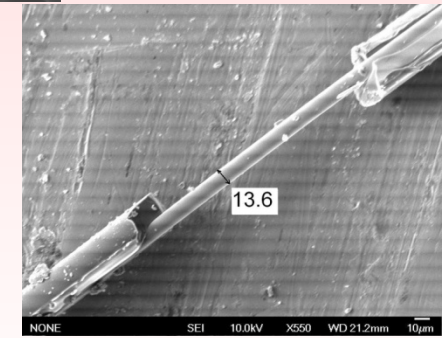
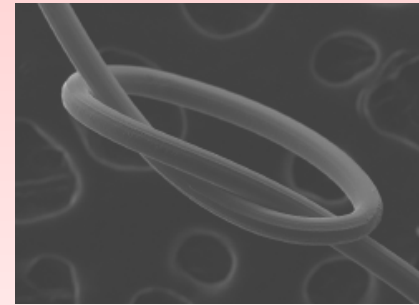
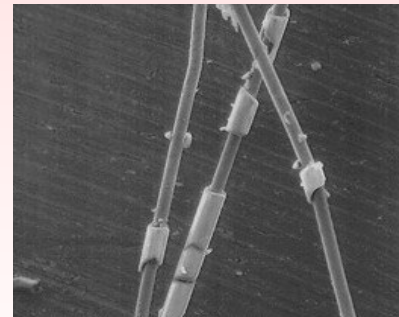
H. Lachowicz, M. Kuzminski, K.L. García, A. Zhukov and M. Vázquez, A. Krzyzhevski, “Influence of Alternative circular magnetic field strength on magnetoimpedance of glass-coated micro-wire⁸”, J. Magn. Magn. Mater. 300 (2006), e88-e-92

Magnetic wires:

- Iron whiskers
- Wiegan magnetic wires
(CoVFe, 1970-th)



Amorphous: milli
(since 80-th) micro } wires
 nano }



Properties

Fast domain walls propagation (after Sixtus-Tonks, 1936)

GMI effect (after E.P. Harrison, et.al *Nature*, 1935, vol. 135, p. 961

and later resurrected by Beach R and Berkowitz A (1994), *APL*, 64, 3652.

Panina L V and Mohri K (1994), *APL*, 65, 1189.)

GMI effect

The **Magneto-Impedance** (MI) effect:

- extremely high sensitivity to external stimulus (magnetic field, stresses, temperature etc)
- relatively low-cost implementation
- suitable for integration into current technological process
- RT effect (not cryogenic)

Conditions of high GMI effect:

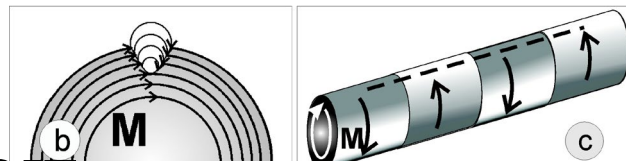
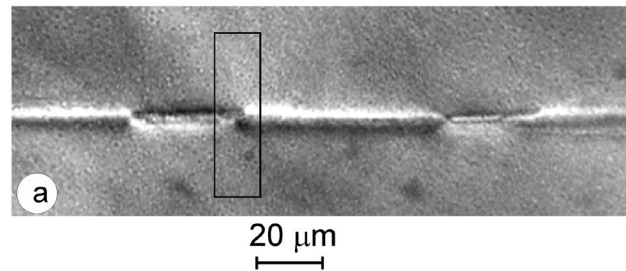
- high transversal magnetic permeability μ and magnetic softness
- high saturation magnetization M_s
- low resistivity ρ

Amorphous μ -wires with vanishing λ_s

• **Reduced dimensions** (metallic nucleus diameter 0.2–100 μm , glass-coating 1–10 μm).

• **High homogeneity low cost** and almost continuous process (1 gram of the alloy allows to obtain about Km of the wire).

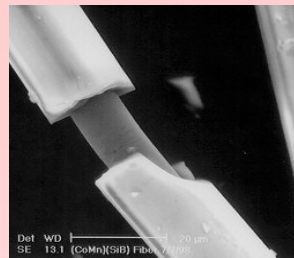
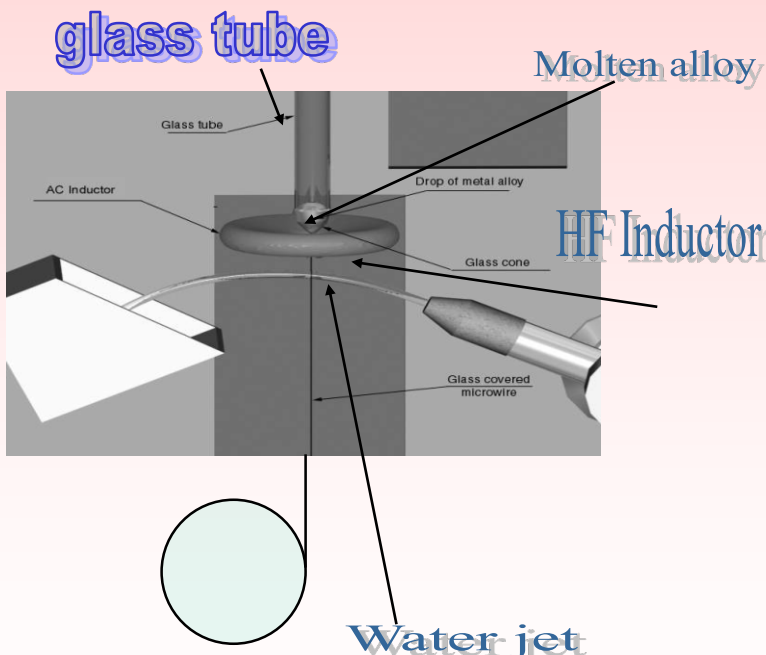
• **Excellent soft magnetic properties**



Glass coated amorphous magnetic microwires

- Co, Ni , Fe and Cu rich compositions

dmetal



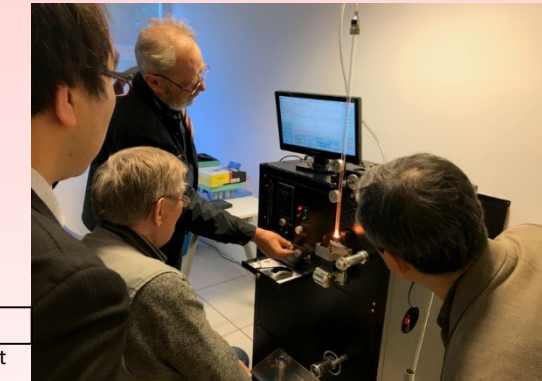
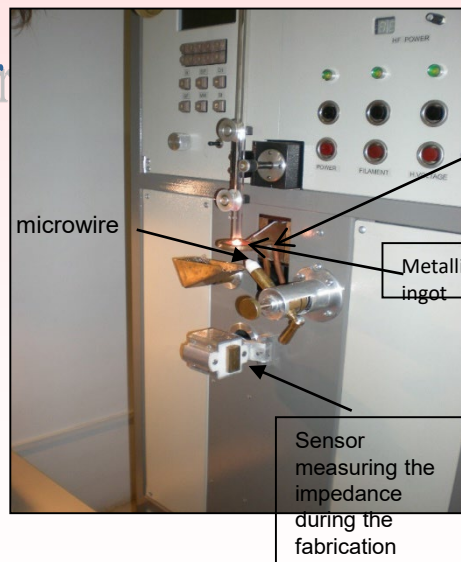
Typical dimensions:

Total diameter 1-120 μm

Metallic nucleus diameter 0.2-100 μm

Glass coating thickness 1-10 μm

Length - few km (up to 10 in 1 bobbin)



Advantages: (functionalities)

1. Unexpensive and simple fabrication method
2. *Excellent soft magnetic properties (if amorphous)*
3. Magnetic bistability (DW propagation)
4. Thin dimensions (Raw materials saving)
5. Biocompatibility (glass-coating)
6. Better corrosion resistance (glass-coating)
7. Robust properties

IOP Publishing
J. Phys.: D: Appl. Phys. 55 (2022) 253003 (40pp)

Journal of Physics D: Applied Physics
<https://doi.org/10.1088/1361-6463/ac48d7>

Topical Review

Advanced functional magnetic microwires for technological applications

Experimental Facilities at UPV/EHU and Tamag

GMI features relevant for applications

1. Value of the effect
2. Linearity
3. Hysteresis
4. Time/temperature stability
5. Low dimensions (high frequency)

Magnetically soft low dimensional magnetic materials are needed

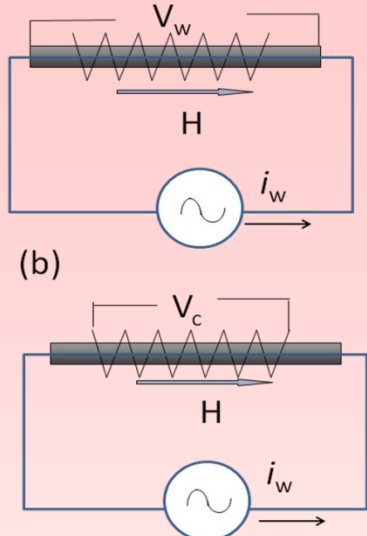
GMI effect (after E.P. Harrison, et.al *Nature*, 1935, vol. 135, p. 961
and later resurrected by Beach R and Berkowitz A (1994), *APL*, 64, 3652.
Panina L V and Mohri K (1994), *APL*, 65, 1189.)

Measurements of GMI

Low-f impedance can be measured by the four-point method.

$\Delta Z/Z$, is defined as:

$$\Delta Z/Z = [(Z(H) - Z(H_{\max})) / Z(H_{\max})]$$



$$Z_{zz} \propto Z = \frac{1 + S_{11}}{1 - S_{11}} Z_0$$

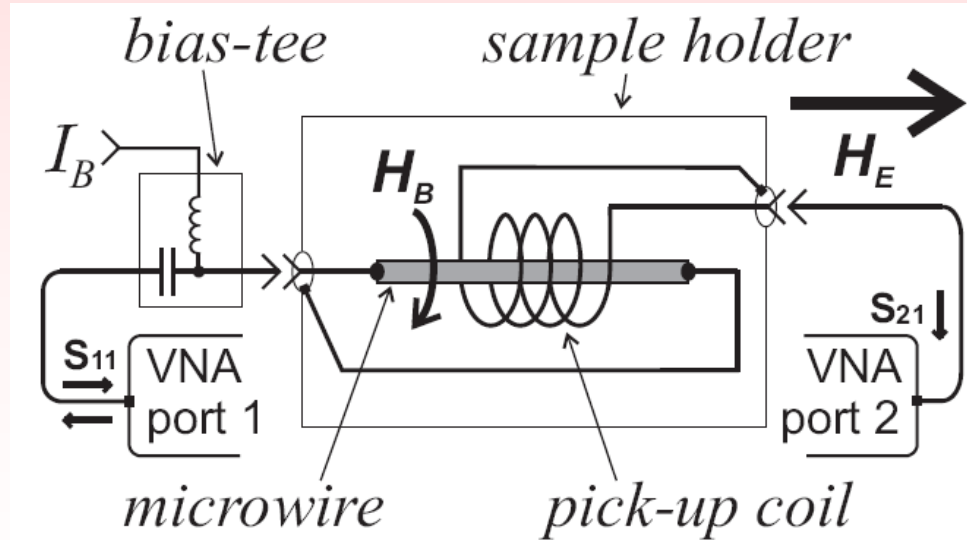
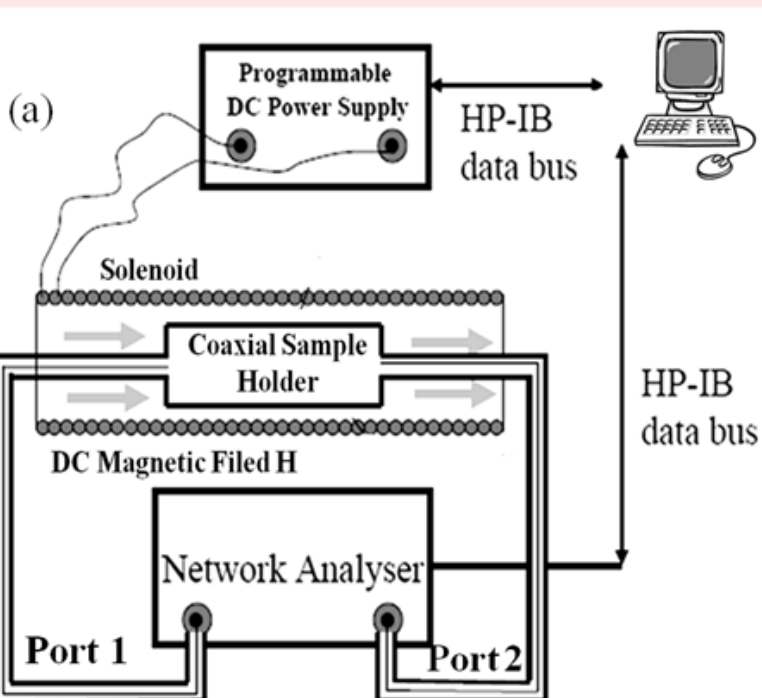
[1]: m_φ, m_r

$$V_w = \xi_{zz} i_w$$

$$i_z \rightarrow h_\varphi \rightarrow [\hat{\mu}]$$

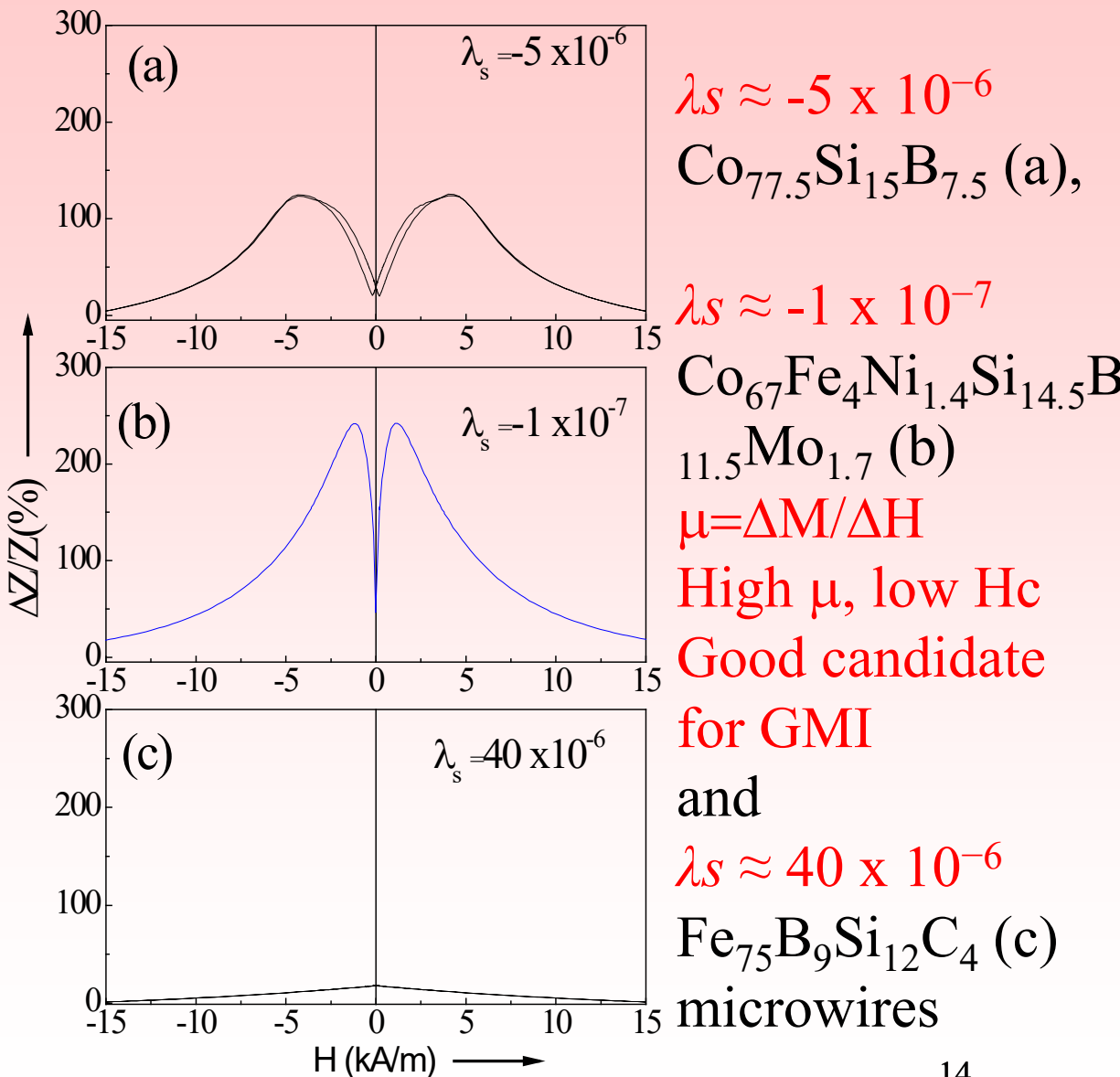
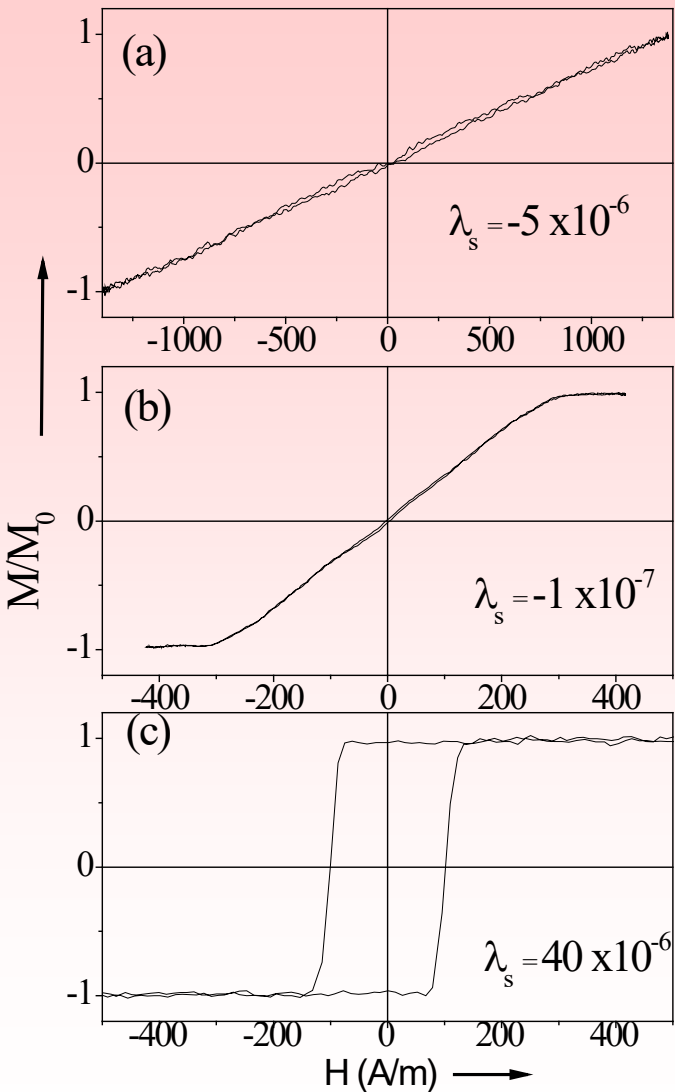
[2]: $m_z \rightarrow V_C$

$$Z_{\varphi z} \propto V_c = S_{21}$$



The impedance was evaluated using Network Analyzer HP8753 at frequency between 10MHz -3GHz .

Magnetic properties and GMI effect of magnetic microwires



Hysteresis loops, shape and value of GMI ratio are different

Factors affecting soft magnetic properties of amorphous alloys

Amorphous materials do not have defects typical for crystalline materials (dislocations, point defects...)

H. Kronmüller (1981) contributions in coercivity of amorphous materials:

Local anisotropy fluctuations (10^{-3} –1 me), $H_c(i)$

Clusters and chemical inhomogeneities (< 1 me), $H_c(SO)$

Surface defects and irregularities (< 5 Me), $H_c(surf)$

Local structural defects (0.1-10 me), $H_c(rel)$

Pinning of DW on defects in magnetostrictive alloys (10-100 Me), $H_c(s)$

$$H_c(\text{total}) = [H_c(s)^2 + H_c(\text{surf})^2 + H_c(SO)^2 + H_c(i)^2]^{1/2} + H_c(\text{rel})$$

или

$$H_c(\text{total}) = H_c(s) + H_c(\text{surf}) + H_c(SO) + H_c(i) + H_c(\text{rel})$$

Magnetostriction

Anisotropy (stresses)

Clusters and chemical inhomogeneities (nanocrystallization)

Defects (surface)

Magnetoelastic energy

Internal stresses in composite microwires

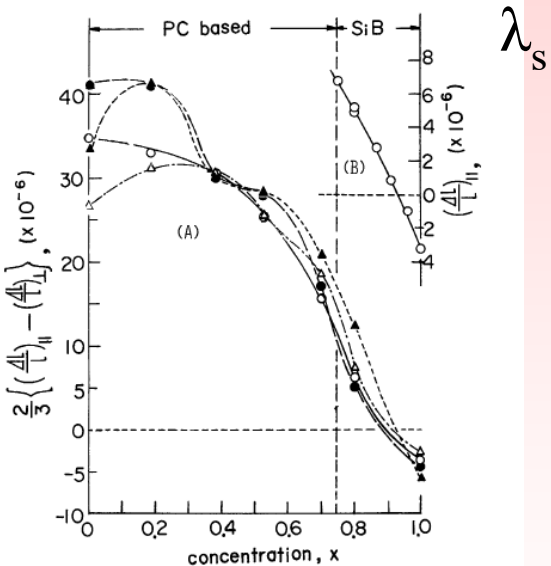
$$K_{me} \approx 3/2 \lambda_s \sigma_i, :$$

Magnetostriction λ_s -determines by the chemical composition

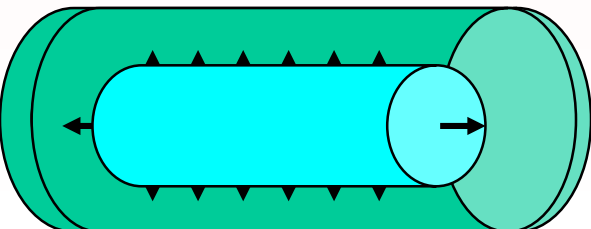
$$\sigma = \sigma_i + \sigma_a$$

σ_a - applied stresses

σ_i -determines by the ratio $\rho = d/D$

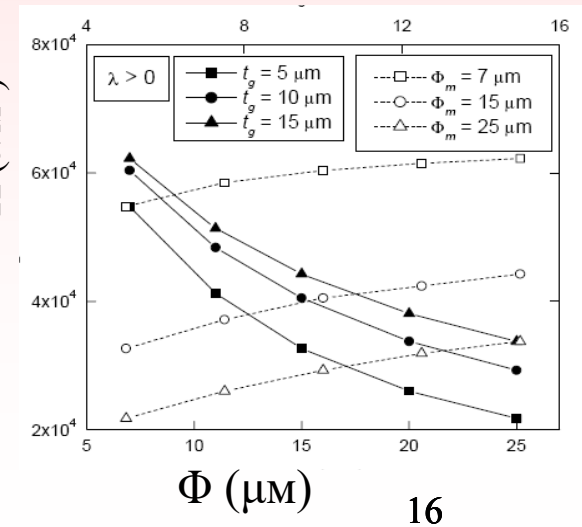
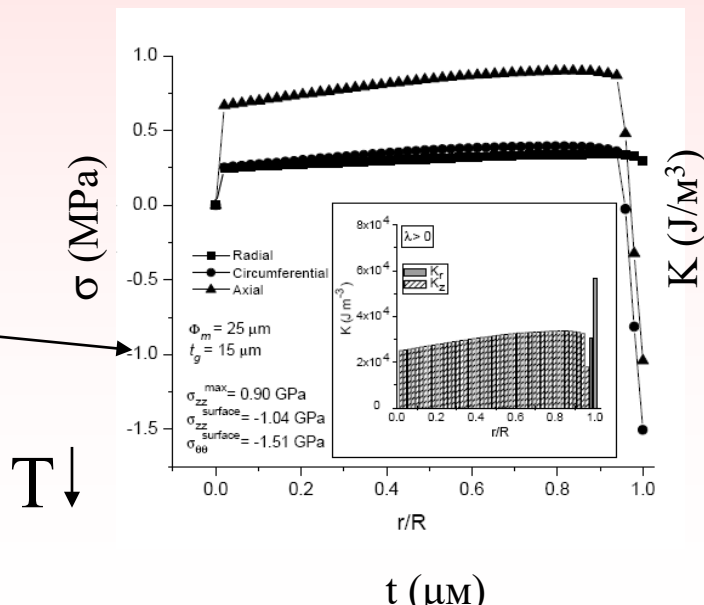
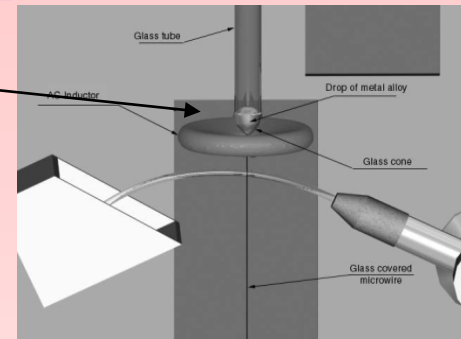


$$\sigma = f(\rho), \rho = d / D$$



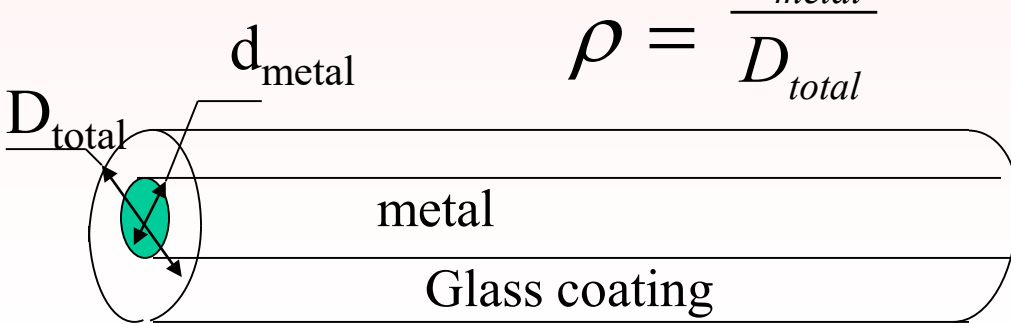
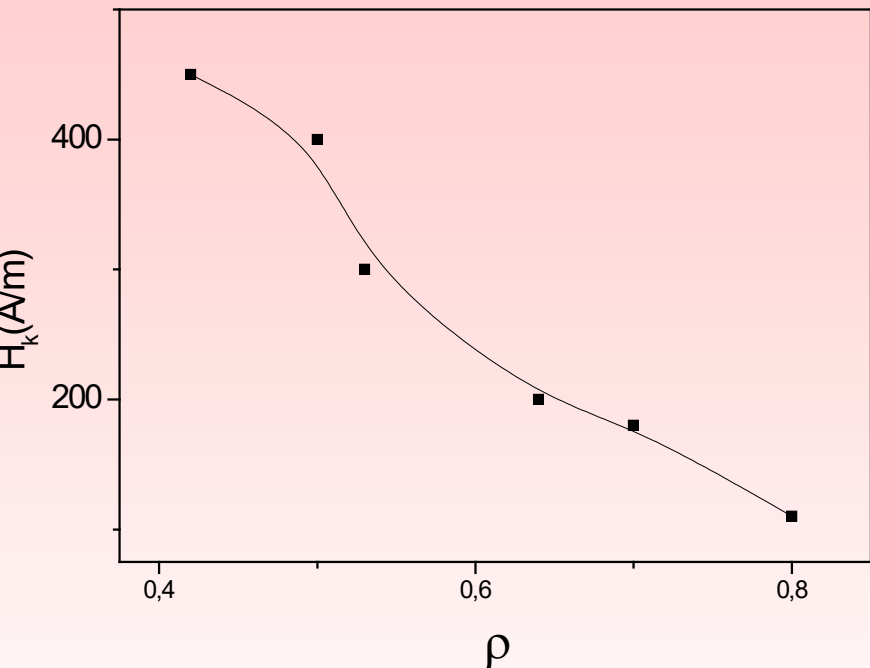
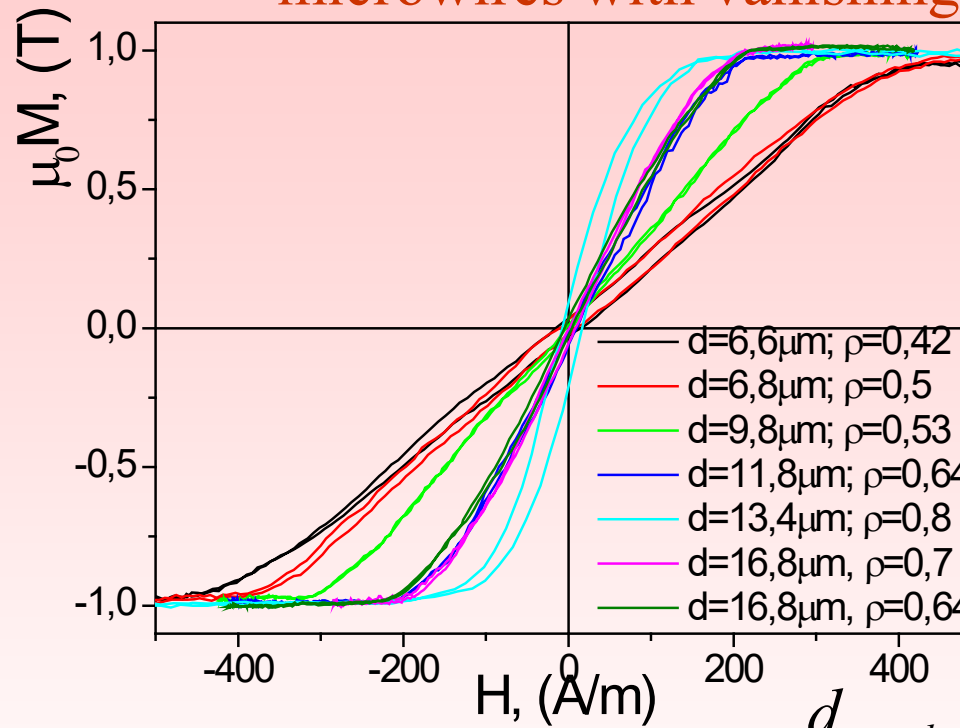
T ↓

Stress appears at simultaneous solidification of metallic alloy inside the glass coating



TAILORING OF GMI EFFECT AND MAGNETIC PROPERTIES

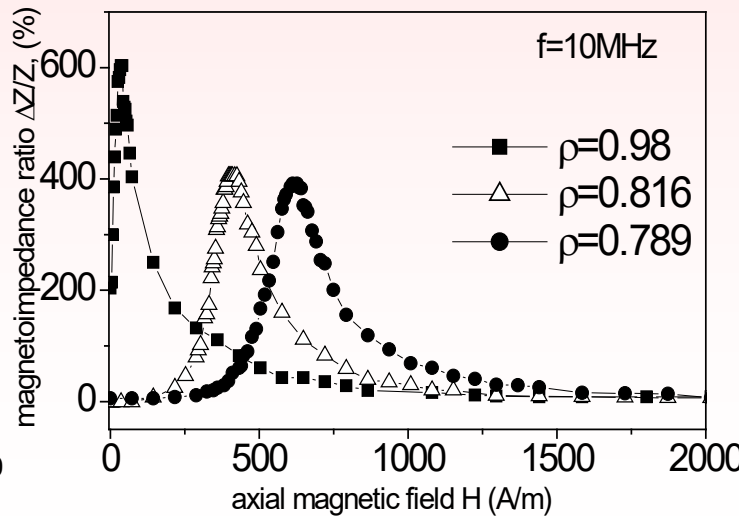
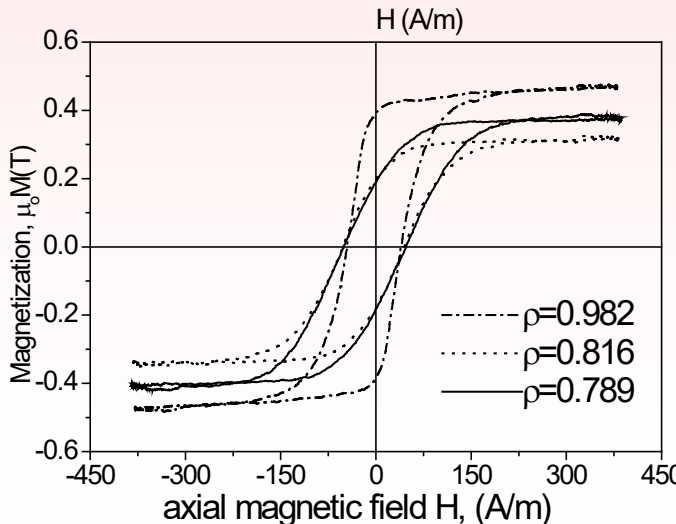
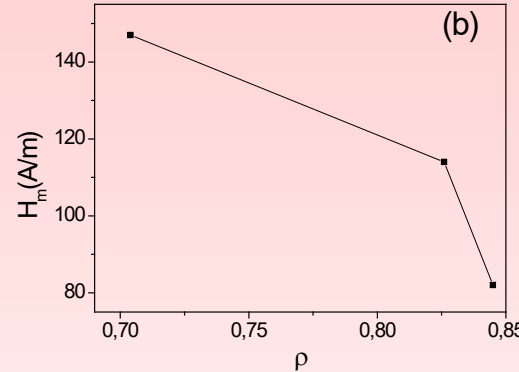
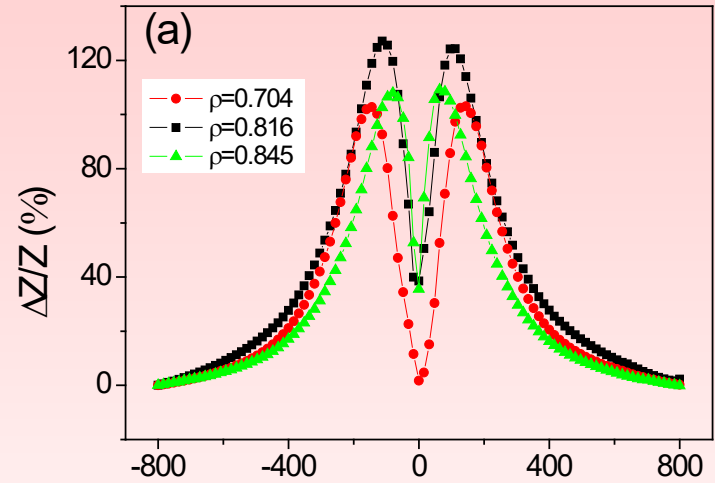
Effect of the samples geometry on the hysteresis loops of Co-rich microwires with vanishing magnetostriction constant.



Correlation with magnetic anisotropy

Effect of internal stresses through the geometry

Effect of ρ -ratio on GMI effect in $\text{Co}_{67,05}\text{Fe}_{3.85}\text{Ni}_{1.4}\text{B}_{11.33}\text{Si}_{14.47}\text{Mo}_{1.69}$ microwire samples with different ρ -ratios (a) and dependence of field of maximums on ρ -ratio (b).



Possibilities:
tailoring of GMI effect
in Co-rich glass coated
microwires by
-Joule heating.
-Choosing adequate
geometry

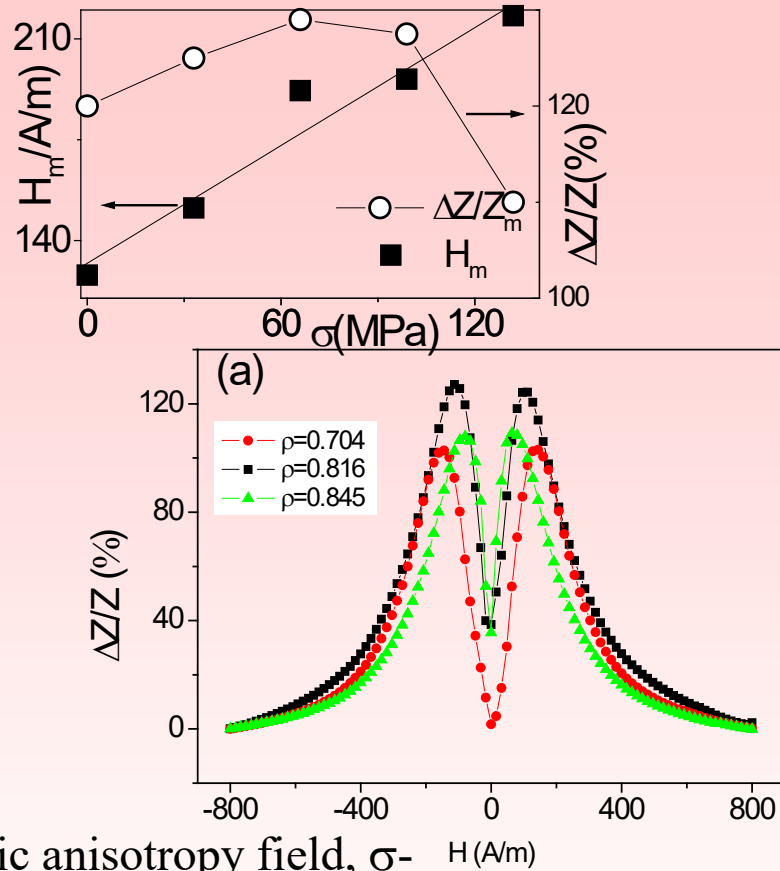
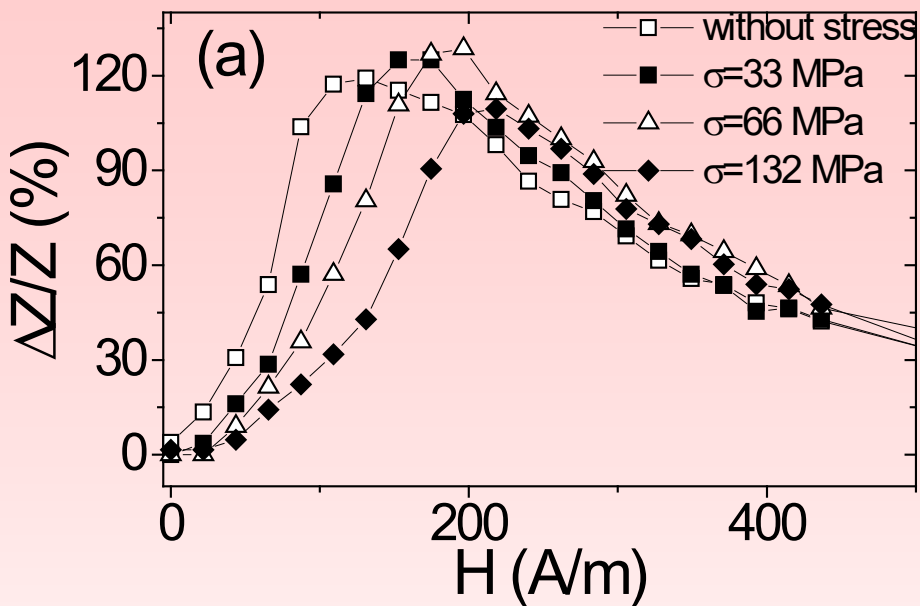
Magnetoelastic
energy

$K_{me} \approx 3/2 \lambda_s \sigma$,
 λ_s – f (chemical
composition)

$$\sigma = \sigma_a + \sigma_i$$



Are stresses always reduce GMI?



The magnetostriiction constant changes with the stress:

$$\lambda_s = (\mu_0 M_s / 3) (dH_k / d\sigma),$$

where $\mu_0 M$ is the saturation magnetization, H_k - magnetic anisotropy field, σ - stresses.

PHYSICAL REVIEW B

VOLUME 35, NUMBER 10

1 APRIL 1987

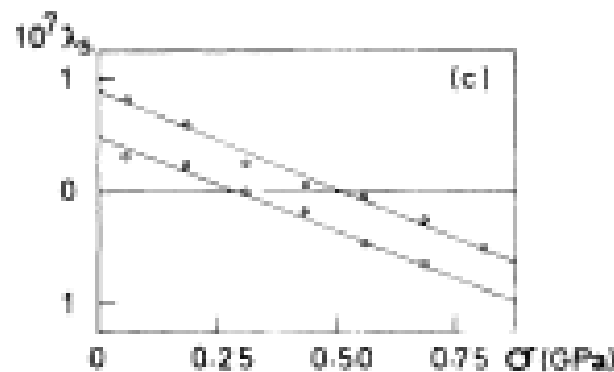
Temperature, stress, and structural-relaxation dependence of the magnetostriiction
in $(Co_{0.94}Fe_{0.06})_7Si_{13}B_{10}$ glasses

J. M. Barandiarán
Departamento de Electricidad y Electrónica, Facultad de Ciencias, Universidad del País Vasco, Apartado 644,
48080 Bilbao, Spain

A. Hernando and V. Madurga
Cátedra de Magnetismo, Facultad de Ciencias Físicas, Universidad Complutense, 28040 Madrid, Spain

O. V. Nielsen
Department of Electrophysics, The Technical University of Denmark, DK-2800 Lyngby, Denmark

M. Vázquez and M. Vázquez-López
Cátedra de Magnetismo, Facultad de Ciencias Físicas, Universidad Complutense, 28040 Madrid, Spain
(Received 21 July 1986)

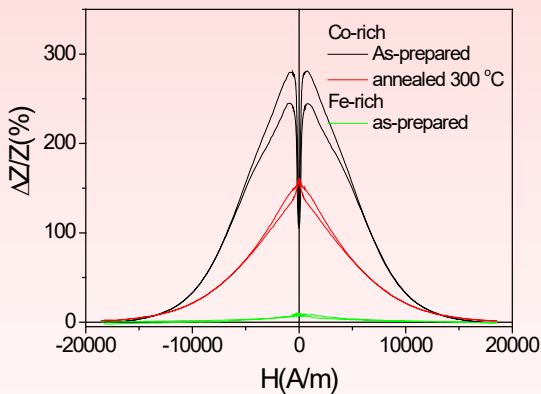


Stress relaxation?

Co-based ($\lambda_s < 0$)

Annealing

Annealing:
 Hysteresis loops and DW dynamics
 -Fe-rich- enhancement of DW velocity
 -Co-rich –induced magnetic bistability

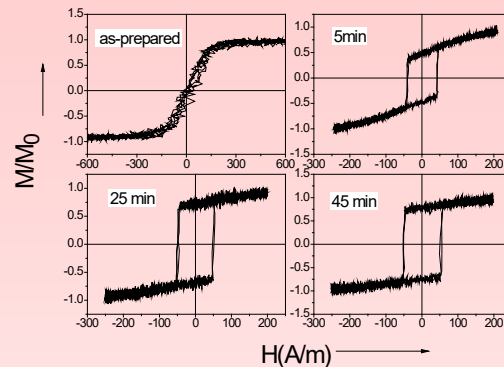


Such hardening was observed in several Co-rich microwires

GMI: For GMI is not a solution!

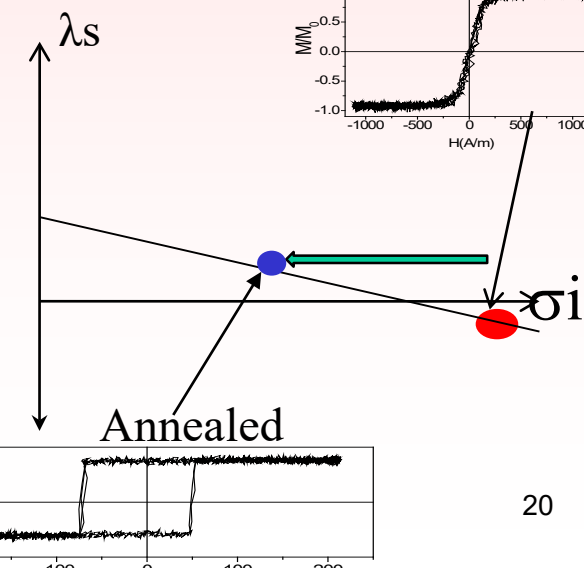
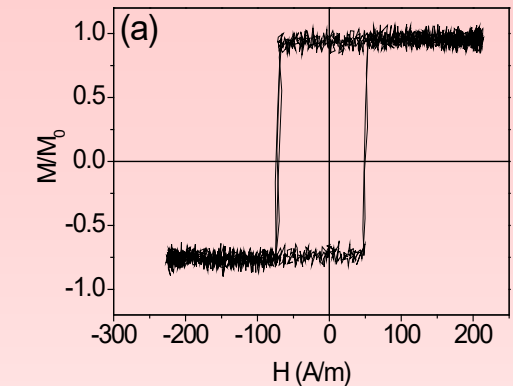
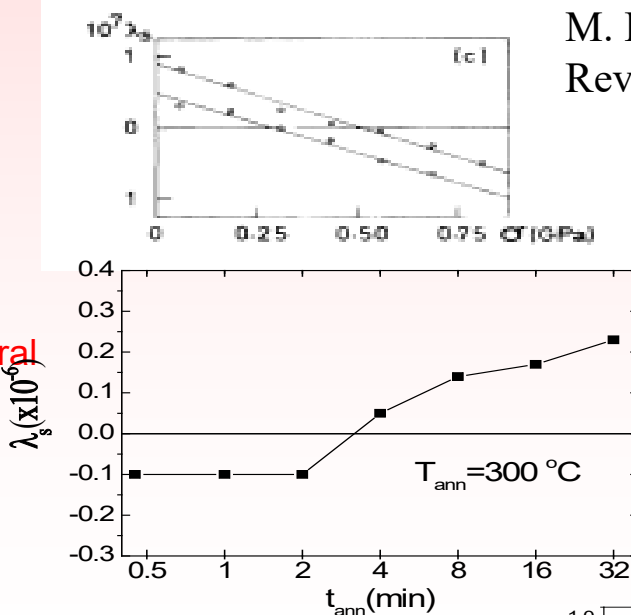
Co-rich – decrease

A. ZHUKOV, et.al J. ELECTRONIC MATERIALS (2015)
 DOI: 10.1007/s11664-015-4011-2



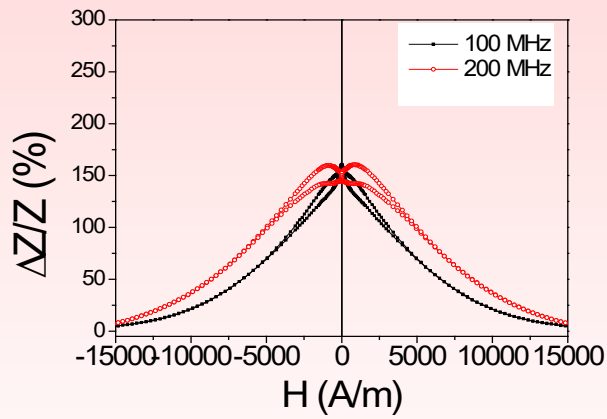
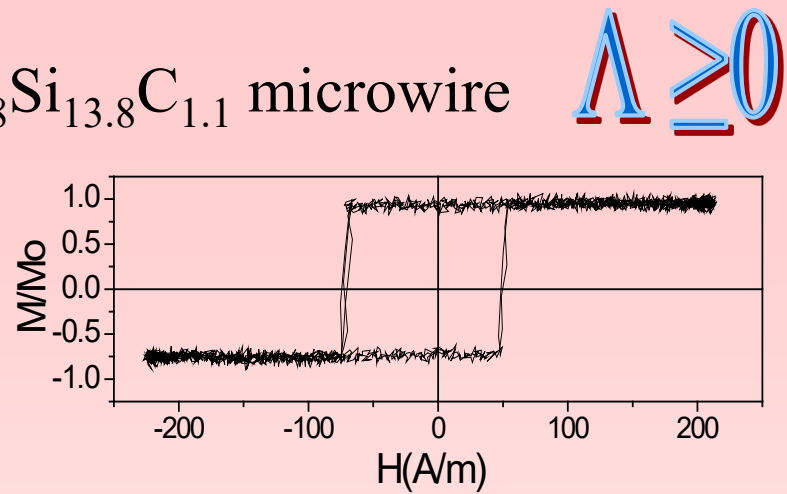
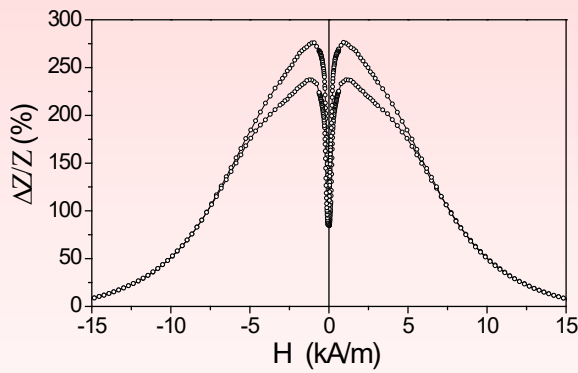
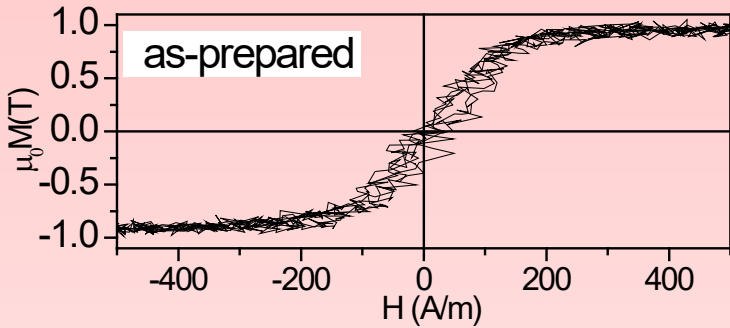
Origin of annealing induced changes in Co-rich microwires

M. Barandiaran, et.all, Phys.
 Rev. B 35 (1987) 5066-5071.
 As-prepared



Magnetostriction

$\lambda \leq 0$



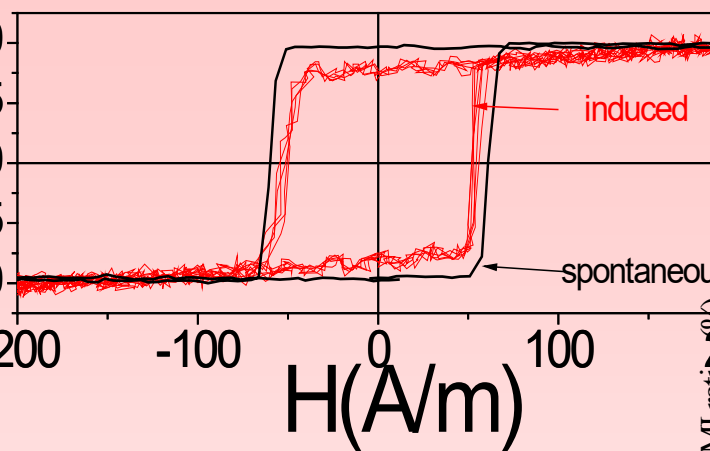
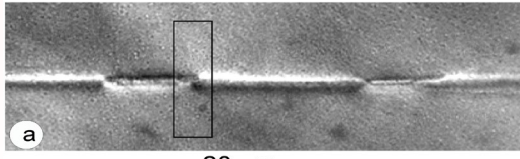
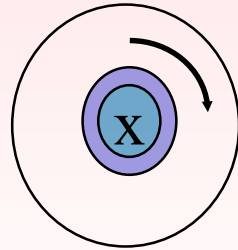
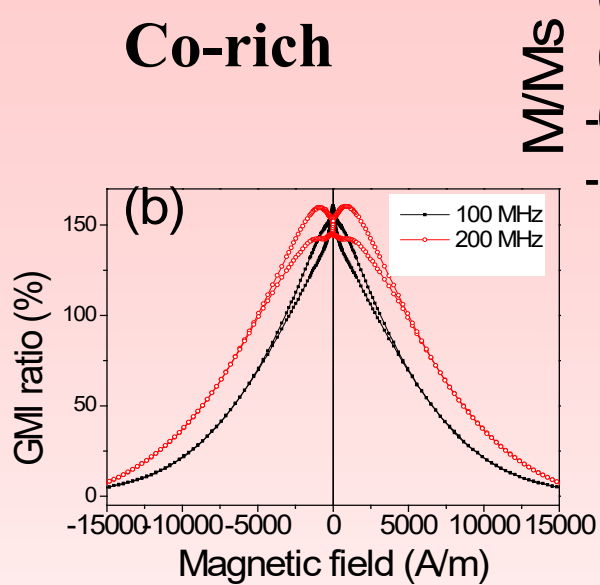
Composition	treatment	$\rho=d/D$	$\lambda_s \times 10^6$
$\text{Co}_{68.7}\text{Fe}_4\text{Ni}_1\text{B}_{13}\text{Si}_{11}\text{Mo}_{2.3}$	As-prepared	0.72	-1.05
$\text{Co}_{68.7}\text{Fe}_4\text{Ni}_1\text{B}_{13}\text{Si}_{11}\text{Mo}_{2.3}$	Annealed (300 °C, 30 min)	0.72	0.42

Recent SAMR Measurements

A.Zhukov, et.al. J.Magn. Magn. Mater., 383 (2015) 232–236

Comparison of hysteresis loops and GMI effect in Co and Fe rich microwires

Co-rich

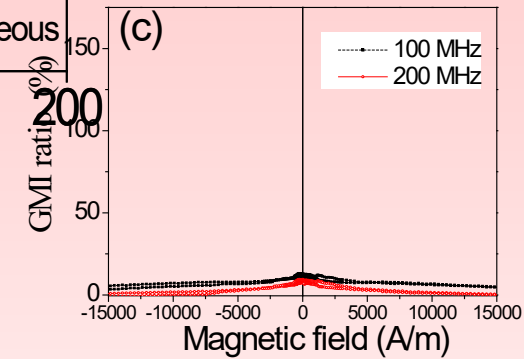


$\lambda \approx 0$

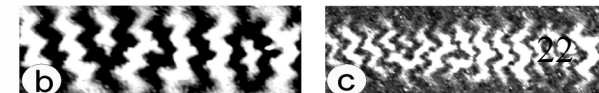
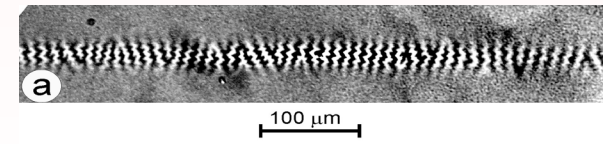
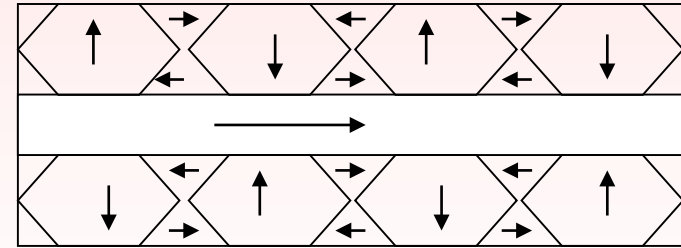
**High GMI and magnetic bistability
be realized in the same sample!**

We can also assume that outer domain shall of the annealed Co-rich microwire exhibiting both fast DW propagation and GMI effect has high circumferential magnetic permeability. This assumption is deduced by much higher GMI ratio of annealed Co-rich microwires as-compared with Fe-rich amorphous microwires.

Fe-rich



$\lambda > 0$

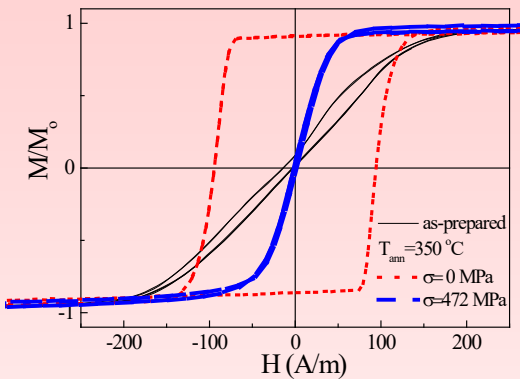
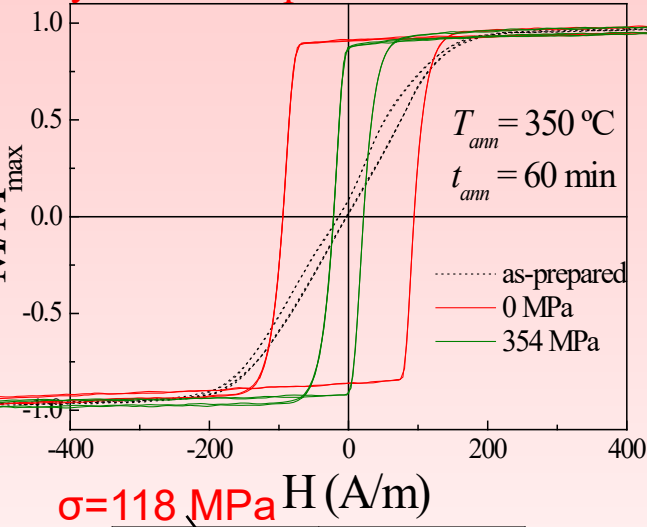


Induced anisotropy Stress-annealing

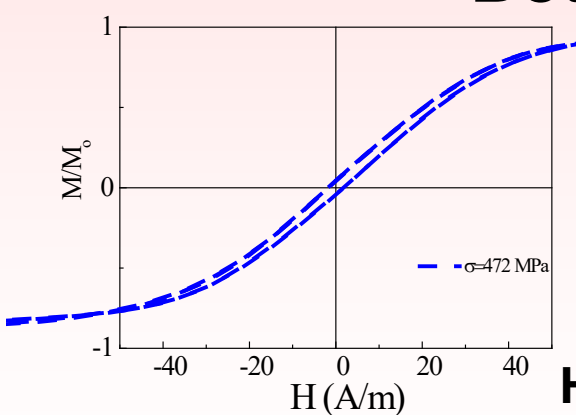
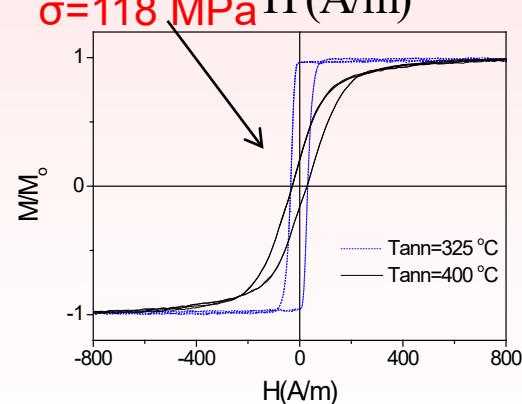
Fe_{3.6}Co_{69.2}Ni₁B_{12.5}Si₁₁Mo_{1.5}C_{1.2}

Co-rich microwires

Hysteresis loops of studied Co-rich microwires stress-annealed at different conditions.



comparison of hysteresis loops of as-prepared, annealed at $T_{\text{ann}} = 350 \text{ }^{\circ}\text{C}$ and stress-annealed at $T_{\text{ann}} = 350 \text{ }^{\circ}\text{C}$ and $\sigma = 472 \text{ MPa}$ microwires.



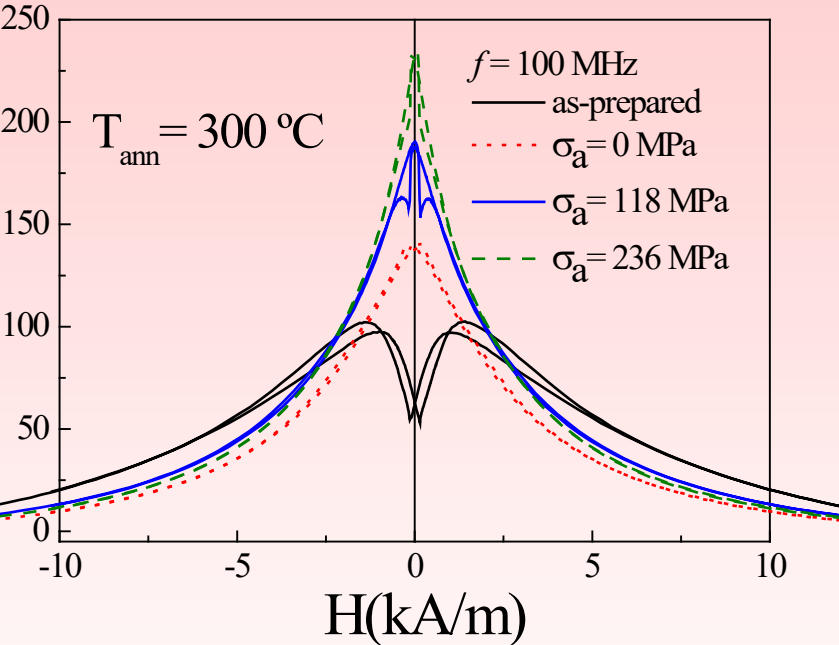
Better magnetic softness

$H_c \approx 2 \text{ A/m}$

At high enough T_{ann} or σ a transverse anisotropy can be induced

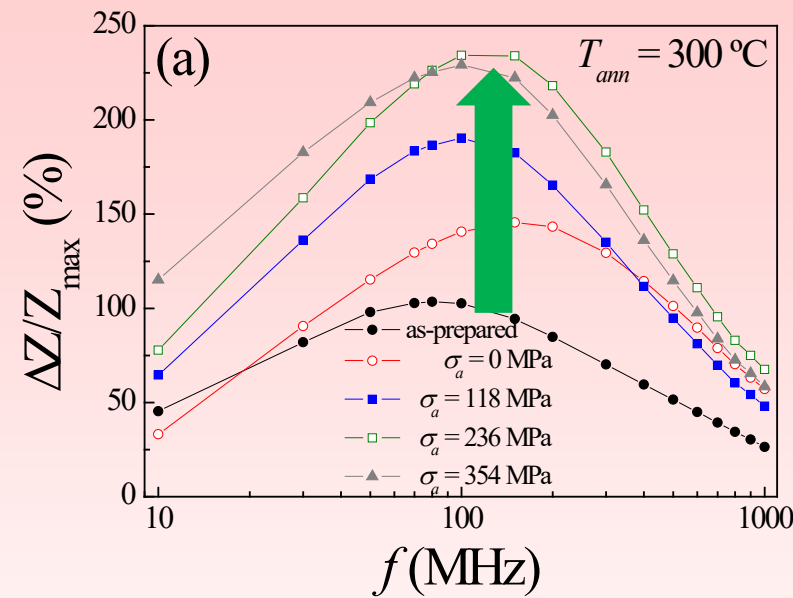
Stress-annealing

$\Delta Z/Z(H)$ dependences of as-prepared and stress-annealed at $T_{ann} = 300$ °C samples at different σ_a measured at 100 MHz.



Co-rich microwires

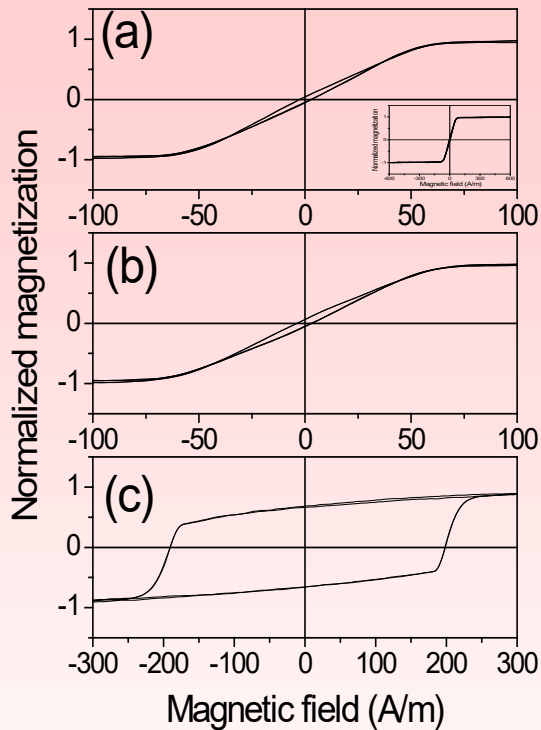
$\Delta Z/Z_{max}(f)$ evaluated for different σ_a -values for the samples annealed at $T_{ann} = 300$ °C



SA allows more remarkable GMI improvement

Origin of MI rising: Right magnetic anisotropy in thin surface layer?

Tailoring by Joule heating

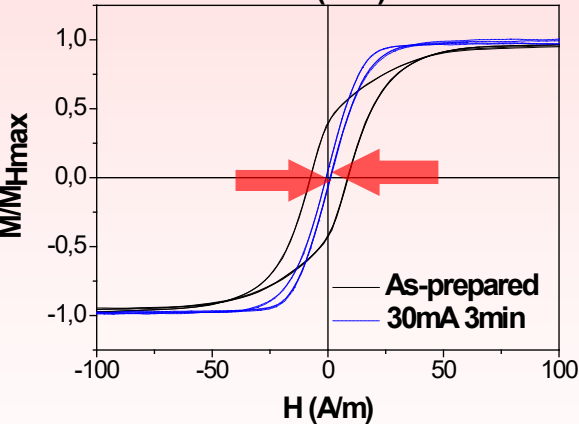
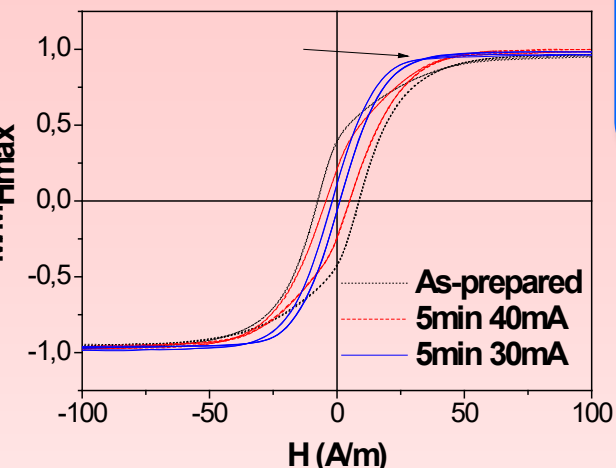


Hysteresis loops of as-prepared (a), Joule heated at 30 mA for 40 min (b) and annealed at conventional furnace at 300° C for 60 min studied microwire.

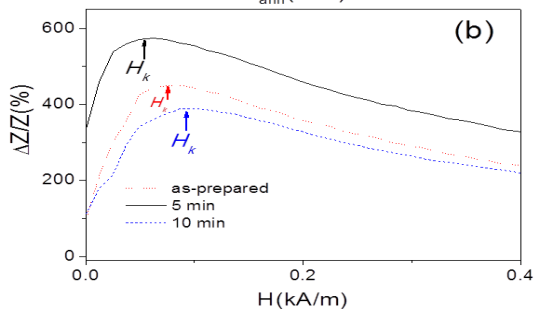
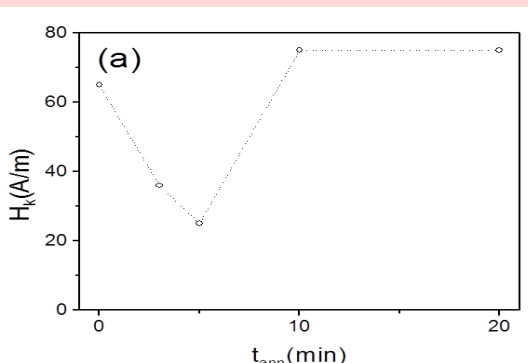
Looks that Joule heating prevents magnetic hardening reported for Co-based microwires after conventional annealing

Induced anisotropy Tailoring by Joule heating

$H_k=25\text{ A/m}$



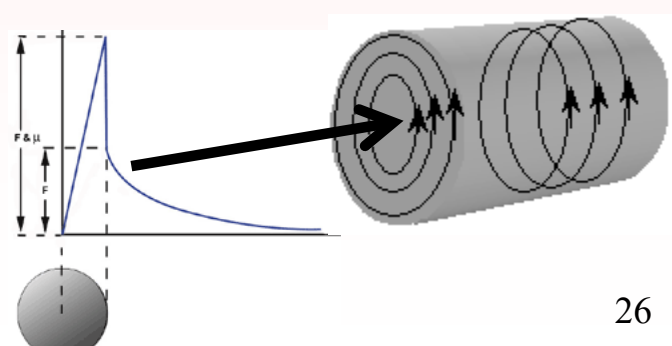
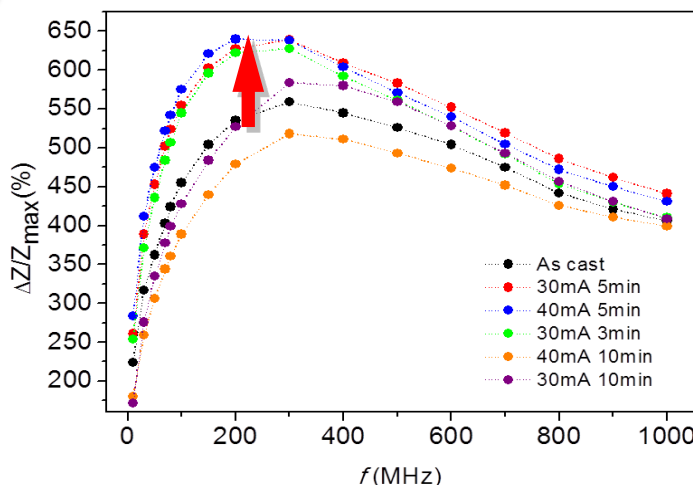
- Internal stresses relaxation
- Induced magnetic anisotropy



$H_c=2 \text{ A/m}$

Circular magnetic field by current:

GMI ratio up to 650%



Looking for the highest GMI effect

Hysteresis loops of as-prepared (a) and annealed at $T_{\text{ann}} = 275 \text{ }^{\circ}\text{C}$ (b), $T_{\text{ann}} = 300 \text{ }^{\circ}\text{C}$ (c) and $T_{\text{ann}} = 350 \text{ }^{\circ}\text{C}$ (d) $\text{Co}_{72}\text{Fe}_{4}\text{B}_{13}\text{Si}_{11}$ sample ($40 \mu\text{m}$).

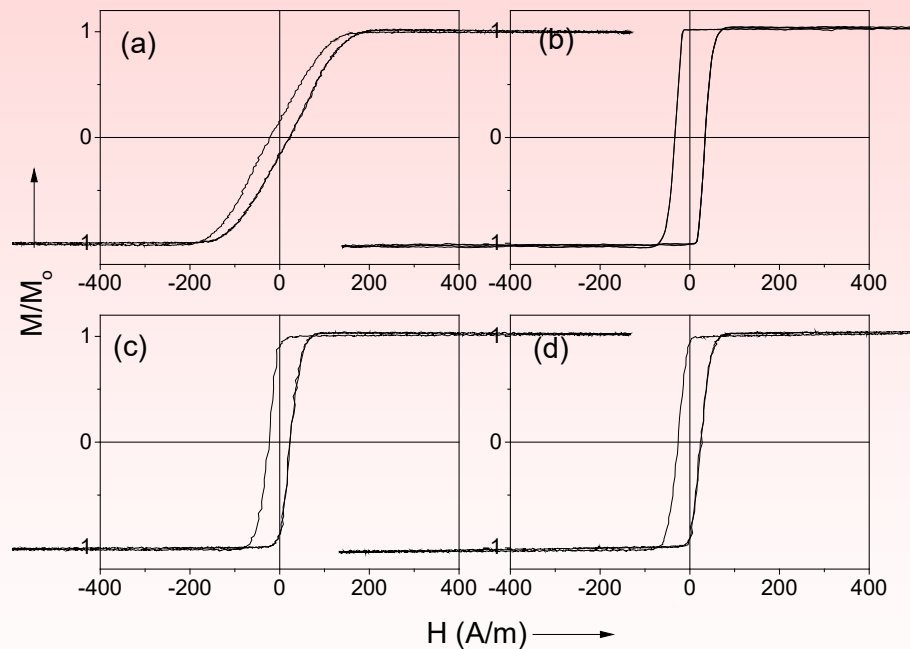
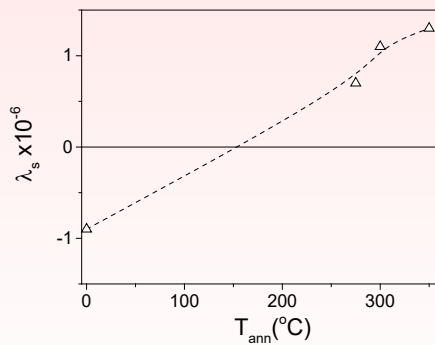


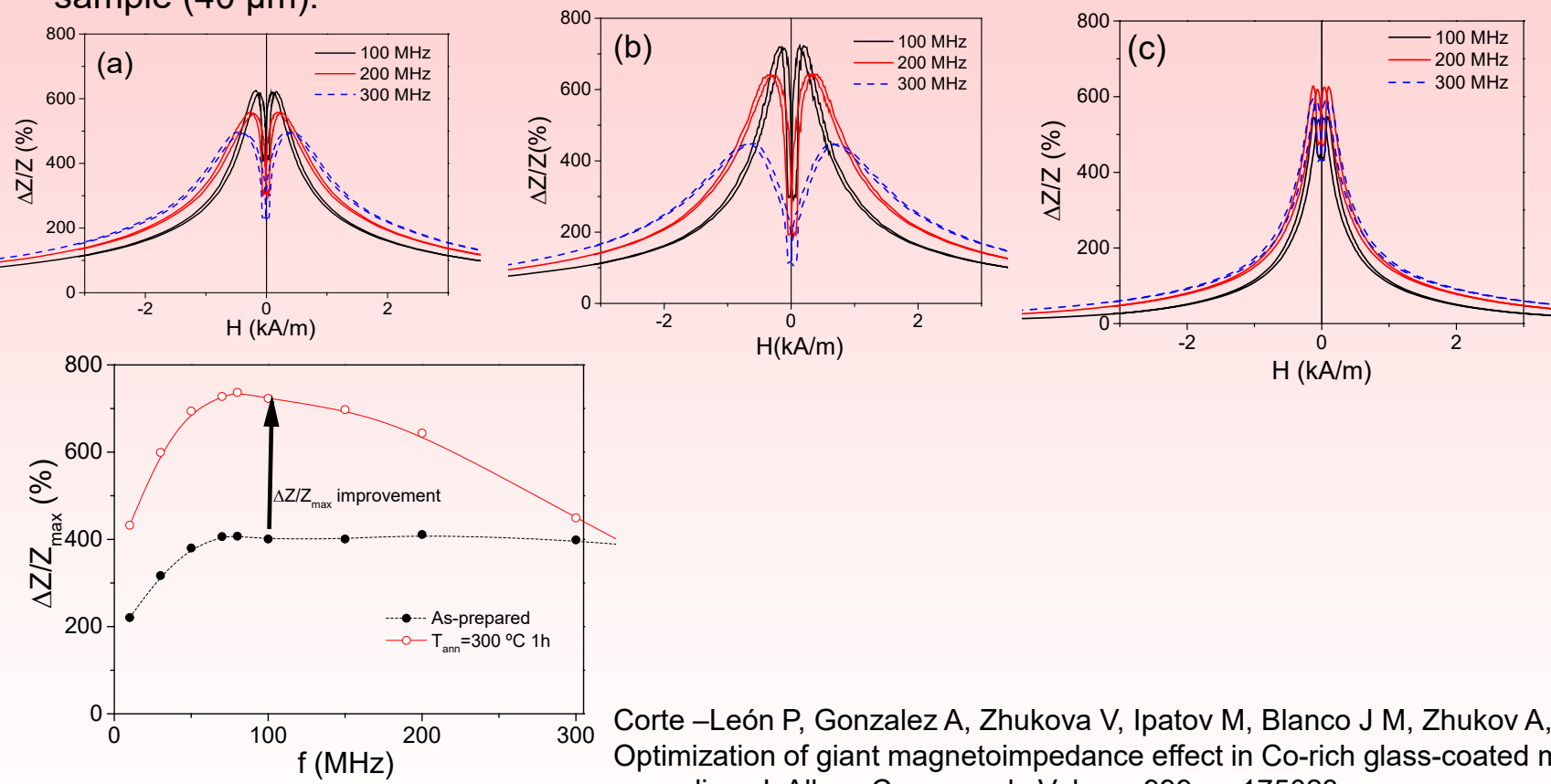
Table 1. The magnetostriction coefficient of as-prepared and annealed $\text{Co}_{72}\text{Fe}_{4}\text{B}_{13}\text{Si}_{11}$ microwires.

Sample	$\lambda_s (\times 10^{-6})$
As-prepared	-9
Annealed at $275 \text{ }^{\circ}\text{C}$	+7
Annealed at $300 \text{ }^{\circ}\text{C}$	+11
Annealed at $350 \text{ }^{\circ}\text{C}$	+13



Looking for the highest GMI effect

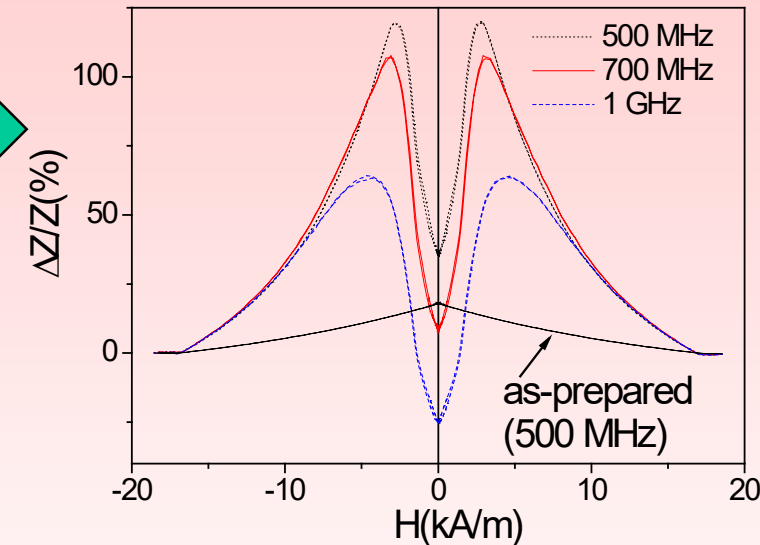
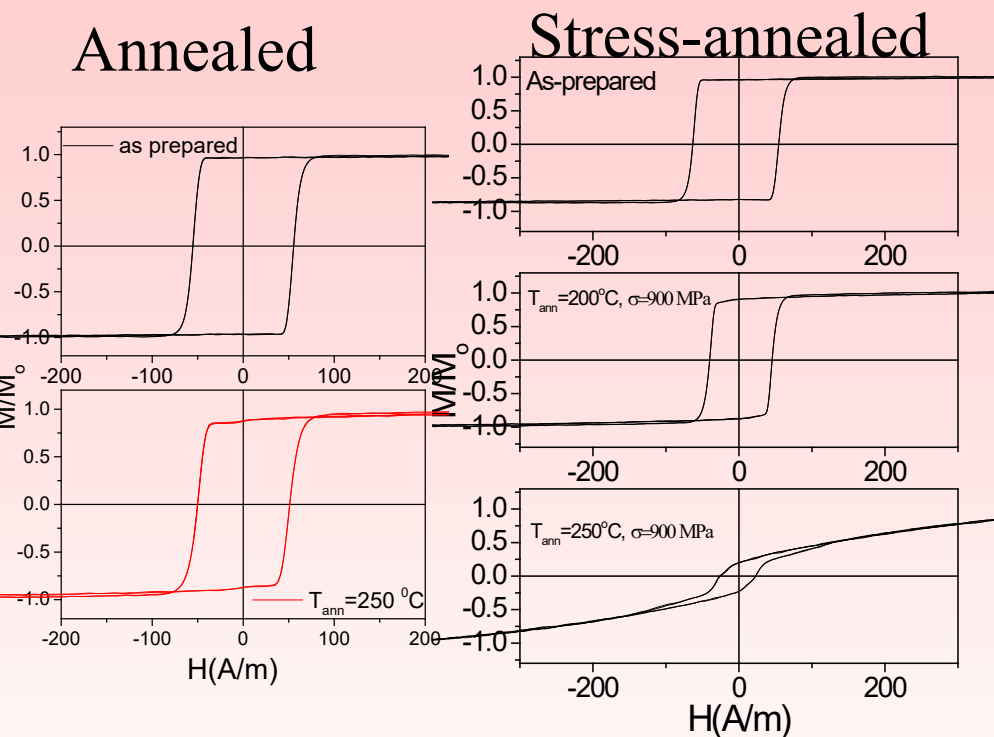
GMI of annealed at $T_{\text{ann}} = 350 \text{ }^{\circ}\text{C}$ (a); $T_{\text{ann}} = 300 \text{ }^{\circ}\text{C}$ (b) $T_{\text{ann}} = 275 \text{ }^{\circ}\text{C}$ (c) Co₇₂Fe₄B₁₃Si₁₁ sample (40 μm).



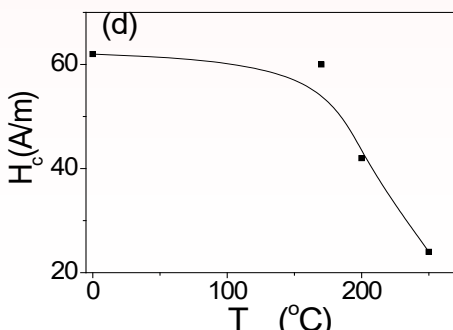
Corte –León P, Gonzalez A, Zhukova V, Ipatov M, Blanco J M, Zhukov A, 2024,
Optimization of giant magnetoimpedance effect in Co-rich glass-coated microwires by
annealing, J. Alloys Compound, Volume 999, p. 175023

Stress-annealing induced Anisotropy and GMI in Fe-rich microwires

Annealed



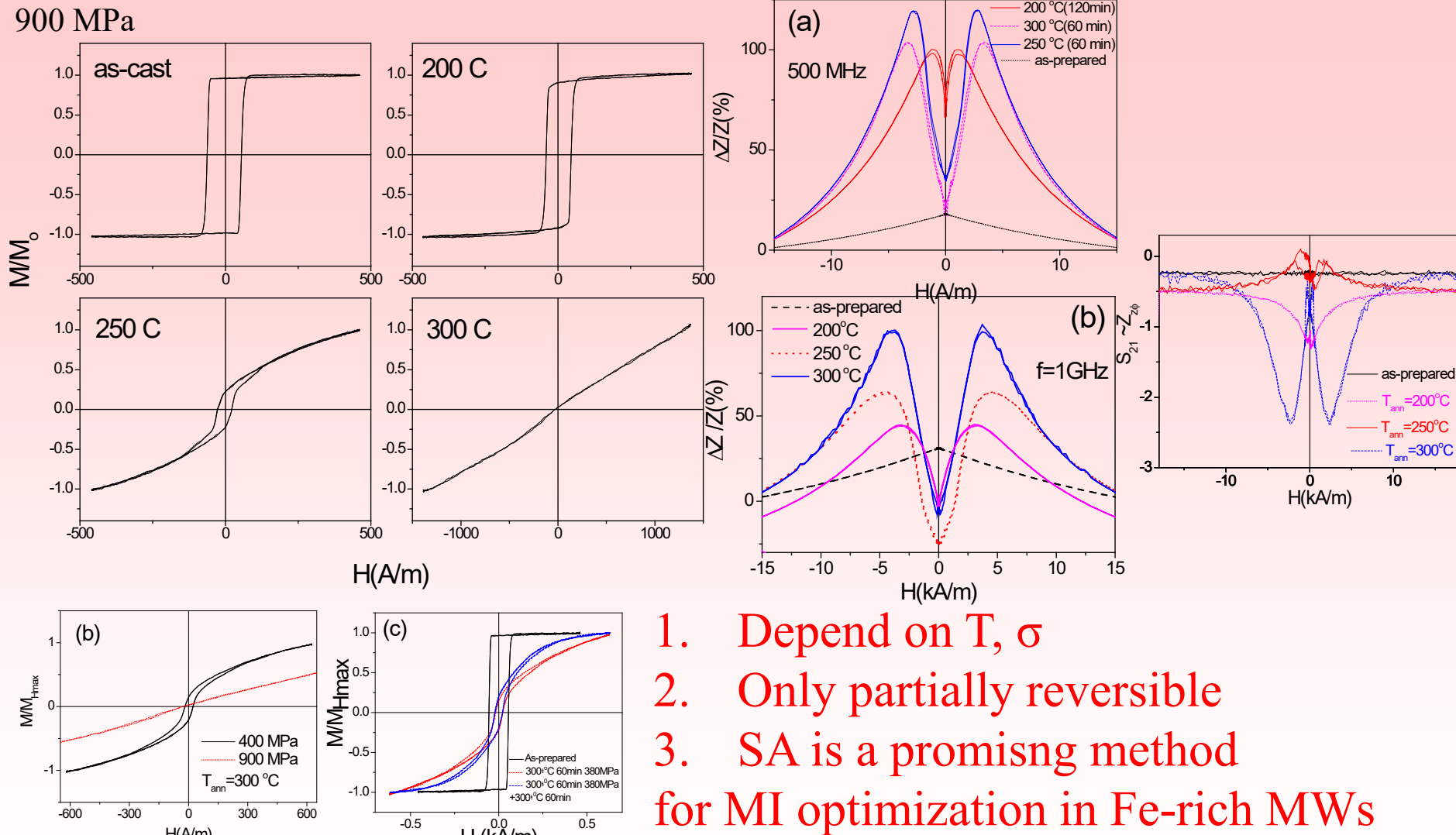
- i) considerable transversal magnetic anisotropy and magnetic softening
- ii) existence of maximum on $\Delta Z/Z(H)$ dependences reflects transversal magnetic anisotropy of stress-annealed



V. Zhukova, M. Ipatov, A. Talaat, J. M. Blanco, M. Churyukanova and A. Zhukov, *J. Alloys Compound (accepted, 2016)* <http://dx.doi.org/10.1016/j.jallcom.2016.10.178>; V. Zhukova, J.M. Blanco, M. Ipatov, J. Gonzalez, M. Churyukanova A., Zhukov, *Scripta Materialia* Vol. 142, 1 January 2018, 10–14, doi: 0.1016/j.scriptamat.2017.08.014

Ways to improve GMI in Fe-rich microwires

Effect of stress annealing on GMI of Fe -rich microwires



1. Depend on T, σ
2. Only partially reversible
3. SA is a promising method for MI optimization in Fe-rich MWs

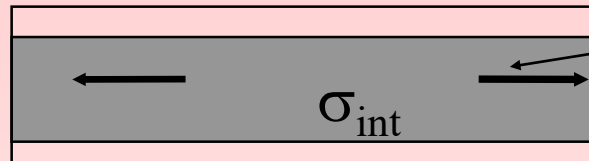
V. Zhukova, M. Ipatov, A. Talaat, J. M. Blanco, M.Churyukanova, S. Taskaev and A. Zhukov, "Effect of stress-induced anisotropy on high frequency magnetoimpedance effect of Fe and Co-rich glass-coated microwires" J. Alloys Compound. 735 (2018) 1818-1825

V. Zhukova, J. M. Blanco, M. Ipatov, M.Churyukanova, S. Taskaev and A. Zhukov, Tailoring of magnetoimpedance effect and magnetic softness of Fe-rich glass-coated microwires by stress- annealing, Sci. Reports 8 (2018) 3202

Origin of stress-induced anisotropy

Amorphous microwires

As-prepared microwire



Internal stresses with mainly axial component

Stress



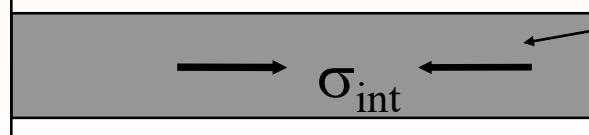
Induction of magnetic anisotropy during stress annealing

Slow Cooling under stress



Stress relaxation in the stressed state at room temperature

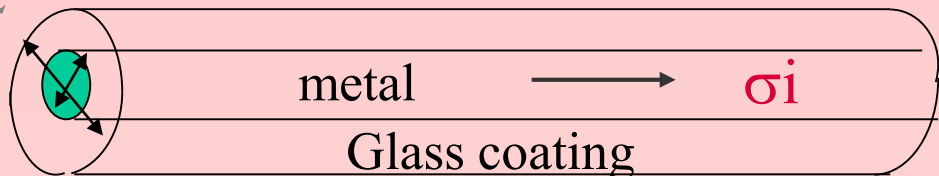
Elimination of the applied stress



Induction of the compressive stresses at room-temperature (so-called “Back stresses”)

31

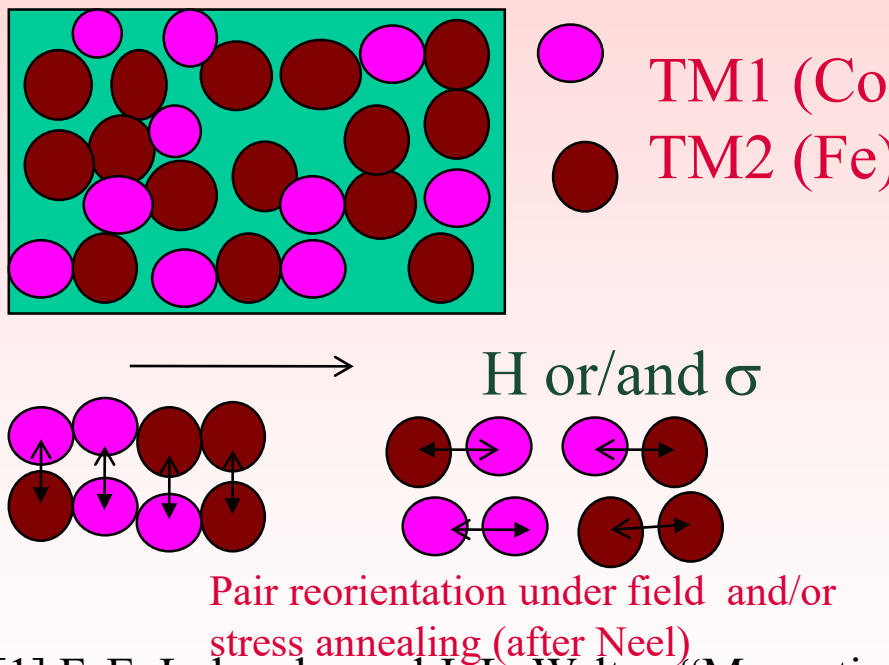
Origin of induced anisotropy 2



Possible origin:

-Stress induced anisotropy (stress from glass coating)?

Origin: Pair ordering usually considered



[1] F. E. Luborsky and J. L. Walter, "Magnetic Anneal Anisotropy in Amorphous Alloys", *IEEE Trans.Magn.* Vol.13 (2), pp.953-956, 1977.

[2] J. Haimovich, T. Jagielinski, and T. Egami, "Magnetic and structural effects of anelastic deformation of an amorphous alloy", *J. Appl. Phys.* Vol. 57, pp. 3581-3583, 1985.

Possible origin 3:

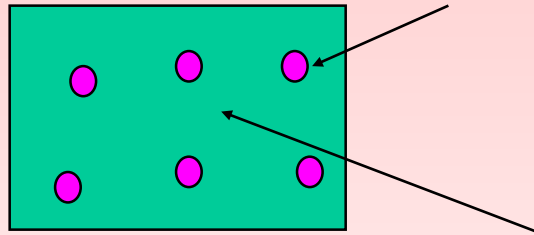
The topological short range ordering (also known as structural anisotropy) can play an important role. This involves the angular distribution of the atomic bonds and small anisotropic structural rearrangements at temperature near the glass transition temperature

Magnetostriction

Nanocrystallization. Method of improvement of magnetic softness and GMI

Structure evolution after annealing

$\text{Cu } FCC$

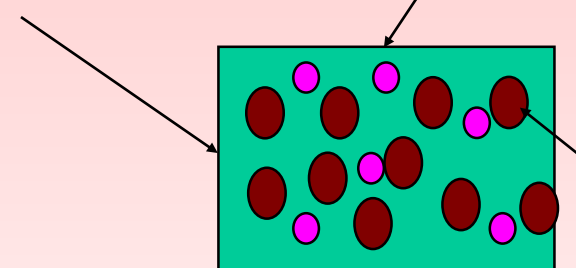


Amorphous phase

$T_{\text{ann}} < T_x$

Amorphous matrix

$\text{Cu } FCC$



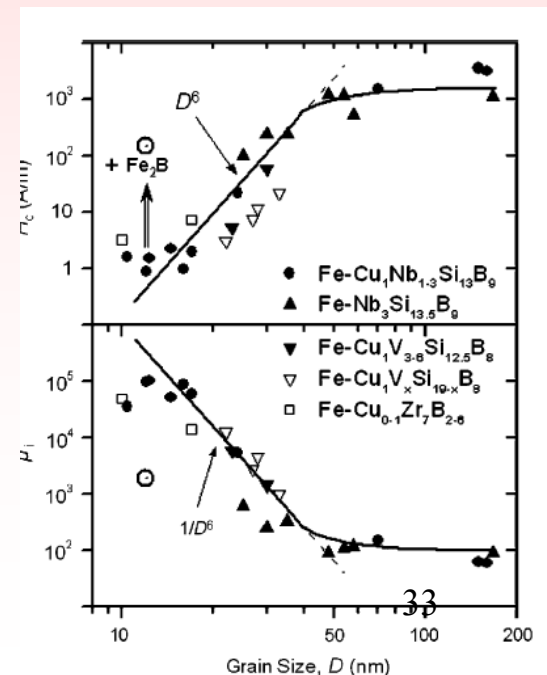
$\text{Fe } BCC$

1. λ_s Amorphous matrix with $\lambda_s > 0$



Nanocrystals with $\lambda_s < 0$

2. Grain size

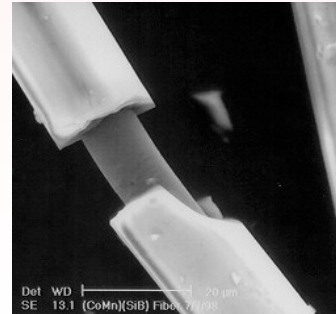
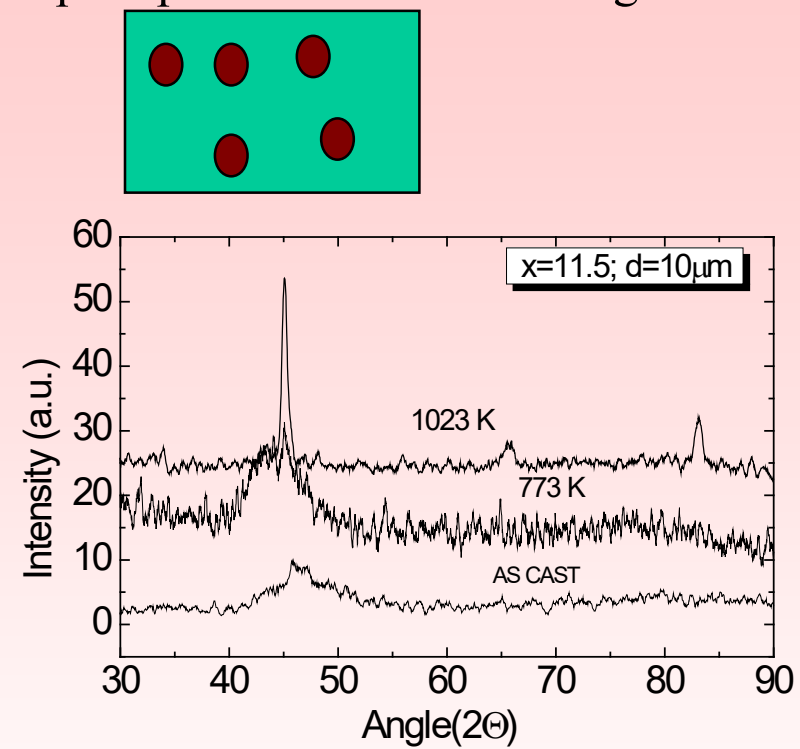
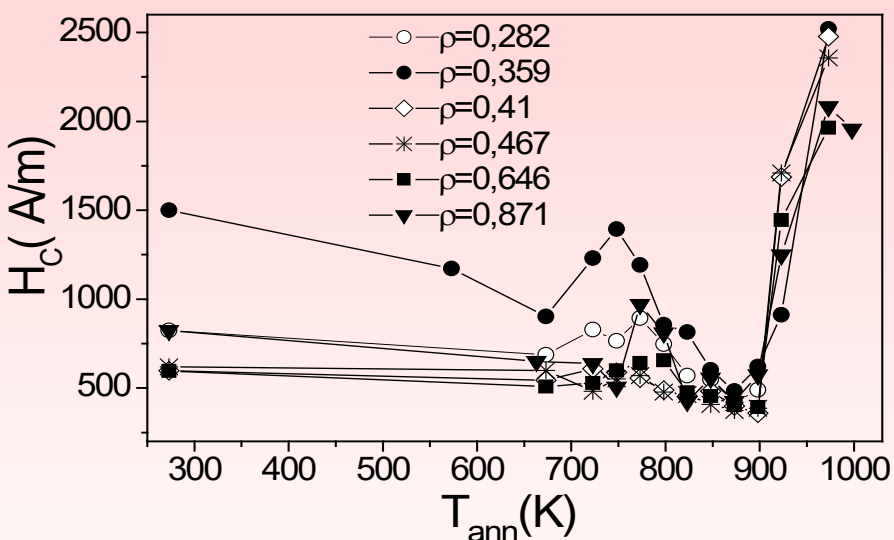


Magnetostriction

Effect of nanocrystallization on magnetic softness of $\text{Fe}_{71.8}\text{Cu}_1\text{Nb}_{3.1}\text{Si}_{15}\text{B}_{9.1}$ microwires

Cu and Nb additions result in nanocrystalites precipitation after annealing :

- High concentration of small grains
- Nanosize of crytsalites 10-20 nm
- Amorphous matrix



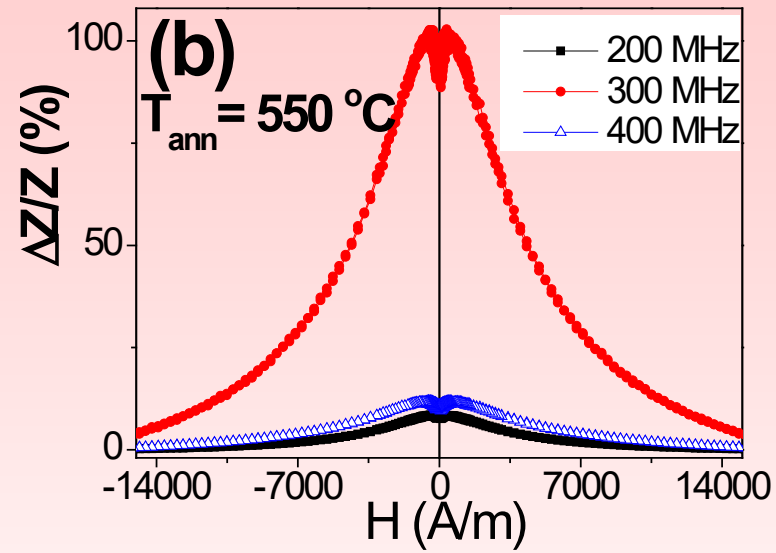
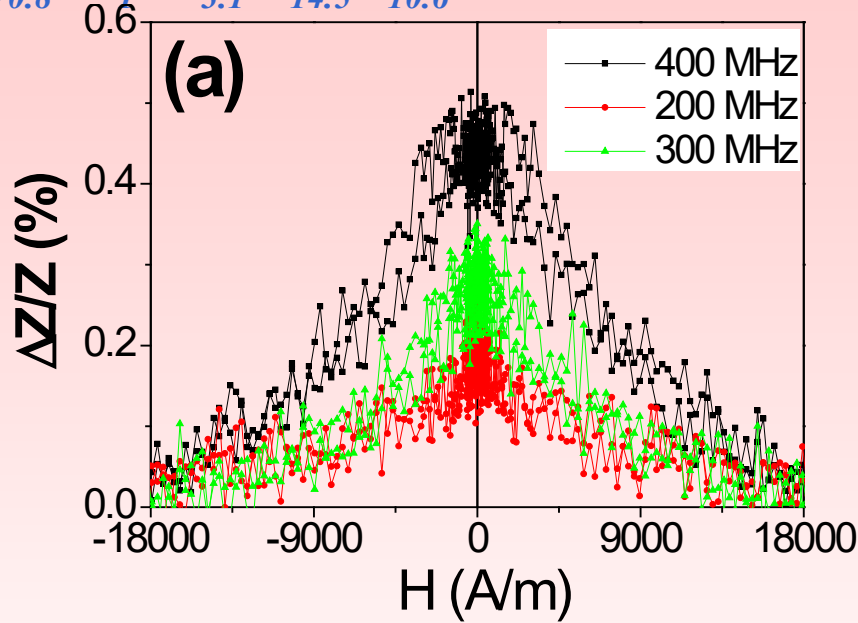
$\rho = d/D$; d – metallic nucleus diameter and D – total diameter

Magnetostriction

Effect of nanocrystallization on GMI of $\text{Fe}_{71.8}\text{Cu}_1\text{Nb}_{3.1}\text{Si}_{15}\text{B}_{9.1}$ microwires

$\Delta Z/Z$ (H) dependences in amorphous and nanocrystalline

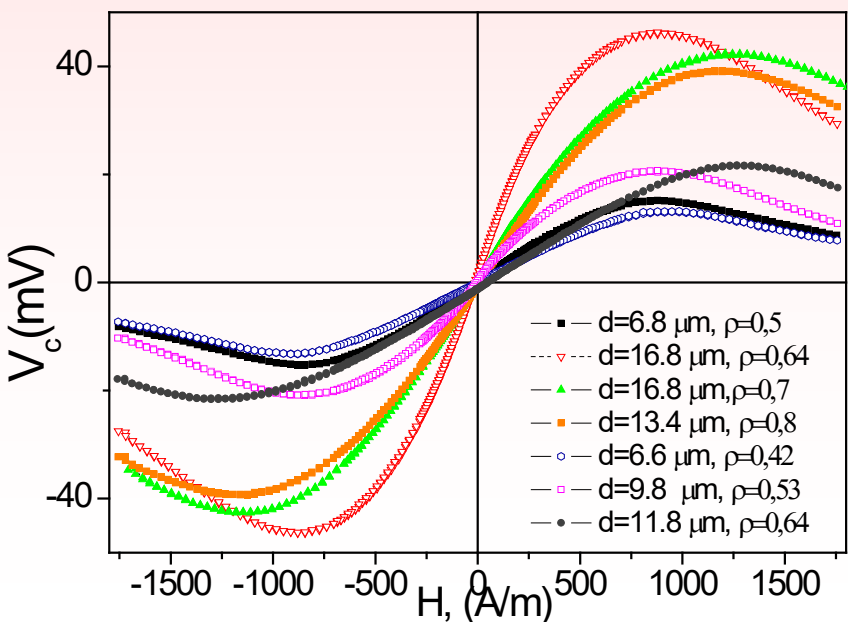
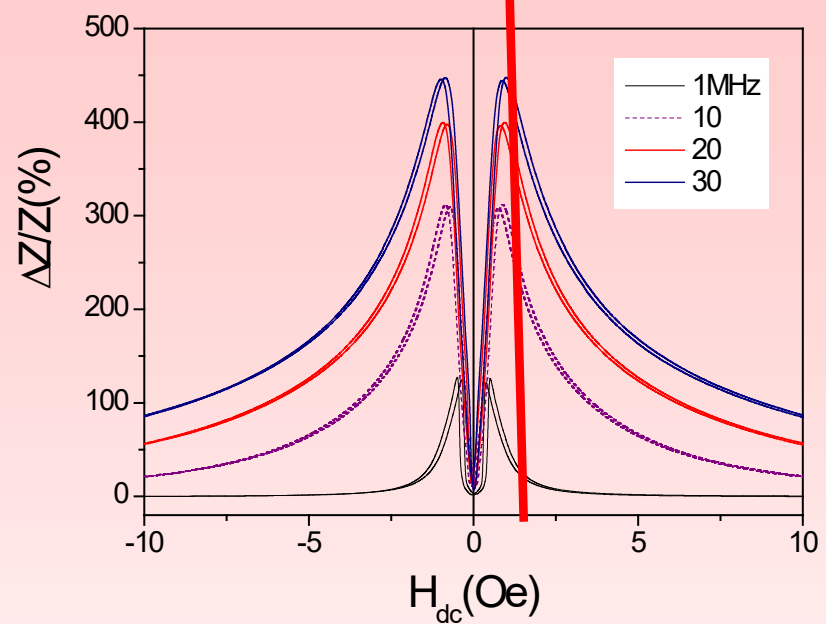
$\text{Fe}_{70.8}\text{Cu}_1\text{Nb}_{3.1}\text{Si}_{14.5}\text{B}_{10.6}$ microwires



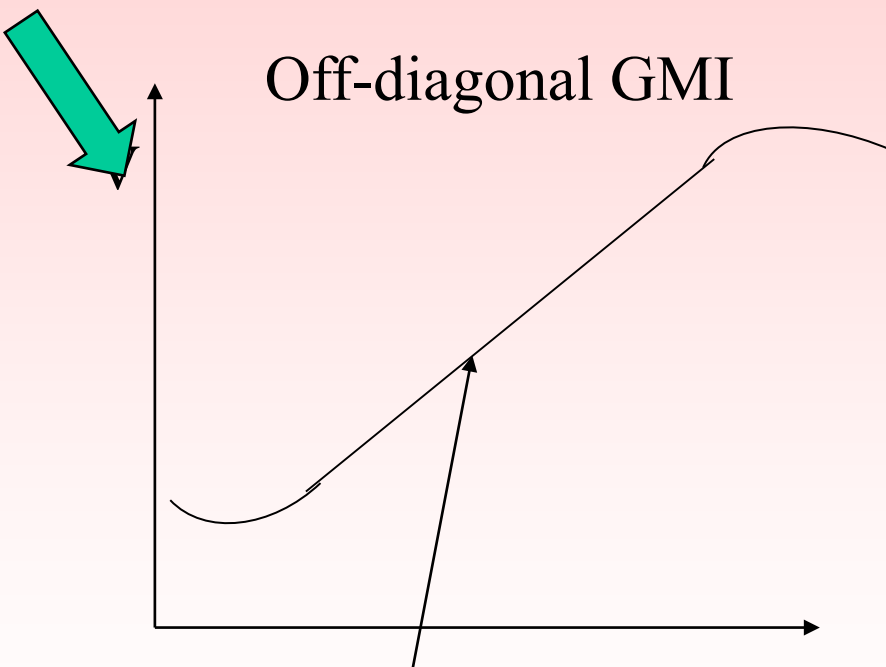
$\Delta Z/Z$ (H) in as-prepared (a), and annealed at 550°C (b)

$\text{Fe}_{70.8}\text{Cu}_1\text{Nb}_{3.1}\text{Si}_{14.5}\text{B}_{10.6}$ microwire with $\rho = 0.65$.

Requests for applications - linearity



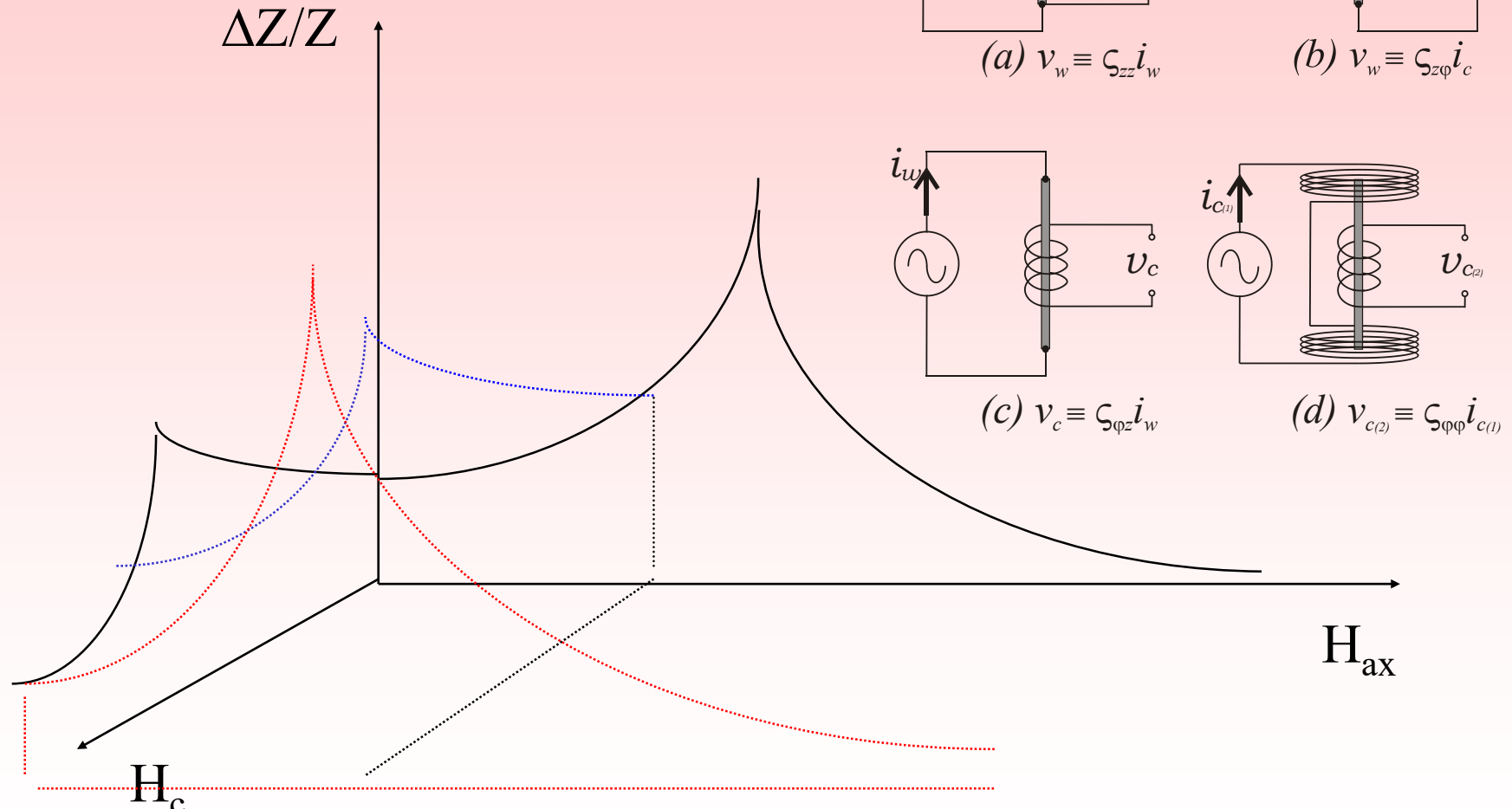
GMI effect, high sensitivity
450%/Oe: 1 Oe = 0,1 mT)
1% MI change $\approx 0,0002$ mT
But non-linear



Good linearity on $V(H)$,
Extended range of linear behaviour
absence of hysteresis

Tensor character of GMI

Schematic representation

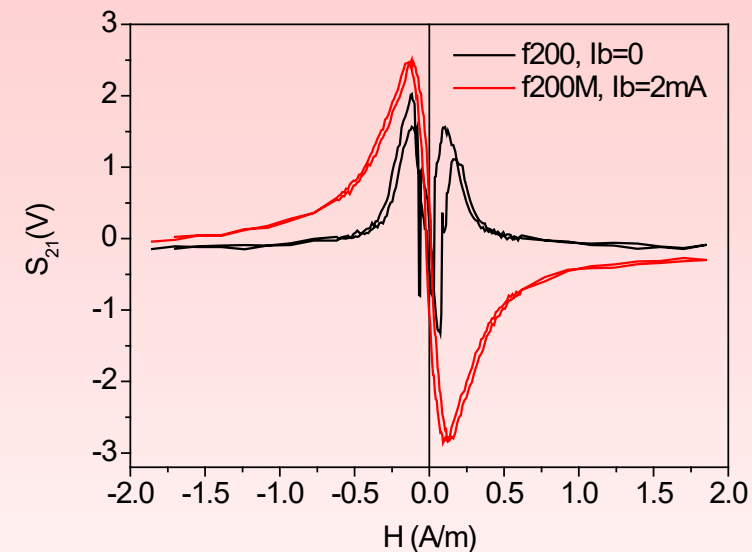


N. A. Usov, A. S. Antonov and A. N. Lagar'kov J Magn Magn Mat **185**, 159 (1998).

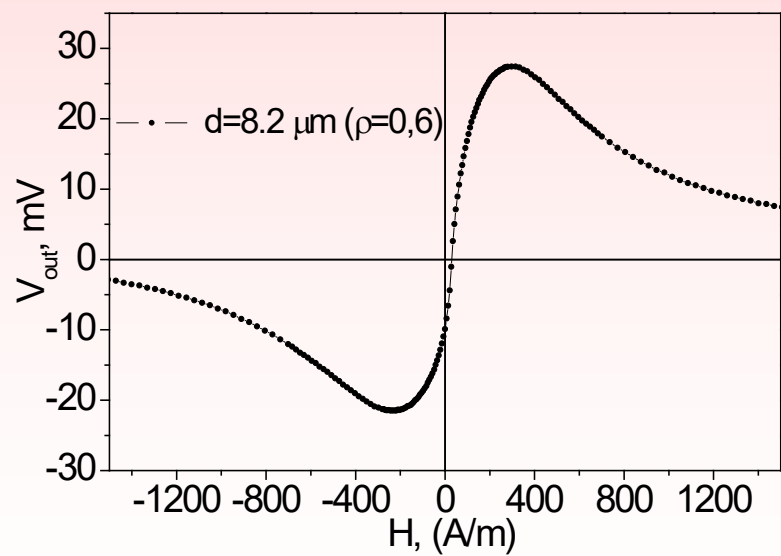
P. Aragoneses, A. Zhukov, J. Gonzalez, J.M. Blanco and L. Dominguez, Sensors and Actuators A, ³⁷ 81/1-3 (2000) 86-90

Off-diagonal GMI effect

Effect of bias current on magnetic field dependence of S_{21} parameter measured at 200 MHz in $\text{Co}_{67.71}\text{Fe}_{4.28}\text{Ni}_{1.57}\text{Si}_{11.24}\text{B}_{12.4}\text{Mo}_{1.25}\text{C}_{1.55}$ microwires



$V_{\text{out}}(H)$ response of $\text{Co}_{67.1}\text{Fe}_{3.8}\text{Ni}_{1.4}\text{Si}_{14.5}\text{B}_{11.5}\text{Mo}_{1.7}$ microwires measured in pulsed excitation



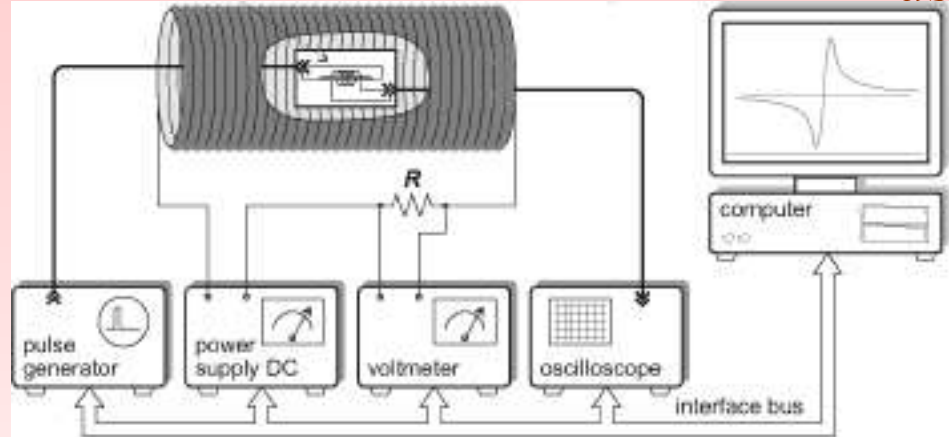
M. Ipatov, V. Zhukova, A. Zhukov, J. Gonzalez, and A. Zvezdin, "Low-field hysteresis in the magnetoimpedance of amorphous microwires", Phys. Rev.B vol. 81, p. 134421, 2010

M. Ipatov, V. Zhukova, J. Gonzalez and A. Zhukov, "Magnetoimpedance sensitive to DC bias current in amorphous microwires" Appl. Phys. Lett vol. 97, p. 252507, 2010.

GMI effect

Linearity: Pulsed GMI

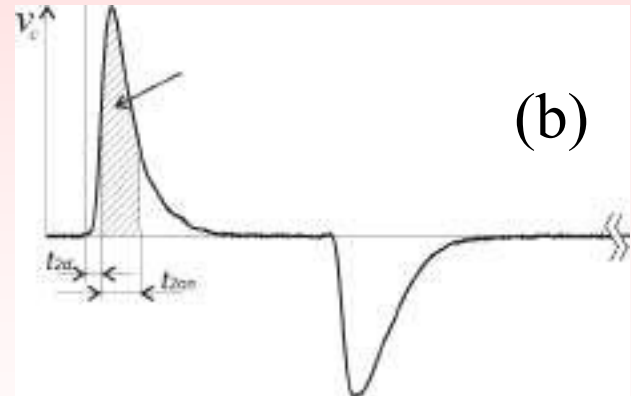
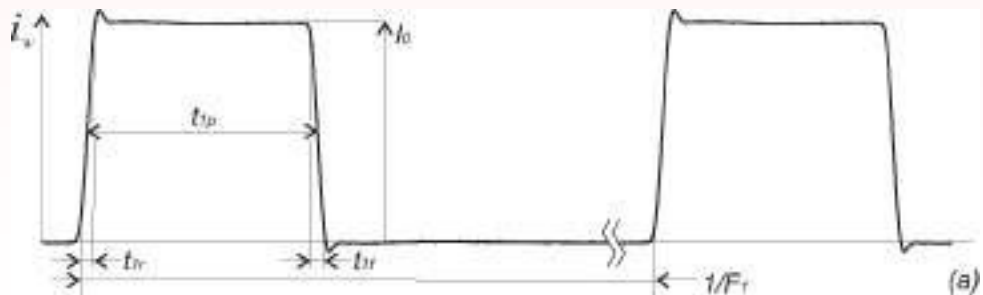
Pulsed GMI: linear field dependence,
useful for circuitry, low noise



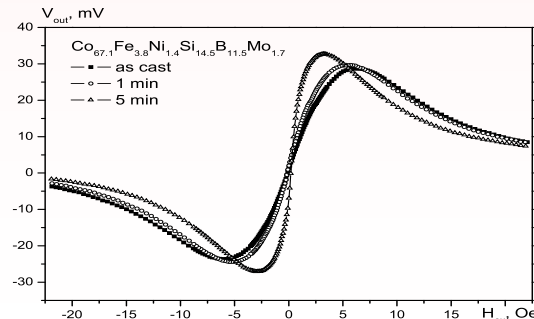
Experimental setup
for MI investigation
with pulse excitation

Excitation current pulse in the wire (a) and
voltage induced in the pickup coil (b)

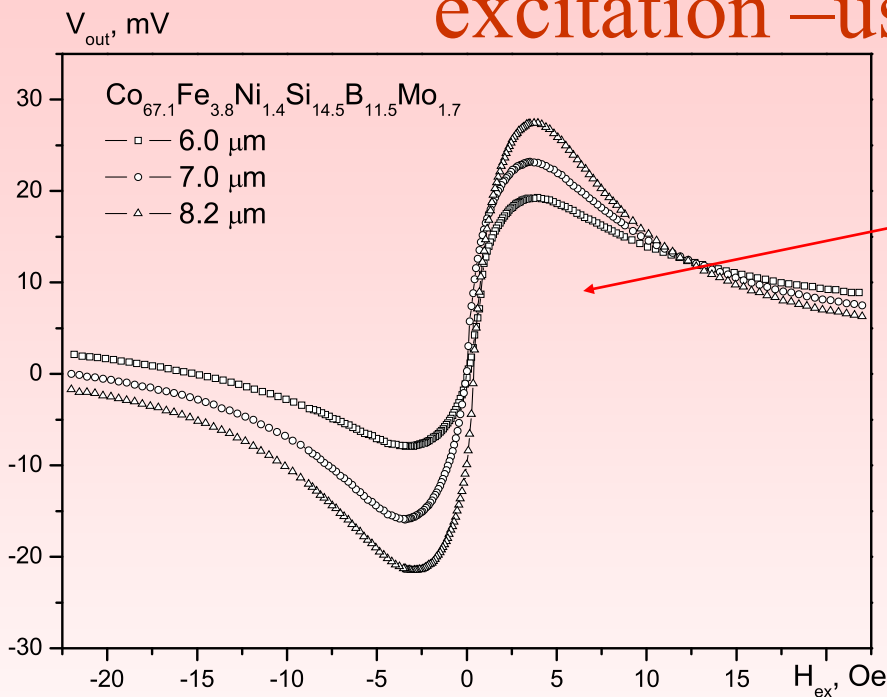
(a)



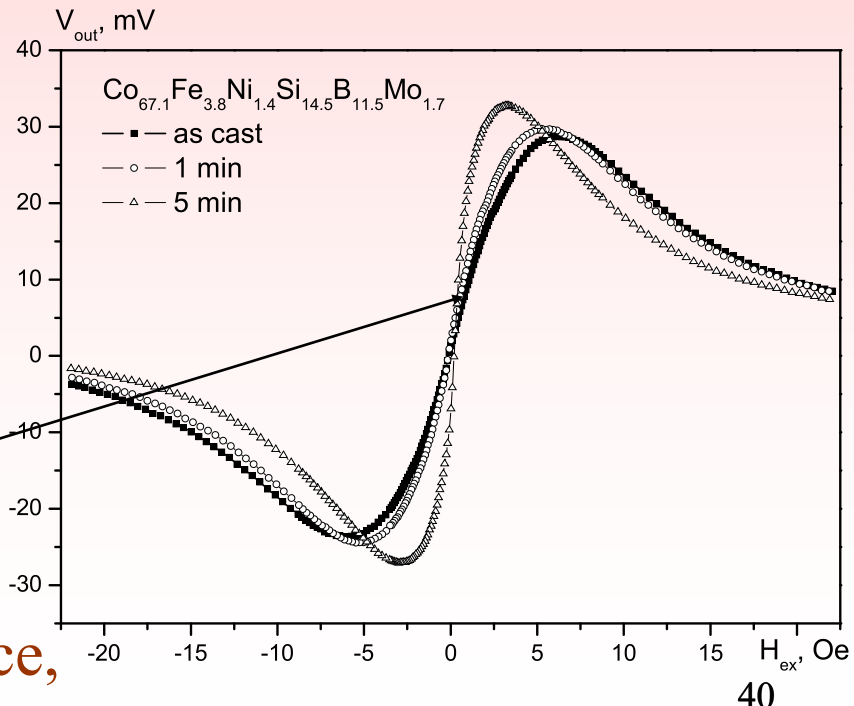
(b)



Off-diagonal GMI of nearly zero magnetostriction $\text{Co}_{67.1}\text{Fe}_{3.8}\text{Ni}_{1.4}\text{Si}_{14.5}\text{B}_{11.5}\text{Mo}_{1.7}$ microwires (pulsed excitation –used in practice)



Asymmetrical shape,
Almost linear region
Linear region and maximum
Position depends on geometry

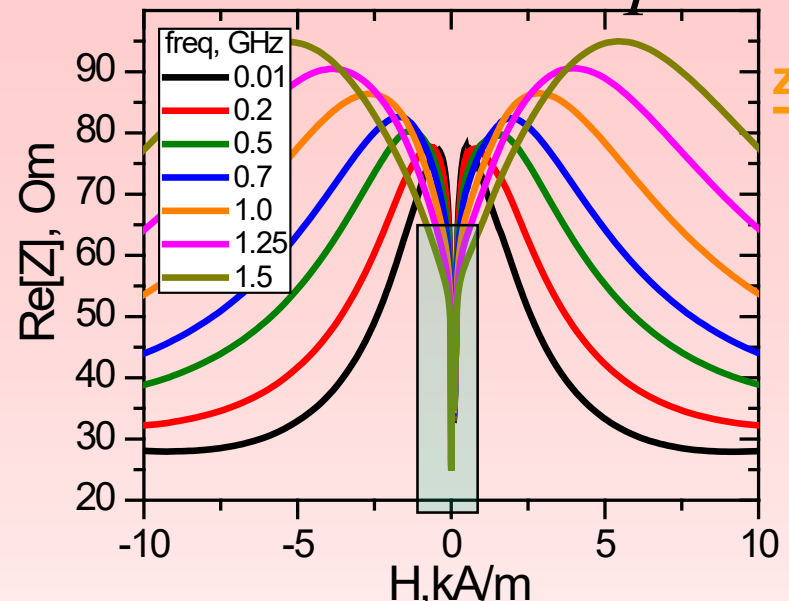


Tailoring of GMI by heat treatment

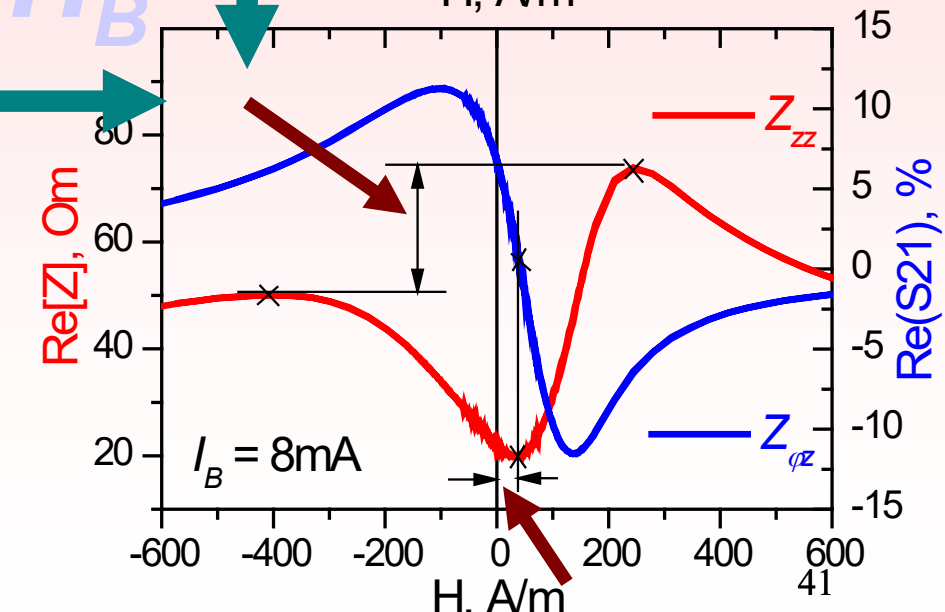
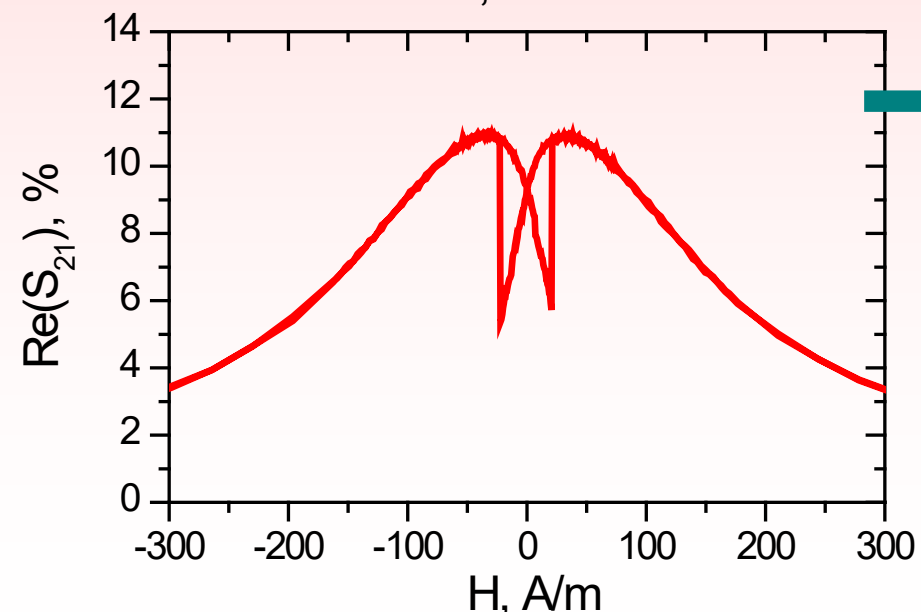
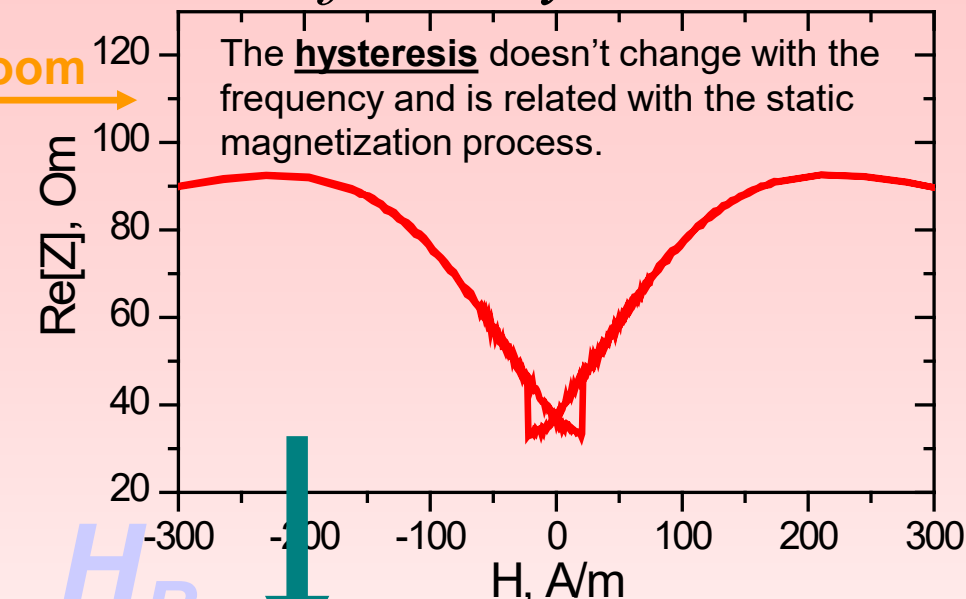
Pulsed GMI: linear field dependence,
useful for circuitry, low noise

GMI effect

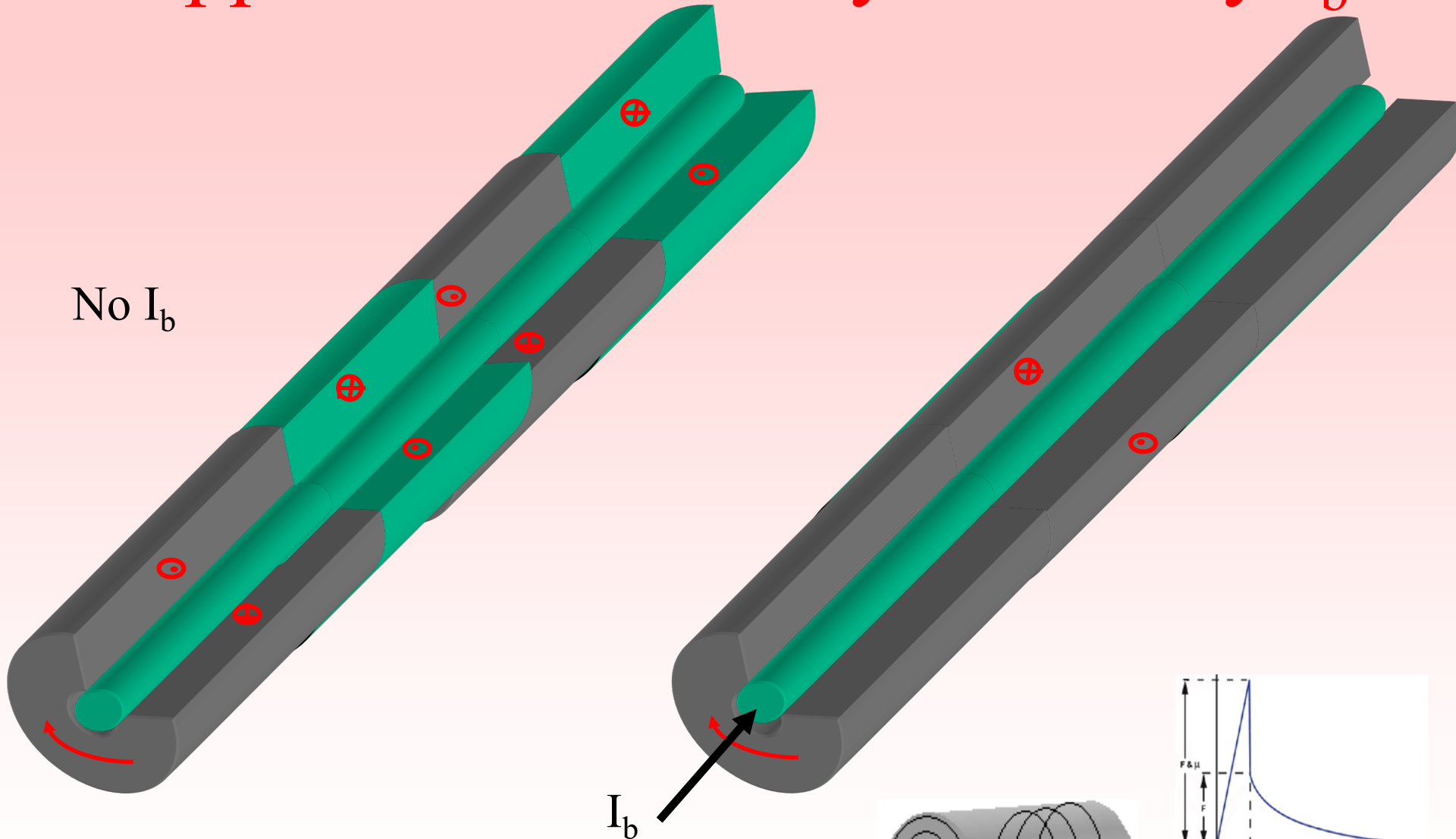
Considerable problem – low field hysteresis



High frequency GMI effect



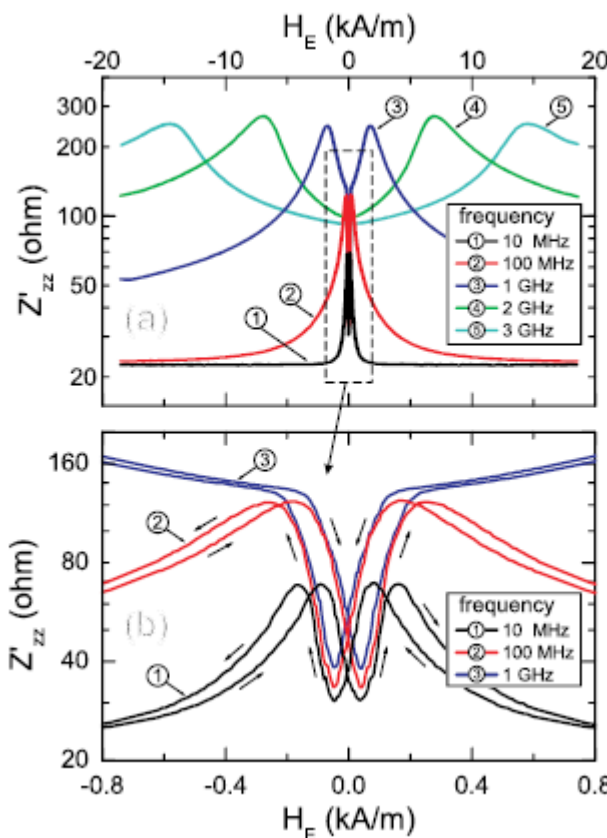
Suppresion of GMI hysteresis by I_b



Circular magnetic field by current
suppresses bamboo-like domain
structure responsible for MI hysteresis

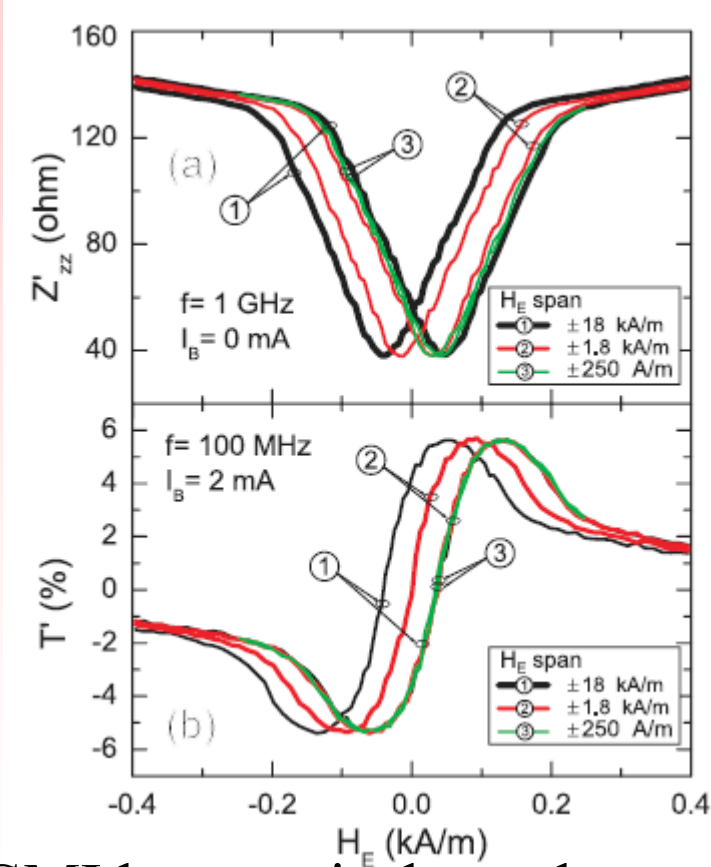
Magnetoimpedance hysteresis in amorphous microwires induced by core–shell interaction

Longitudinal MI measured at different frequencies.



GMI hysteresis persists at all f

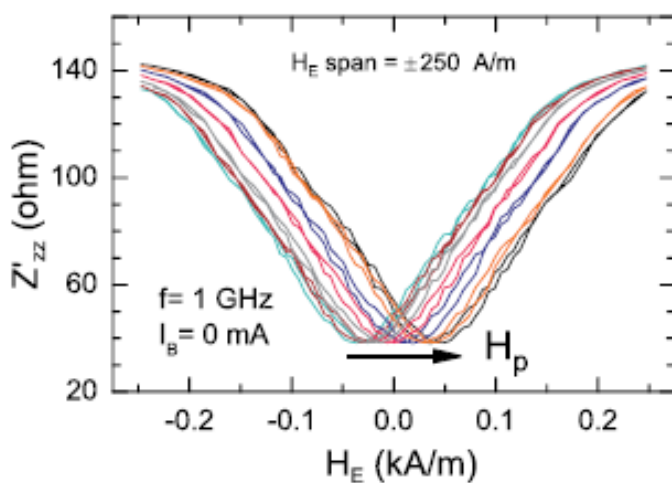
Longitudinal Z_{zz} (a) and off-diagonal $Z \phi z$ (b) MI measured for 3 different magnetic field spans.



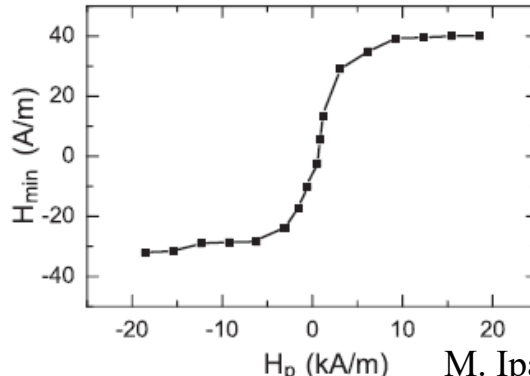
GMI hysteresis depends on magnetic history

Magnetoimpedance hysteresis in amorphous microwires induced by core–shell interaction

Effect of H_p pulse applied before measurements on shift of the longitudinal MI.

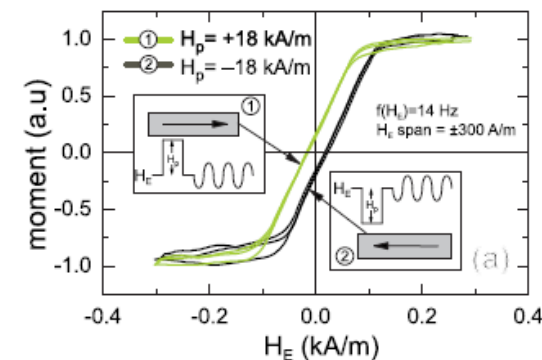


Dependence H_{min} as a function of the applied pulse of magnetic field H_p . Field H_{min} corresponding to the field at which the MI dependence $Z_{zz}(H_E)$ exhibits a minimum

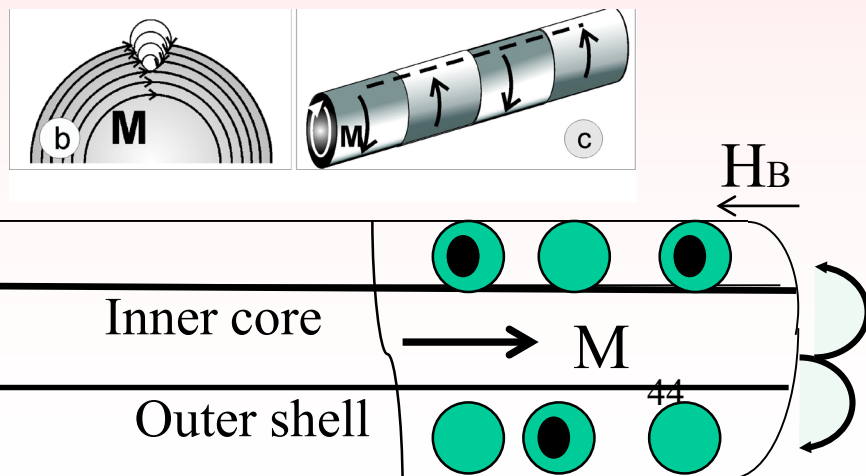


First, pulses H_p of the axial magnetic field H_E with positive or negative amplitudes between 18 and 0.3 kA/m were applied. After each pulse, the MI dependence was measured within a HE span of ± 250 A/m.

Hyst. loop
also depends on
 H_p !



Considering domain structure consisting of an inner core and an outer shells, we supposed that the observed effect of magnetic history of the microwire on the MI arises from the interaction between them (core-shell interaction).



Thin μ wires

Giant Magneto-impedance effect

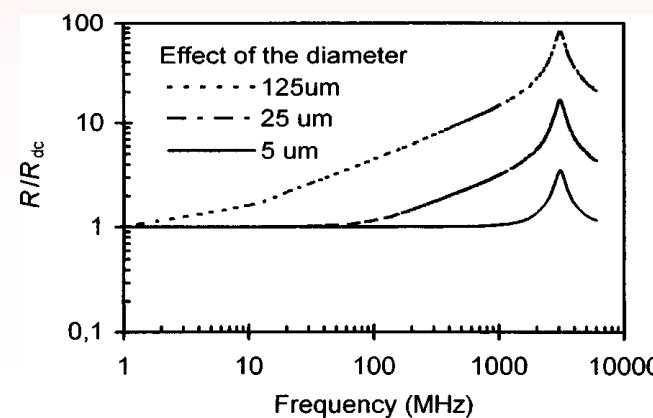
At high frequencies, of the order of GHz, the magnetization rotation is strongly influenced by the gyromagnetic effect. With increasing the frequency the GMI peaks are shifted to static fields where **sample is magnetically saturated**. At this frequency range strong changes of the sample's impedance have been attributed to the ferromagnetic resonance (FMR).

The criteria for determining the frequency regions is probably the ratio of skin depth to transversal dimensions of the sample (δ/a):

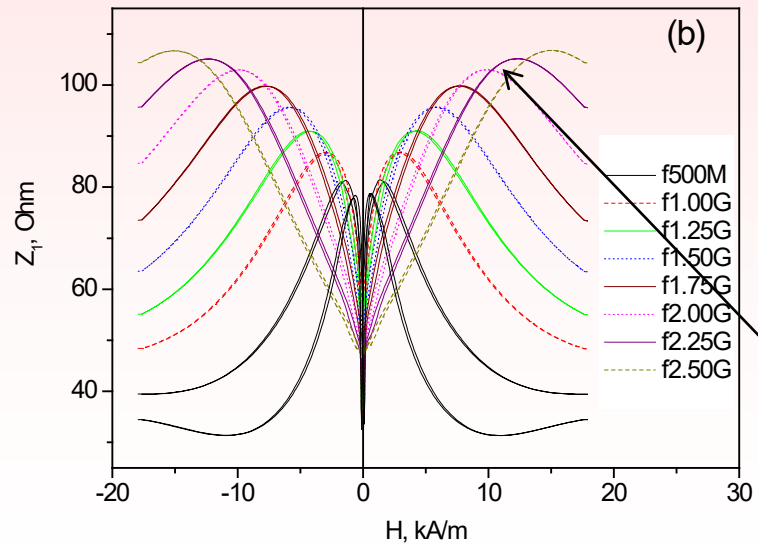
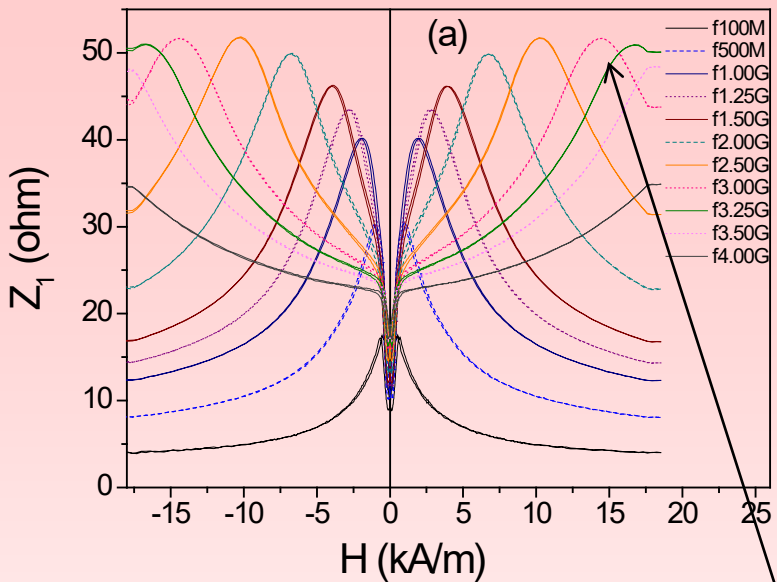
$\delta/a \gg 1$ indicates a **weak skin effect** regime, while $\delta/a \ll 1$ indicate a **strong skin effect**.

δ/a ratio also depends on many other parameters, such as sample dimensions, material properties, magnetic field, etc.

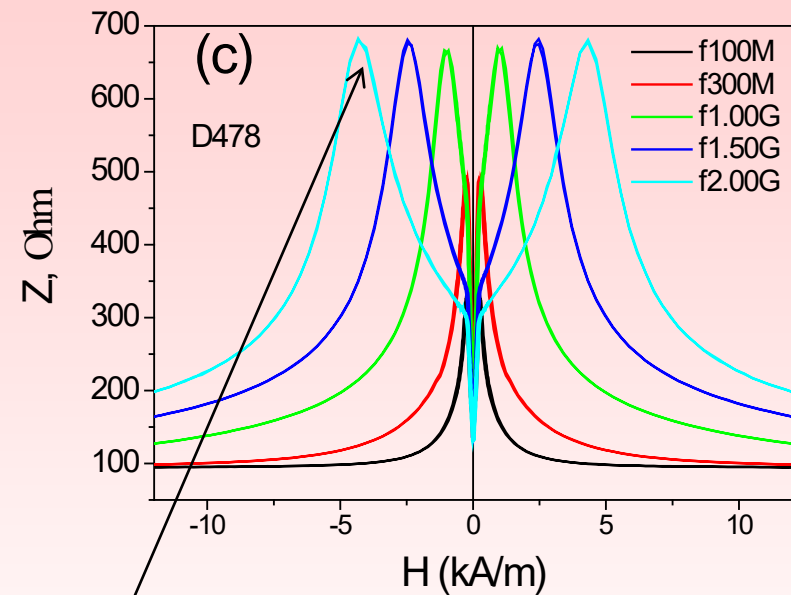
As thinner wire as higher GMI frequency !



Experiments: Frequency dependence of GMI effect



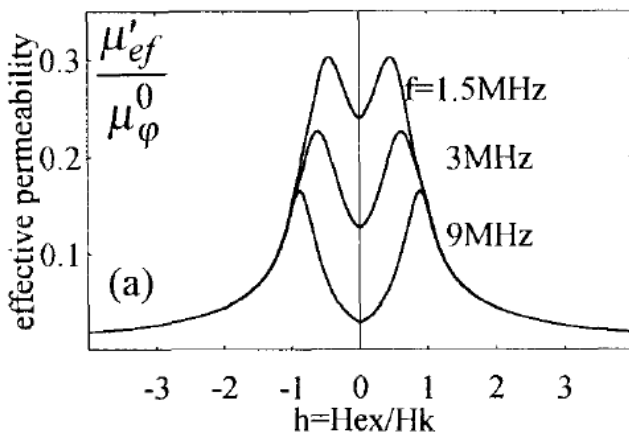
$Z_1(H)$ dependence of $\text{Co}_{66}\text{Cr}_{3.5}\text{Fe}_{3.5}\text{B}_{16}\text{Si}_{11}$ (a) and $\text{Co}_{67}\text{Fe}_{3.85}\text{Ni}_{1.45}\text{B}_{11.5}\text{Si}_{14.5}\text{Mo}_{1.7}$ (b) and $\text{Co}_{67.71}\text{Fe}_{4.28}\text{Ni}_{1.57}\text{Si}_{11.24}\text{B}_{12.4}\text{Mo}_{1.25}\text{C}_{1.55}$ microwires measured at different frequencies



V. Zhukova, M. Ipatov and A Zhukov, "Thin Magnetically Soft Wires for Magnetic Microsensors", *Sensors* 9: 9216-9240, 2009.

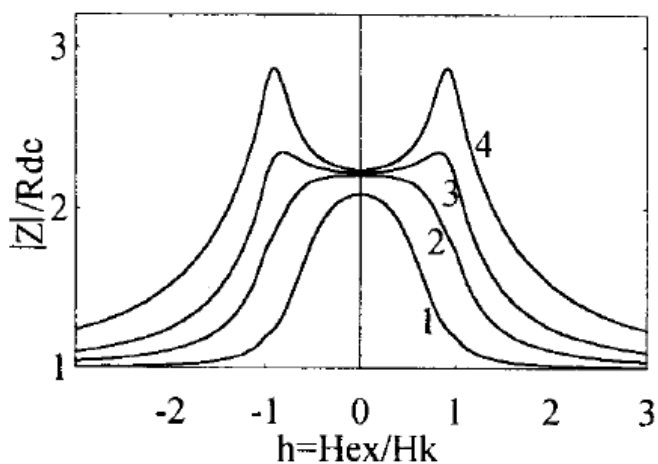
High enough magnetic fields

Frequency dependence of GMI effect: interpretation

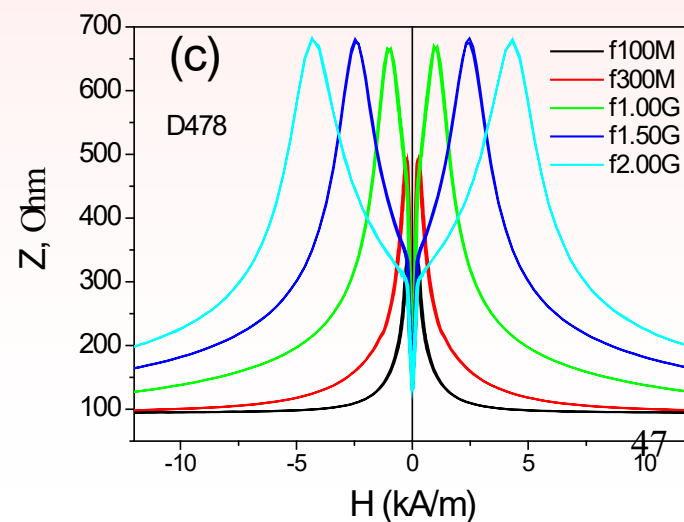


L. V. Panina, K. Mohri, T. Uchyama, and M. Noda,
IEEE TRANS. MAGN. VOL. 31, (1995), 1249

position of μ and Z maximum
becomes closer to $h(H_{ex}/H_k) = 1$ with
increasing frequency



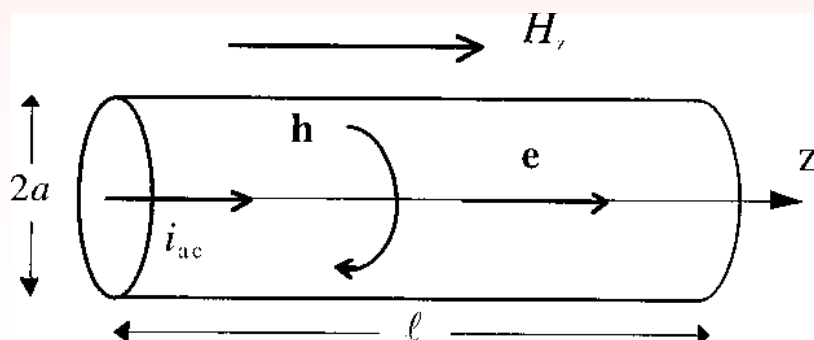
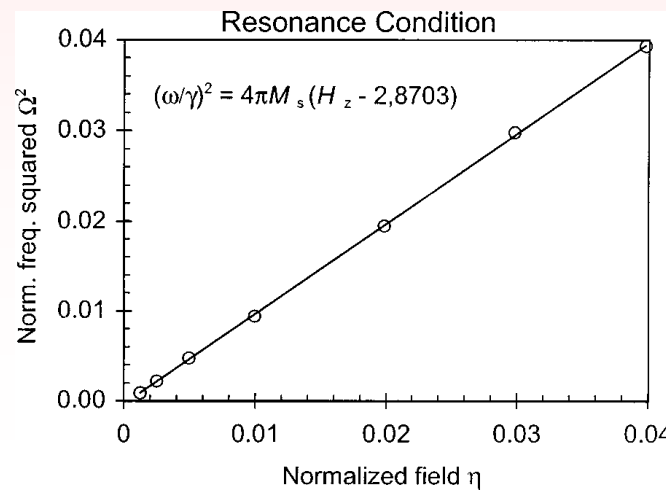
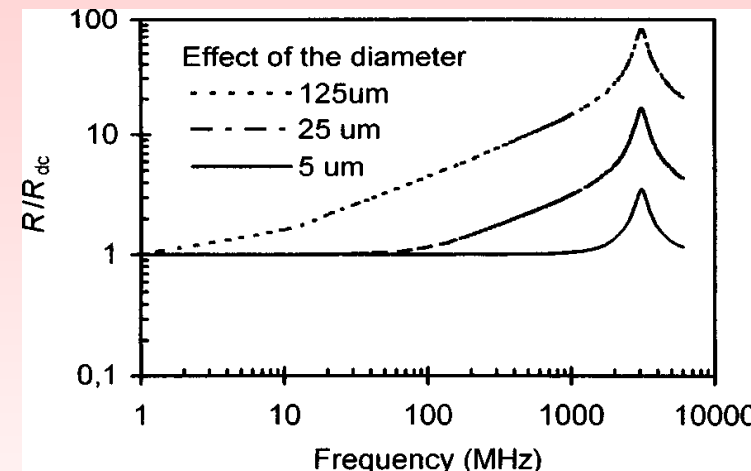
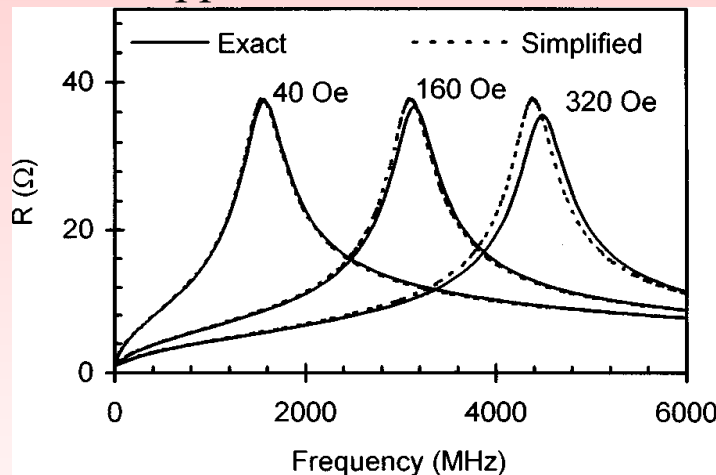
Experimental data (above presented) –
H_k is too high (kA/m) ?
FMR?



Frequency dependence of GMI effect: interpretation

D. Ménard, M. Britel, P. Ciureanu, and A. Yelon, JAP, 84, 5 (1998), 2805:
high field, or linear GMI, for which the cylindrical magnetic conductor is nearly
saturated along its axis ($H > 10$ Oe) in absence of domain
structure or wall motion,

Similar approach L. Kraus & M. Vazquez



Application for MI effect - Sensors

❖ High sensitive electronic compass

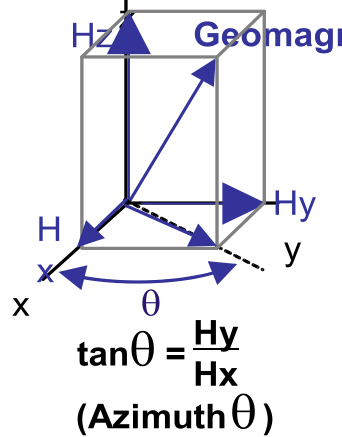
- ❖ Positional sensor ❖ Motion-sensing controllers ❖ Operating attitude automated control.

Motion Sensor = 3D magnetic sensor + 2/3D accelerometer

It determines the attitude of mobile devices relative to geomagnetism and gravity, and by analyzing the attitude and speed, other aspects of movement such as acceleration, translational speed and rotational speed can be calculated.

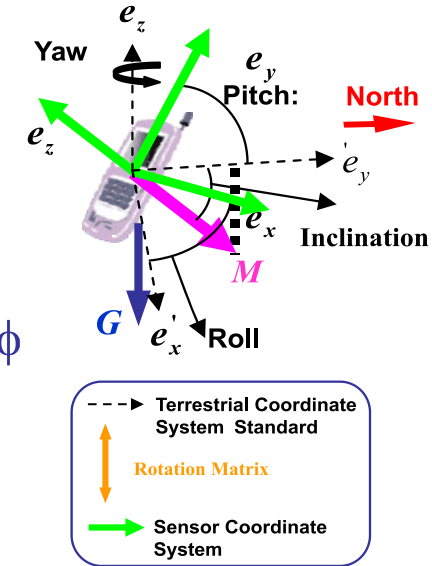
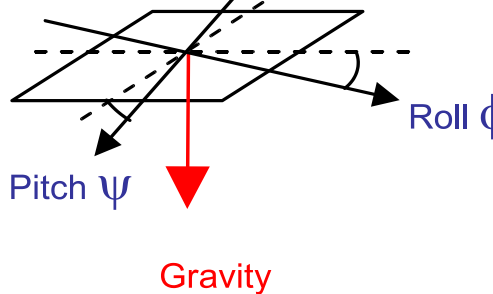
Attitude Detection Principles

3-Axis Magnetic Sensor



Horizontal Detection
Determination of translational/rotational movement

2-Axis Accelerometer



Source: Aichi Micro Intelligent Corporation

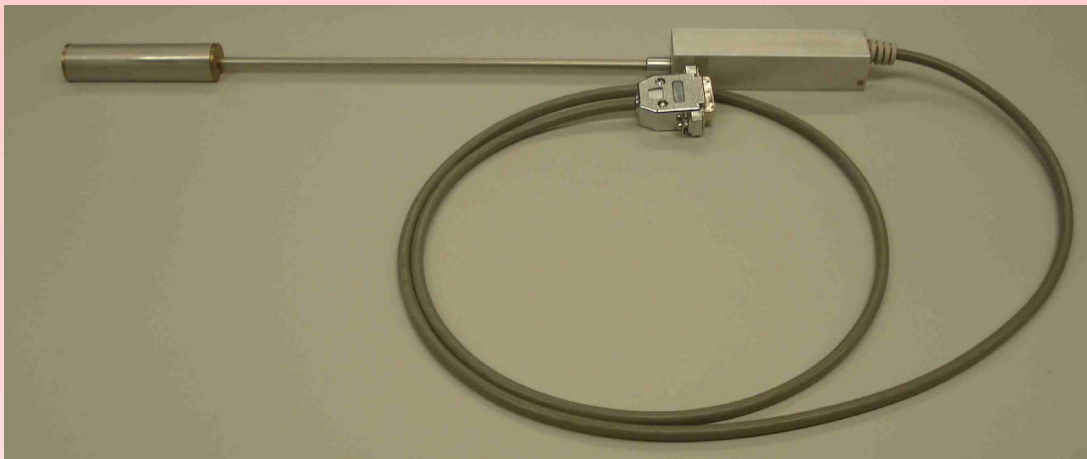
- ❖ Navigation functions combining the motion sensor with a GPS:

Intelligent Transportation System,

Control of operating attitude in unmanned helicopters, robots, automobiles, etc.

Requirements: high sensitivity at low H (up to few Oe)

Designed by us magnetometer



Technical characteristics

Channel number

3 (X, Y, Z components);

Size of the 3-component sensing element

cube with 14 mm edge;

Input voltage of the channel, not less

± 4.5 V;

Dynamic range, not less

± 2.5 Oe;

Frequency range, not less

1 kHz;

Power voltage

0 + 5.5V;

Consuming current

~ 250 mA;

Transmission coefficient of the channels

Channel X

1.58V per 1Oe;

Channel Y

1.57V per 1Oe;

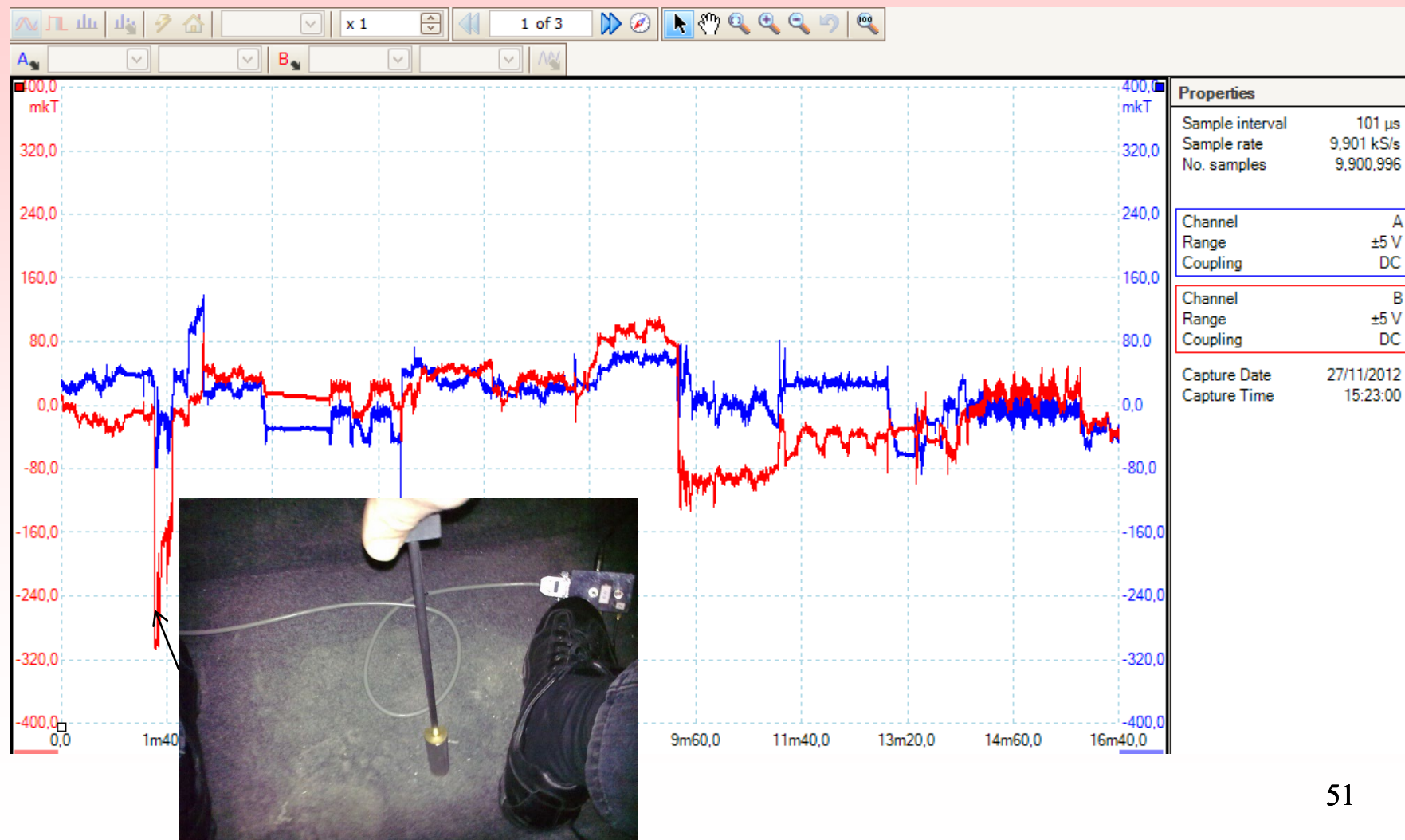
Channel Z

1.69V per 1Oe.

Noise level (resolution)

≈ 10 nT

MAGNETIC FIELD MEASUREMENTS WITH GMI MAGNETOMETER inside the electric car (FIAT Turin Nov. 2012) (FP7 project)



MAGNETIC FIELD MEASUREMENTS WITH GMI MAGNETOMETER (Turin

Nov. 2012), (FP7 project)

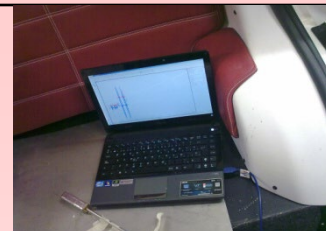
Frame 4, Start time 15:45:55



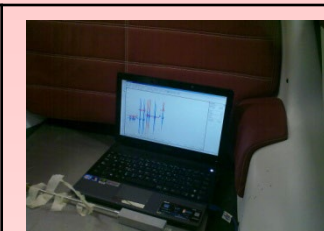
15:47



15:49



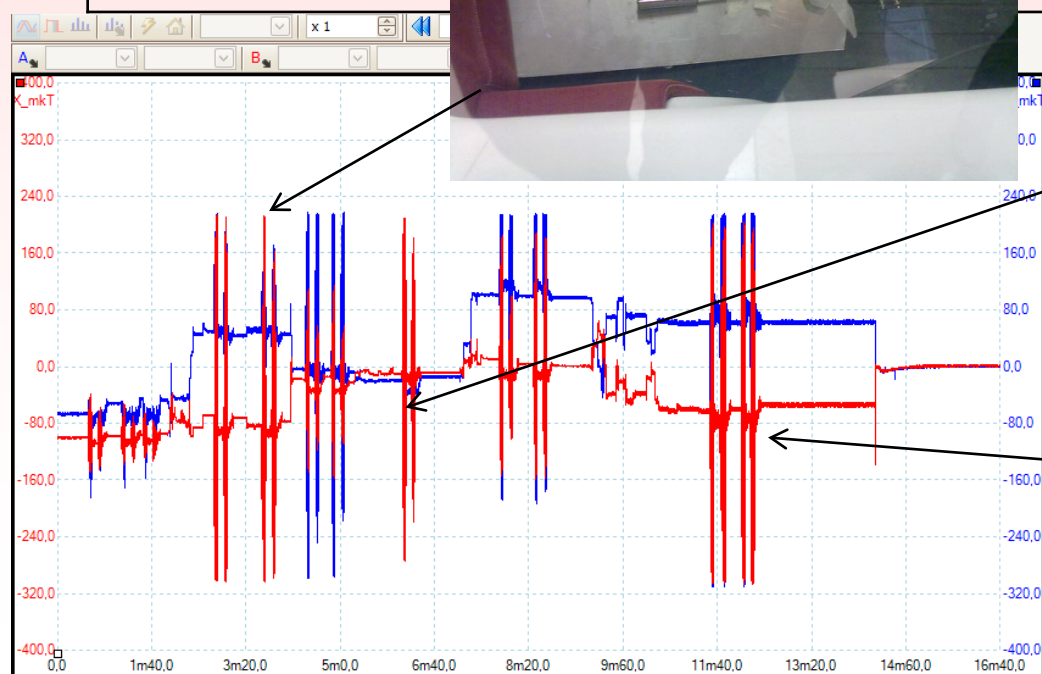
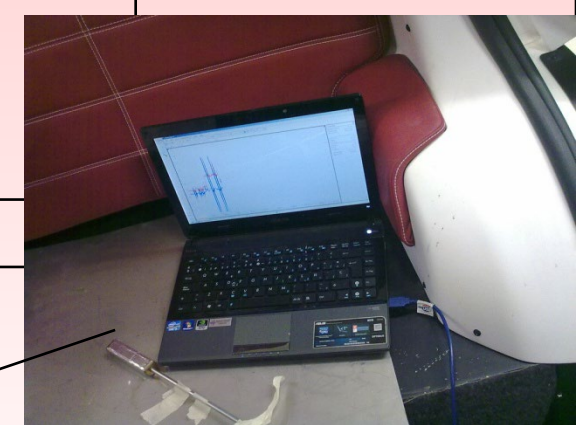
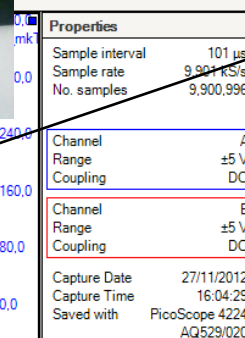
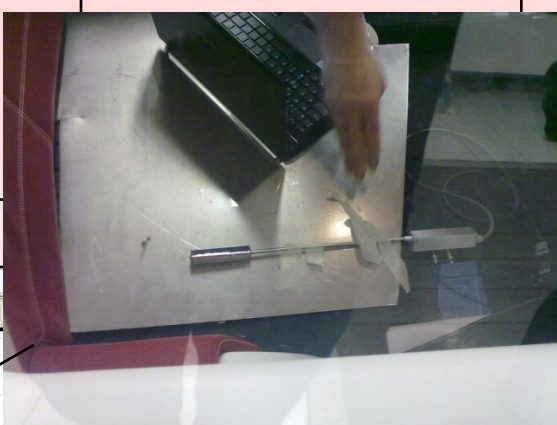
15:51



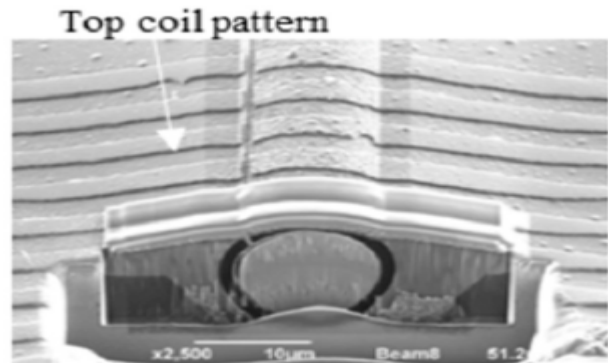
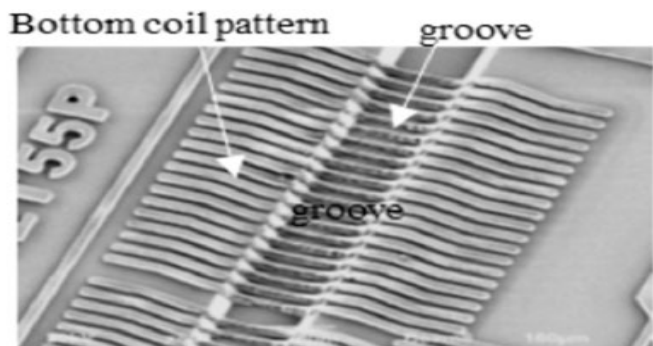
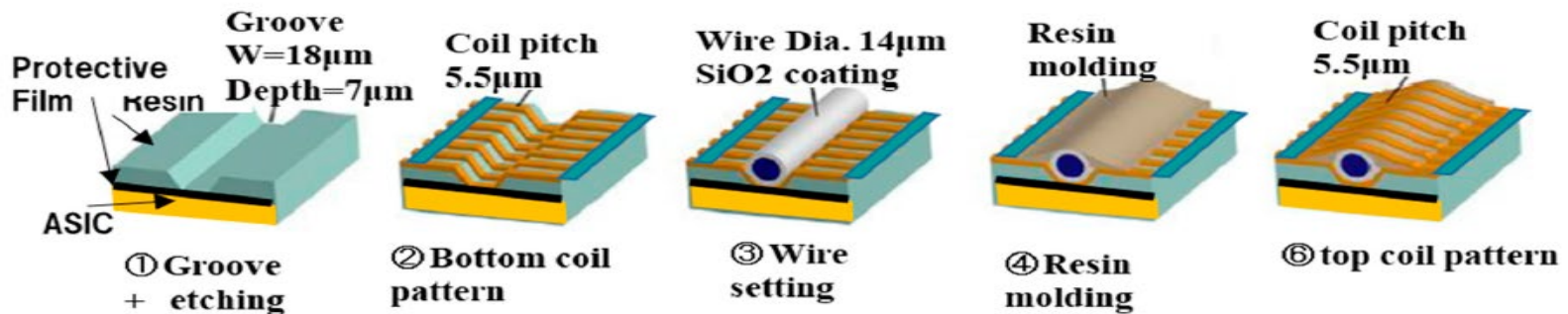
15:55



16:00



Microwires and compatibility with integrated circuits



 **sensors**

 MDPI

Article
The Development of ASIC Type GSR Sensor Driven by GHz Pulse Current [†]

Yoshinobu Honkura ^{1,*} and Shinpei Honkura ^{2,*}

Sensors **2020**, *20*, 1023; doi:10.3390/s20041023

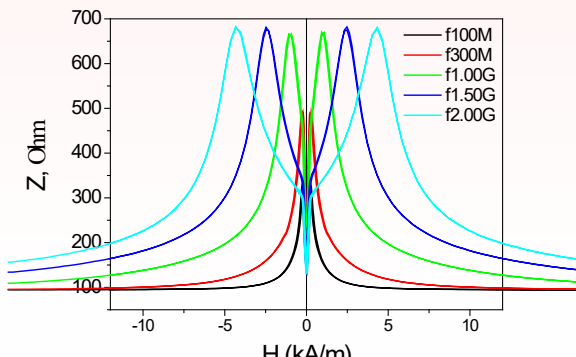
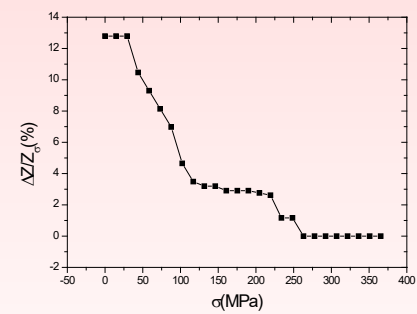
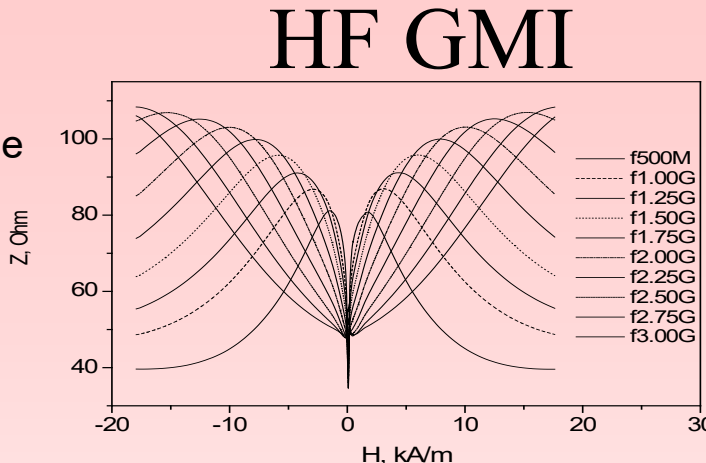
Smart composites: contactless sensor technology

The components of tuneable composite metamaterial:

- (1) strong dispersion of the effective permittivity in microwave range of composite containing metallic wires
- (2) Magneto-Impedance (MI) in Magnetically Soft Microwires.

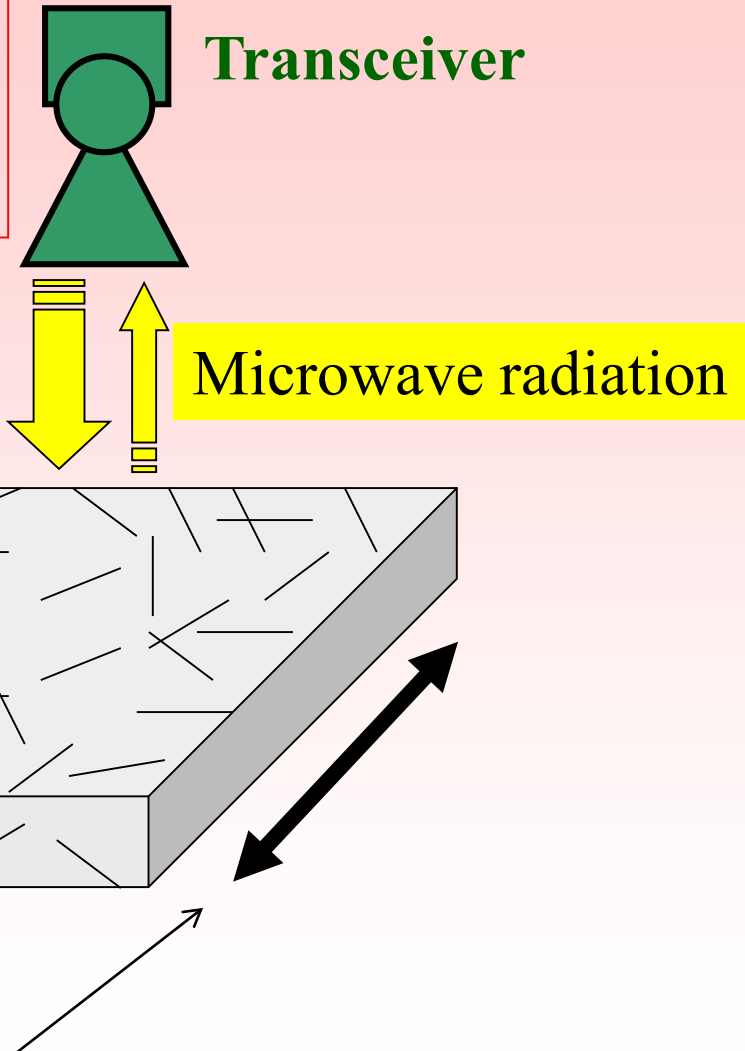


Tuneable Microwave Composites



Free-space microwave sensing technique: embedded short ferromagnetic microwires

There is no bulk conductivity (percolation) through the microwire network! Embedded short microwire inclusions (any conductive) play the role of microwave scatterers ("antennas") which form the effective dipole response of the composite sample in free space.

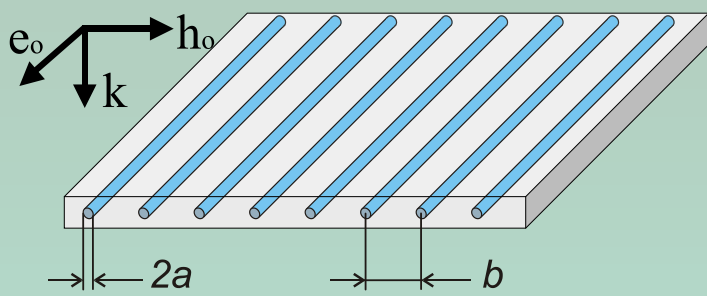


External stimuli: strain, compression, magnetic field, or heating

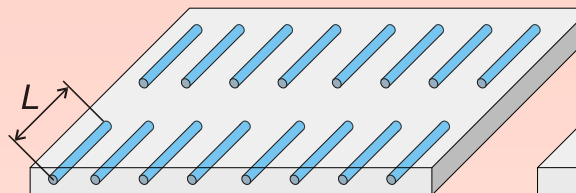
Composites with unusual dispersion of permittivity

4

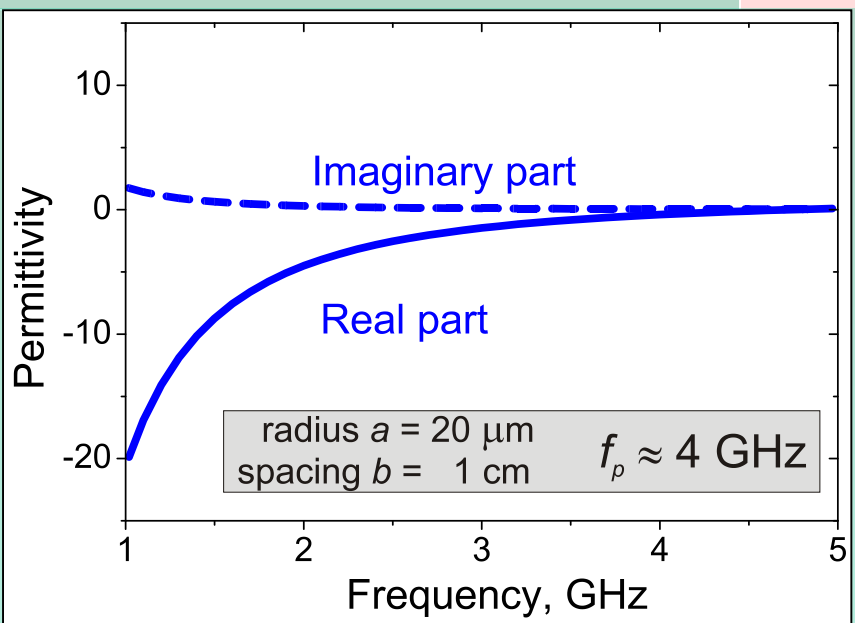
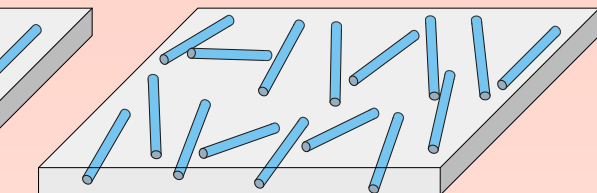
1. Ordered long wire inclusions



2. Ordered short wire inclusions (0.5-5 cm)



3. Arbitrary directed short wire inclusions (0.5-5 cm)

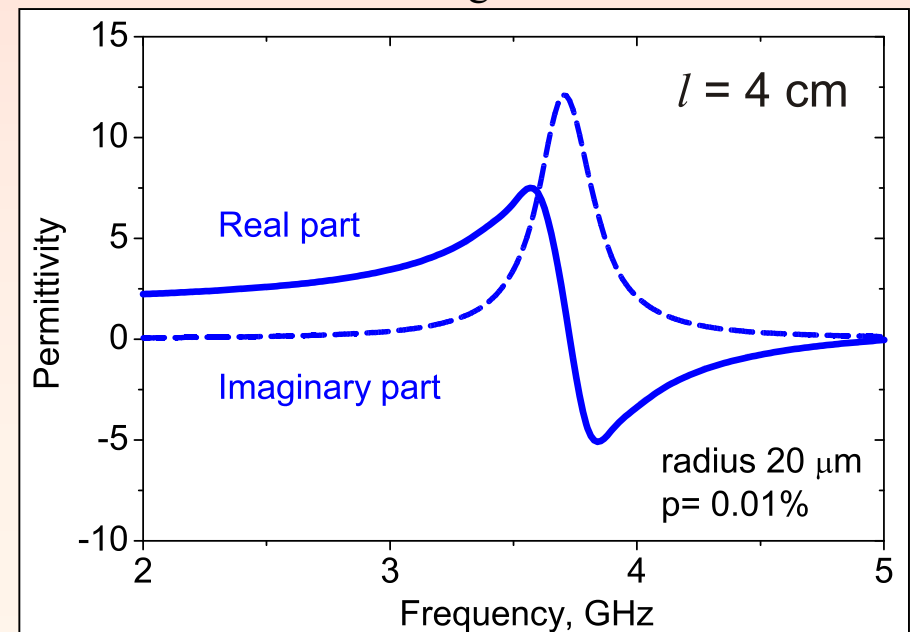


Ordered thin long wire structures behave like a **plasma** in the microwave region with a plasma frequency:

$$\omega_p^2 = \frac{2\pi c^2}{b^2 \ln(b/a)}$$

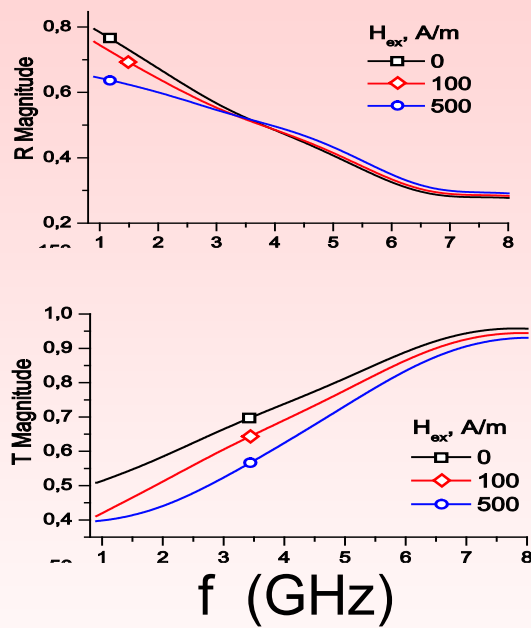
The short wire composites are characterized by **resonance type** of the ϵ_{ef} as the wires behave as dipole antennas with the resonance at half wave length:

$$\omega_{res} = \frac{\pi c}{l \sqrt{\epsilon_d}}$$

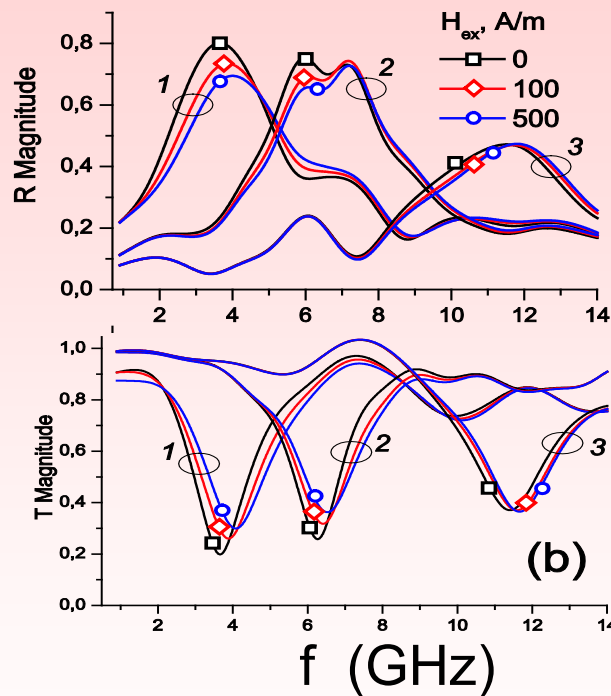


Smart composites with magnetic wire inclusions

Spectra of R , T for
composites with long wires
with H_{ex} as a parameter
($H_{ex} = 0, 100, 500$ A/m).



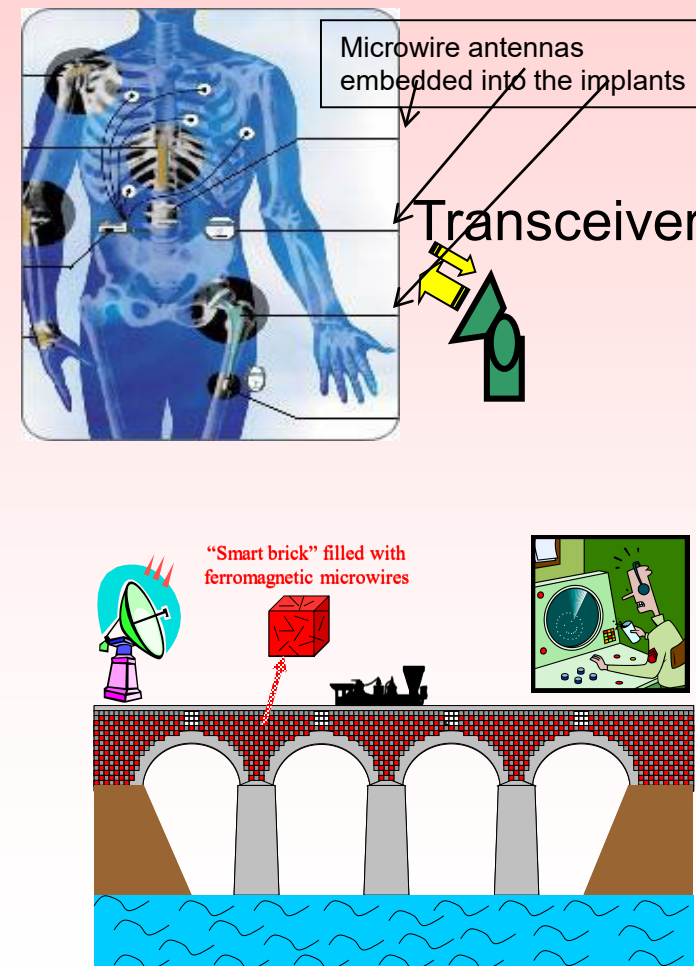
Spectra of R , T of
composites with cut wires
of length 40 (1), 20 (2)
and 10 (3) mm with the
field as a parameter.



reflection R and transmission T spectra

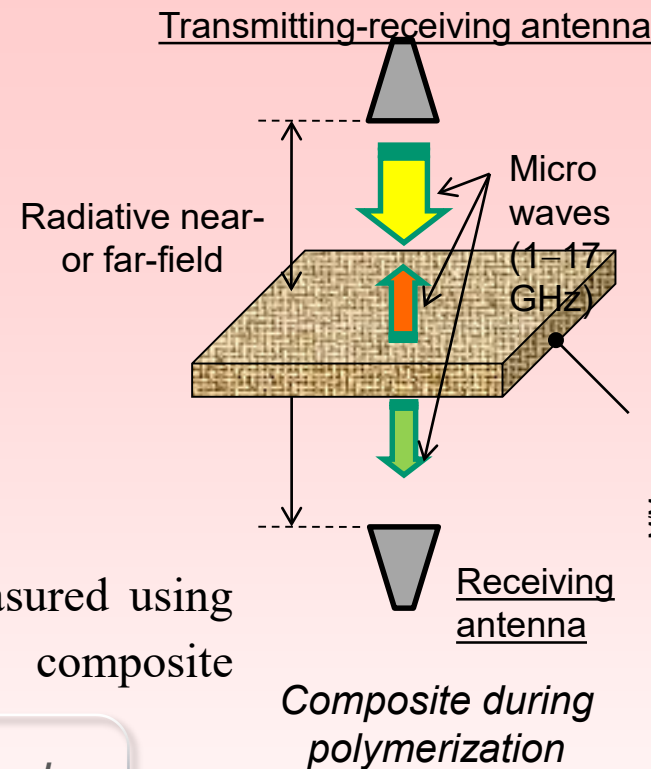
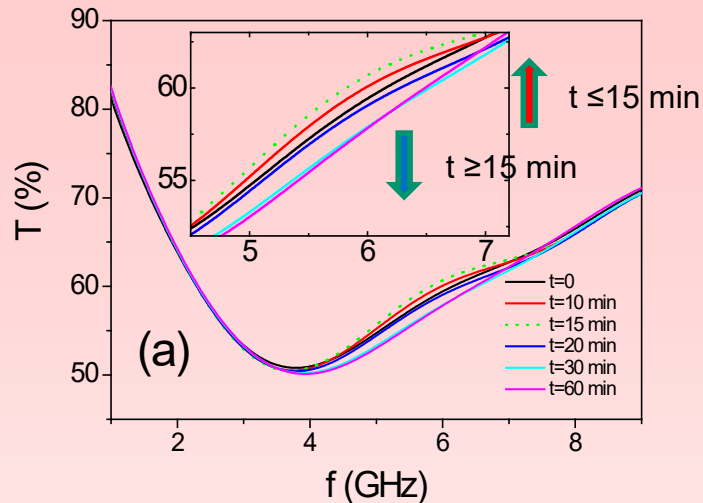
experiment

Applications:

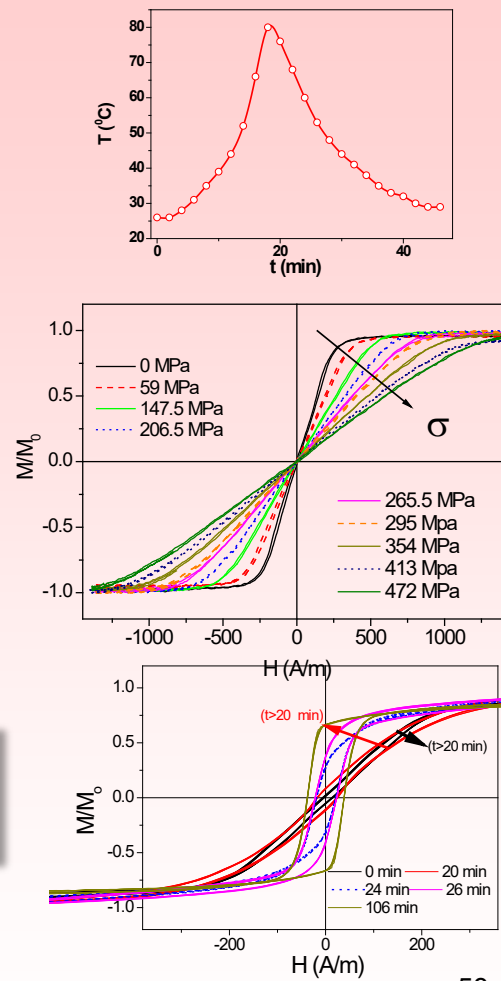
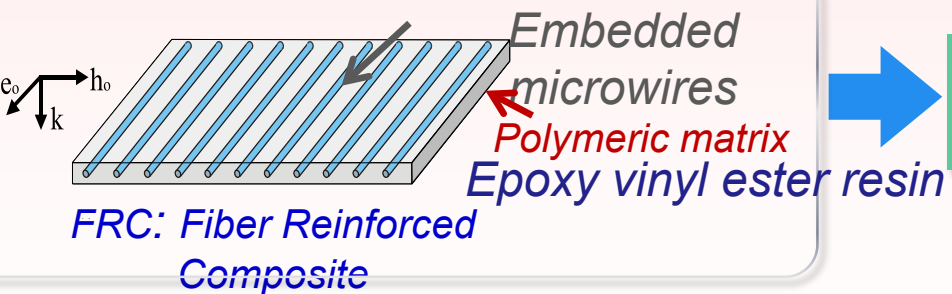


Composites monitoring

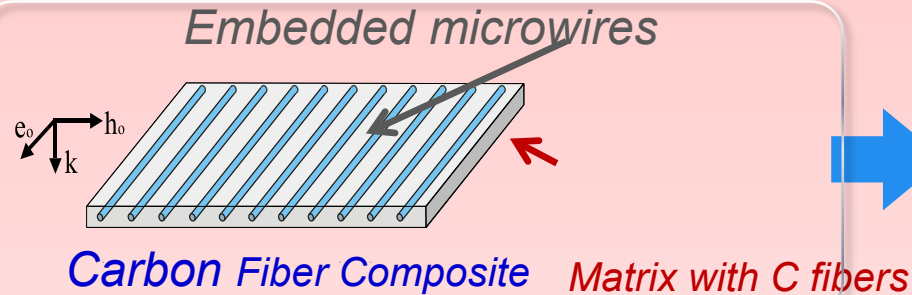
Recent results



The Transmission, T parameters measured using free-space system during the composite solidification.



Composite structures in aircraft industry



Free-space Measurements



Aerospace Composites
digitally sensorised from
manufacturing to end-of-life

Both magnetic and mechanical properties are relevant !
Main problem: high electrical conductivity of Carbon fibre (different to Polymer matrix). Magnetic field (low f modulating) allows separate signal from magnetic wires

Modulation magnetic field (80 Hz) OFF and ON, at 2 GHz

Line colors: yellow-S11; green-S22, blue and magenta: S12 and S21 respectively



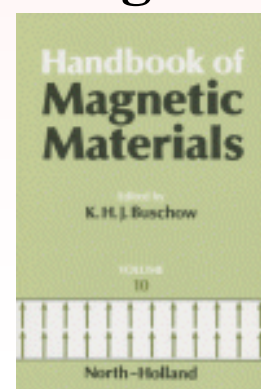
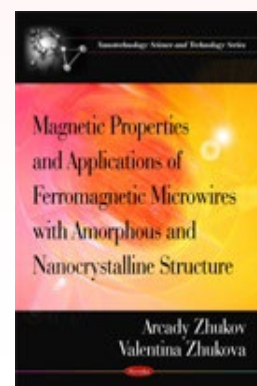
ITE consortium



Conclusions

- Soft magnetic microwires exhibit **high GMI effect** in a wide frequency range suitable for the magnetic field detection, stress and temperature monitoring. But **one should pay attention on stress relaxation and magnetostriction coefficient**.
- GMI effect and its frequency dependence that can be **tailored the magnetoelastic anisotropy**, i.e. modifying the microwires geometry or relaxing the stresses by heat treatment
- Features of **high frequency GMI effect** can be described using **FMR-like approximation**.
- **GMI hysteresis** can be related with bamboo-like domain structure and can be suppressed by the bias magnetic field. The other origin of GMI hysteresis is the **bias field from the inner core (core-shell interaction)**
- **HF GMI can be used for composite monitoring**

Thank you for
the attention!



“Advances in Giant Magnetoimpedance Materials” by A. Zhukov, M. Ipatov and V. Zhukov (issue October 2015)